Fitted Numerical Methods for Delay Differential Equations Arising in Biology

Eihab Bashier Mohammed Bashier

A Thesis submitted in partial fullfillment of the requirements for the degree of Doctor of Philosophy in the Department of Mathematics and Applied Mathematics at the Faculty of Natural Sciences, University of the Western Cape

Supervisor: Professor Kailash C. Patidar

May 2009

KEYWORDS

Mathematical Biology

Delay differential equations

Singular perturbations

Positivity preserving numerical methods

Bifurcation Analysis

Fitted operator finite difference methods

Fitted mesh finite difference methods

Convergence analysis

Matrix stability analysis

Fourier stability analysis

ABSTRACT

Fitted Numerical Methods for Delay Differential Equations Arising in Biology

E.B.M. Bashier

PhD thesis, Department of Mathematics and Applied Mathematics, Faculty of Natural Sciences, University of the Western Cape.

This thesis deals with the design and analysis of fitted numerical methods for some delay differential models that arise in biology. Very often such differential equations are very complex in nature and hence the well-known standard numerical methods seldom produce reliable numerical solutions to these problems. Inefficiencies of these methods are mostly accumulated due to their dependence on crude step sizes and unrealistic stability conditions. This usually happens because standard numerical methods are initially designed to solve a class of general problems without considering the structure of any individual problems. In this thesis, issues like these are resolved for a set of delay differential equations. Though the developed approaches are very simplistic in nature, they could solve very complex problems as is shown in different chapters.

The underlying idea behind the construction of most of the numerical methods in this thesis is to incorporate some of the qualitative features of the solution of the problems into the discrete models. Resulting methods are termed as fitted numerical methods. These methods have high stability

properties, acceptable (better in many cases) orders of convergence, less computational complexities and they provide reliable solutions with less CPU times as compared to most of the other conventional solvers. The results obtained by these methods are comparable to those found in the literature. The other salient feature of the proposed fitted methods is that they are unconditionally stable for most of the problems under consideration.

We have compared the performances of our fitted numerical methods with well-known software packages, for example, the classical fourth-order Runge-Kutta method, standard finite difference methods, dde23 (a MAT-LAB routine) and found that our methods perform much better.

Finally, wherever appropriate, we have indicated possible extensions of our approaches to cater for other classes of problems.

May 2009.
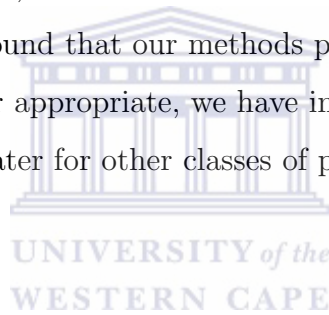
DECLARATION

I declare that *Fitted Numerical Methods for Delay Differential Equations Arising in Biology* is my own work, that it has not been submitted before for any degree or examination at any other university, and that all sources I have used or quoted have been indicated and acknowledged by complete references.

Eihab Bashier Mohammed Bashier   May 2009

Signed . . . .

ACKNOWLEDGEMENT

First and foremost, I would like to thank with all sincerity the almighty God Allah (Glory to Him) who gave me the strength to do this research and made all difficult tasks very easy.

My deepest gratitude is due to my supervisor Professor Kailash C. Patidar who was more a closed friend than a supervisor. Without his great ideas and big efforts this work would not have been done. Special thanks go to his wife Mrs. Pramila Patidar who always had encouraging smiles and lots of patience whenever we had borrowed lots of hours for our research discussions at their home. Her nice tea and tasty Indian food have been a powerful fuel for our minds and a source for many ideas in this thesis.
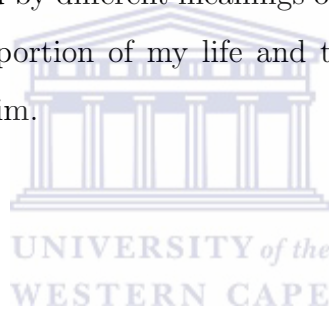
I would like to thank the University of Khartoum who funded me for this PhD programme and gave me study leave to carry out this research. Particular thanks to Dr. Mohsin H. A. Hashim (the Dean of Faculty of Mathematical Sciences at the University of Khartoum) and Mrs. Islah Shaaban (the training manager at the Adminstration of teaching assistants, at the University of Khartoum) who have been of great assistance throughout the programme.

The all time support from my wife is unforgettable. Coming to a new country, adapting to the new environment and doing research in very difficult circumstances was not possible without the moral support that my wife has given me.

Finally, I would like to thank many professors at the University of the Western Cape (in particular, Prof. JvB Donker, Prof. R Christie, Prof. P Witbooi and Dr. L Holtman) and also to all my friends across the campus.

DEDICATION

I dedicate this work to my parents who have devoted their lives for us and who have been giving their continuous wishes to me for success; to my lovely wife and son with whom I have been inspired by different meanings of life; to my dear brothers and sister with whom I shared big portion of my life and to my supervisor who has been my friend ever since I knew him.

Contents

List of Tables

List of Figures

xiii

List of Publications

Part of this thesis has been submitted in the form of the following research papers:

1. Eihab B.M. Bashier and Kailash C. Patidar, A robust fitted operator finite difference method for a singularly perturbed delay parabolic partial differential equation, submitted for publication.

2. Eihab B.M. Bashier and Kailash C. Patidar, A fitted numerical method for a system of partial delay differential equations, submitted for publication.

3. Eihab B.M. Bashier and Kailash C. Patidar, An almost second order fitted mesh numerical method for a singularly perturbed delay parabolic partial differential equation, submitted for publication.

4. Eihab B.M. Bashier and Kailash C. Patidar, A second order fitted operator finite difference method for a singularly perturbed delay parabolic partial differential equation, submitted for publication.

5. Eihab B.M. Bashier and Kailash C. Patidar, A fitted numerical method for a delayed model of two competitive species, submitted for publication.

6. Eihab B.M. Bashier and Kailash C. Patidar, Fitted numerical methods for a system of first order delay differential equations, submitted for publication.

7. Eihab B.M. Bashier and Kailash C. Patidar, An efficient fitted operator method to solve delayed singularly perturbed differential difference equation, submitted for publication.

Chapter 1

General Introduction

1.1 Introduction

Delay differential equations (DDEs) have a wide range of application in modelling problems in biology. Dynamics of viruses, blood cells populations, predator-prey models, competitive and co-operative species, etc, are just to mention a few. In a model that describes the dynamics of a virus, a delay may represent the latent period of the virus [57]. In a model that describes the dynamics of the blood cells population, a time delay may represent the time taken by the bone marrow to reproduce new cells to replenish cells that have been cleared in the past [91]. A little differently in a predator-prey model, delay can be used to represent the densities of the predator and prey at a previous time [47].

In addition to the time, when another independent variable is considered in a DDE model, then the resulting model is termed a delay partial differential equation (DPDE). Like DDEs, these DPDEs also model a wide range of applications in the world of mathematical biology. The position of the species [25], the level of maturation [123], the age, etc, are some of the instances when it is worth considering DPDEs instead of DDEs. Many biological models describe the diffusion of some species through DPDEs. It is possible that the diffusion parameter is very small and hence the resulting model

is almost a singularly perturbed delay parabolic partial differential equation. Such examples of small diffusions can be found in Murray [110].

The DDEs arising in biology have different levels of difficulties. Some of them have small delays [84] while others have large delays; some of them are nonlinear [29]; some of them are non-stiff while others are very stiff [65, 137, 138, 144]; some of them are highly singularly perturbed [84, 85], and so on. In many of the above cases, the resulting DDEs are discontinuous in nature and hence pose challenging problems when one solves these DDEs either analytically or numerically.

Some problems with constant time delays constitute an important class of the DDE models. On their dde23 tutorial [129], Shampine and Thompson wrote about this class of DDEs that "*Although DDEs with delay of more general form are important, this is a large and useful class of DDEs. Indeed, Baker, Paul and Wille' write that the lag functions that arise most frequently in the modelling literature are constants....*".

In many of the DDE models, the time delay parameter acts as a bifurcation parameter. As the delay parameter passes through some critical value, a couple of complex conjugating eigenvalues of the system cross the imaginary axis at some pure imaginary points and stable periodic Hopf bifurcating solutions occur. Then, when the delay parameter crosses its critical value, the real parts of these eigenvalues cross to the positive real axis causing an equilibrium to loose its stability. However, to the best of our knowledge to date, the issue of determining whether and when a bifurcation occurs is not completely resolved till date. Some bifurcation analysis tools based on novel programming tools are designed but it seems that no concrete analytical tools are currently available.

Due to the complex nature of the governing equations, analytical investigations have become very difficult and therefore one has to rely mostly on some numerical methods. Many of these numerical methods for solving DDEs are based on step-by-step methods for solving initial value problems (IVPs). Examples to these are Runge-Kutta methods [7, 39, 130, 139], multi-step methods [60, 68] and pseudospectral methods [98].

The general deficiencies of the standard finite difference methods in solving problems

with complex structures such as nonlinearity, stiffness, singular perturbations and high oscillations are well-known in the literature. While explicit methods can solve such differential equations with low computational cost, they have the drawback that their stability regions are very small and hence severe restrictions on the time and space step-sizes will be required in order to achieve satisfactory results. On the other-hand, the implicit methods do have wider stability regions but the associated computational complexities are very high, and furthermore, they cannot achieve more than one order as compared to explicit methods that use the same number of stages [20]. However, due to some inherent errors in the models, it becomes very expensive to retrieve the true information because most of the numerical methods available so far fail in providing reliable results. This is mostly due to the fact that essential qualitative features of the solutions have not been embedded into the numerical schemes.

Our main goal in this thesis is therefore to design numerical methods which can inherit some of the qualitative features of the solution with the hope of obtaining results which are which are consistent to the desired dynamics as possible. Particular problems we are focusing on include a number of delay and partial delay differential equation models from biology, few of which are mentioned below.

1.2   Some delay differential equations (DDEs) arising in biology

In this section, we survey some DDE models that arise in biology.

Hutchinson [62] proposed a logistic delay population model of the form

$$\dot{N}(t) = rN(t)\left(1 - \frac{N(t-\tau)}{K}\right), \tag{1.2.1}$$

where r is the growth rate, K is the carrying capacity, $N(t)$ is the size of population at time t. The delay τ in this model represents a maturation time (The model was proposed originally to describe the dynamics of Daphnia population and the time delay

represents the time taken from the eggs formation until those eggs hatch).

The Hutchinson's model has another form that can be obtained by substituting $N(t)$ instead of $-1 + N(t)/K$ in model (1.2.1). This leads to

$$\dot{N}(t) = rN(t - \tau)(1 + N(t)). \qquad (1.2.2)$$

Mackey and Glass [91] proposed two possible models to describe the change of density of Hematopoietic cells in the blood that is circulating in the human body. They assumed that the cells are lost at a rate proportional to their concentration. After the reduction of cells, the bone marrow requires six days to release new mature cells to replenish the deficiency. Denoting by $P(t)$ the density of the Hematopoietic cells at time t, their two models are given by

$$\dot{P}(t) = \frac{\beta_0 \theta^n}{\theta^n + P^n(t - \tau)} - \gamma P(t), \qquad (1.2.3a)$$

and

$$\dot{P}(t) = \frac{\beta_0 \theta^n P(t - \tau)}{\theta^n + P^n(t - \tau)} - \gamma P(t), \qquad (1.2.3b)$$

where β_0, θ, n and γ are constants and the delay τ is the time taken from the reduction of the cells until the release of the new mature cells.

Gurney et al. [53] proposed a DDE to describe the Nicolson's blowflies model. This model takes the form

$$\dot{N}(t) = aN(t - \tau)e^{-bN(t-\tau)} - dN(t), \qquad (1.2.4)$$

where $N(t)$ denotes the size of the population at time t, a is the maximum per capita rate of producing eggs per day, d is the death rate in the adult population, and τ is time taken from the birth of a member until it becomes mature.

Cooke and van den Driessche [29] proposed a model to describe the growth of a

single species model. The model is of the form

$$\dot{N}(t) = B(N(t-\tau))N(t-\tau)e^{-d_1\tau} - dN(t), \qquad (1.2.5)$$

where $N(t)$ denotes the population of the mature individuals of the species and $d_1 \geq 0$ and $d > 0$ are the death rates of the immature and mature populations, respectively. The time delay $\tau > 0$ is the maturation time. The function $B(N(t-\tau))$ is termed as the birth function and gives the rates by which new individuals of the species are produced by a mature individual.

Gopalsamy et al. [48] proposed a delayed model to describe the growth of a population with limited food source. For this model, it is assumed that the growth rate of the population is proportional to the rate of the food supply. The model is given by

$$\dot{N}(t) = rN(t)\left(\frac{K - N(t-\tau)}{K + rcN(t-\tau)}\right), \qquad (1.2.6)$$

where $N(t)$ is the size of population at time t, r is the intrinsic growth rate of the population, K is the carrying capacity and $c > 0$ is a constant.

Mackey et al. [93] developed a DDE model describing the periodic oscillations of blood cells in people infected by chronic myelogenous leukemia. Their model is a stem cell model of the form

$$\dot{P}(t) = -\gamma P(t) + \beta(N(t))N(t) - e^{-\gamma\tau}\beta(N(t-\tau))N(t-\tau), \qquad (1.2.7a)$$

$$\dot{N}(t) = -(\beta(N(t)) + \delta)N(t) + 2e^{-\gamma\tau}\beta(N(t-\tau))N(t-\tau), \qquad (1.2.7b)$$

where $P(t)$ is the population of the proliferating cells and $N(t)$ is the population of the resting G_0 cells. The parameters $\gamma > 0$ and $\delta > 0$ are the deaths rates of the proliferating and resting cells. The birth function $\beta(N(t))$ is given by the formula

$$\beta(N(t)) = \frac{\beta_0\theta^n}{\theta^n + N^n(t)},$$

where β_0 and θ are constants.

Villasana and Radunskaya [142] presented a model describing the competition between the tumor cells and the immune system. The model consists of four DDEs. In this model, three populations and a cycle-phase-specific drug are considered. The three populations are the immune system, the tumor cells during the interphase and the tumor cells during mitosis. The model is given by

$$\dot{T}_I = 2a_4 T_M - (c_1 I + d_2) T_I - a_1 T_I(t - \tau), \tag{1.2.8a}$$

$$\dot{T}_M = a_1 T_I(t - \tau) - d_3 T_M - a_4 T_M - c_3 T_M I - k_1(1 - e^{-k_2 u}) T_M, \tag{1.2.8b}$$

$$\dot{I} = k + \frac{\rho I(T_I + T_M)^n}{\alpha + (T_I + T_M)^n} - c_2 I T_I - c_4 T_M I - d_1 I - k_3(1 - e^{-k_4 u}) I, \tag{1.2.8c}$$

$$\dot{u} = -\gamma u, \tag{1.2.8d}$$

with the initial data

$$T_I(\theta) = \phi_1(\theta), \; \theta \in [-\tau, 0]$$

$$T_M(\theta) = \phi_2(\theta), \; \theta \in [-\tau, 0]$$

$$I(\theta) = \phi_3(\theta), \; \theta \in [-\tau, 0]$$

$$u(0) = u_0,$$

where $T_I(t)$ denotes the population of tumor cells during interphase at time t, $T_M(t)$ is the population of tumor cells during mitosis at time t, $I(t)$ is the population of immune system cells at time t and $u(t)$ is the amount of drug present at time t. The delay τ is the maturation time of the cell. The constant a_4 denotes the cell reproduction rate whereas the constant a_1 denotes the rate at which the cells cycle. The constants c_1 and c_2 denote the rate by which immune cells are lost by interaction with tumors cells. The constants d_1, d_2 and d_3 denote the natural death rates of the immune, immature and mature tumor cells, respectively. The Michaelis-Menten term $\rho I(T_I + T_M)^n / (\alpha + (T_I + T_M)^n)$ represents the nonlinear growth of the immune population due to stimulus by the tumor cells, where the parameters ρ, α, and n depend on the type of tumor being considered

and the status of the immune system. Tumor chemotherapy causes tumor cells not to continue their cycles, hence, they die naturally during the mitosis.

Berreta and Kuang [14] developed a DDE model to describe the viral infection of bacteria, to replicate themselves. The model consists of three compartments representing the susceptible and infected bacteria and the virus with densities $S(t)$, $I(t)$ and $P(t)$, respectively. In the absence of viruses, it has been assumed that the bacterial population density grows according to a logistic equation with carrying capacity C and a constant intrinsic growth rate α. In the presence of viruses, the total bacterial population has been divided into two subclasses: the susceptible bacteria $S(t)$ and the virus infected bacteria $I(t)$. The rate of infection per unit time is given by $kS(t)P(t)$ where k denotes the effective per bacteria phage absorption constant rate. The infected bacteria which are under the genetic control of virulent phages, replicate phages inside themselves up to the death by lysis after a latency time τ. On the lysis death of an infected bacteria (τ time units from the infection), b copies (on average) of assembled phages are released in the solution. The constant b is termed the virus replication factor. The death rate of the infected bacteria (which might be different to the lysis death) is given by a constant μ_i. The death rate of the virus is given by a constant μ_P. Using these notations and terminology, the model is given by

$$
\begin{aligned}
\dot{S}(t) &= \alpha S(t)\frac{S(t)+I(t)}{C} - kS(t)P(t), & \text{(1.2.9a)} \\
\dot{I}(t) &= -\mu_i I(t) + kS(t)I(t) - e^{-\mu_i \tau}S(t-\tau)P(t-\tau), & \text{(1.2.9b)} \\
\dot{P}(t) &= \beta - \mu_P P(t) - kS(t)I(t) + be^{-\mu_i \tau}S(t-\tau)P(t-\tau). & \text{(1.2.9c)}
\end{aligned}
$$

In [148], Yoshida and Hara formulated an SIR model with density dependant birth

and death rates in a population governed by logistic growth. The model is given by

$$
\begin{aligned}
\dot{S}(t) &= -\frac{\beta S(t)I(t-\tau)}{N(t-\tau)} - \left(d + (1-a)\frac{rN(t)}{K}\right)S(t) \\
&\quad + \left(b - a\frac{rN(t)}{K}\right)N(t), &\text{(1.2.10a)} \\
\dot{I}(t) &= \frac{\beta S(t)I(t-\tau)}{N(t-\tau)} - \left(d + (1-a)\frac{rN(t)}{K}\right)I(t) - \lambda I(t), &\text{(1.2.10b)} \\
\dot{R}(t) &= \lambda I(t) - \left(d + (1-a)\frac{rN(t)}{K}\right)R(t), &\text{(1.2.10c)}
\end{aligned}
$$

where β is the effective per capita contact rate constant of infective individuals, $a \in [0,1]$ is a convex combination constant, b and d are the natural growth and death rates, $r = b - d > 0$ is the intrinsic growth rate, $K > 0$ is the carrying capacity of the population, the delay parameter τ is the latent period of the virus and λ is the recovery rate on the infected population.

Yan and Liu [147] considered an SEIR model with a constant time delay. The model is given by

$$
\begin{aligned}
\dot{S}(t) &= bS(t) + bE(t) + bR(t) - \mu S(t) - \gamma\frac{S(t)I(t)}{N(t)}, &\text{(1.2.11a)} \\
\dot{E}(t) &= \gamma\frac{S(t)I(t)}{N(t)} - \gamma\frac{S(t-\tau)I(t-\tau)}{N(t-\tau)}e^{-\mu\tau} - \mu E(t), &\text{(1.2.11b)} \\
\dot{I}(t) &= -\mu I(t) + \gamma\frac{S(t-\tau)I(t-\tau)}{N(t-\tau)}e^{-\mu\tau} - \alpha I(t), &\text{(1.2.11c)} \\
\dot{R}(t) &= -\mu R(t) + f\alpha I(t), &\text{(1.2.11d)}
\end{aligned}
$$

where $N(t) = S(t) + E(t) + I(t) + R(t)$ is the total population, $S(t)$ is the susceptible population, $E(t)$ is the exposed population, $I(t)$ is the infectious population and $R(t)$ is the recovered population. The delay τ represents the latent period, the constants b and μ are the birth and natural death rates, respectively; γ is the expected number of contacts per unit multiplied by the probability of transmission given contact and α is the removal rate. The probability that an individual survive the whole latent period is $e^{\mu\tau}$. The delayed term $\gamma S(t-\tau)I(t-\tau)e^{-\mu\tau}/N(t-\tau)$ gives the number of individuals

who survive the latent period τ and become infectious at time t.

Zhang et al. [150] formulated an SIR epidemic model with incubation time and saturated incidence rate. In their model, they assumed that susceptibles satisfy a logistic equation and the incidence term is of saturated form with the susceptible. They determined the threshold value $\mathcal{R}_0$ and showed that the dynamics of the model is determined by this value together with the delay which represents the incubation time length. Their model is given by

$$
\dot{S}(t) = r\left(1 - \frac{S(t)}{K}\right) - \beta\frac{S(t)}{1 + \alpha S(t)}I(t - \tau), \tag{1.2.12a}
$$

$$
\dot{I}(t) = \beta\frac{S(t)}{1 + \alpha S(t)}I(t - \tau) - (\mu_1 + \gamma)I(t), \tag{1.2.12b}
$$

$$
\dot{R}(t) = \gamma I(t) - \mu_2 R(t), \tag{1.2.12c}
$$

where $r > 0$ is the intrinsic growth rate, K is the carrying capacity of the population, α is the parameter that measures the inhibitory effect, γ is the natural recovery rate of the infective individuals and μ_1 and μ_2 represent the per capita death rates of infectious and recovered, respectively.

Busenberg and Huang [19] studied a delayed Hutchinson population model with diffusion. The model is given by

$$
\frac{\partial u}{\partial t} = c\frac{\partial^2 u}{\partial x^2} + ku(t, x)\left(1 - u(t - \tau, x)\right), \tag{1.2.13}
$$

with initial data

$$
u(\theta, x) = \varphi(\theta, x), \; \theta \in [-\tau, 0]
$$

and homogeneous Dirichlet boundary conditions

$$
u(t, 0) = u(t, \pi) = 0,
$$

where $c > 0$ and $k > 0$ are constants.

So et al. [133] studied a delay diffusive version of the Nicolson's blowflies model. The model is given by

$$\frac{\partial u}{\partial t} = c\frac{\partial^2 u}{\partial x^2} - au(t,x) + bu(t-1,x)e^{-u(t-1,x)}, \qquad (1.2.14)$$

with initial data

$$u(\theta, x) = \varphi(\theta, x), \ \theta \in [-1, 0]$$

and homogeneous Dirichlet boundary conditions

$$u(t, 0) = u(t, \pi) = 0,$$

where $c > 0$, $k > 0$, $a > 0$ and $b > 0$ are constants.

Zhou et al. [151] considered a system of two delayed diffusive partial differential equations to describe the competition of two species $u(t,x)$ and $v(t,x)$ living in the same environment. The model is given by

$$\frac{\partial u}{\partial t}(t, x) = \frac{\partial^2 u}{\partial x^2}(t, x) + \kappa u(t, x)\left(1 - a_1 u(t - \tau, x) - b_1 v(t - \tau, x)\right), \quad (1.2.15\text{a})$$

$$\frac{\partial v}{\partial t}(t, x) = \frac{\partial^2 v}{\partial x^2}(t, x) + \kappa v(t, x)\left(1 - a_2 u(t - \tau, x) - b_2 v(t - \tau, x)\right), \quad (1.2.15\text{b})$$

where $0 < x < \pi$ and $t > 0$, subject to the initial data

$$u(t, x) = u^0(t, x), \quad v(t, x) = v^0(t, x), \quad t \in [-\tau, 0], \qquad (1.2.16)$$

and Dirichlet boundary conditions

$$u(t, 0) = u(t, \pi) = v(t, 0) = v(t, \pi) = 0, \ t \geq 0. \qquad (1.2.17)$$

On the other hand, Li et al. [86] considered also a system of two delayed diffusive partial differential equations to describe the dynamics (densities) of two cooperative species living in the same community, where the existence of each one enhances the growth of the other. Their model is given by

$$\frac{\partial u}{\partial t}(t, x) = \lambda_1 \frac{\partial^2 u}{\partial x^2}(t, x) + u(t, x)\left(r_1 - a_1 u(t - \tau, x) - b_1 v(t - \tau, x)\right), \quad (1.2.18a)$$

$$\frac{\partial v}{\partial t}(t, x) = \lambda_2 \frac{\partial^2 v}{\partial x^2}(t, x) + v(t, x)\left(r_2 - a_2 u(t - \tau, x) - b_2 v(t - \tau, x)\right), \quad (1.2.18b)$$

where $0 < x < \pi$ and $t > 0$, subject to the initial data

$$u(t, x) = u^0(t, x), \quad v(t, x) = v^0(t, x), \quad t \in [-\tau, 0] \qquad (1.2.19)$$

and Dirichlet boundary conditions

$$u(t, 0) = u(t, \pi) = v(t, 0) = v(t, \pi) = 0, \ t \geq 0. \qquad (1.2.20)$$

The constants $\lambda_1 > 0$ and $\lambda_2 > 0$ represent the diffusivity of the two species whereas $r_1 > 0$ and $r_2 > 0$ are the intrinsic growth rates of the two species.

Some other relevant models can be found in [2, 76, 110].

1.3 Literature review on some analytical and semi-numerical methods for solving DDEs

In this section we describe some of the well-known methods (analytical as well as semi numerical) for solving the delay differential equations.

Method of steps:

Consider a DDE of the form

$$\dot{y}(t) = f(t, y(t), y(t - \tau)), t \in [0, T],$$ (1.3.1)

$$y(\theta) = \varphi_0(\theta), \theta \in [-\tau, 0].$$ (1.3.2)

The basic idea behind the method of steps [9] is to transform the DDE model (1.3.1)-(1.3.2) to a sequence of a finite number of ODEs through dividing the domain of the DDE into sub-domains, in each of which the DDE is transformed into ODE. Then to solve these ODEs starting from the first sub-domain using the given history function (1.3.2). The solution in the first domain is used as a history for the next sub-domain, and this process is repeated until the domain of the DDE is covered.

We will assume that $T = K\tau$ for some positive integer K. Then the space $[0, T] = [0, K\tau]$ can be written as

$$[0, T] = \cup_{m=1}^{K} [(m - 1)\tau, m\tau].$$

In the sub-domain $[0, \tau]$, the DDE is transformed into an IVP of the form

$$\dot{y}(t) = f(t, y(t), \varphi_0(t - \tau)), \ t \in [0, \tau]$$ (1.3.3)

$$y(0) = \varphi_0(0).$$ (1.3.4)

Let $\varphi_1(t)$ be the solution of the IVP (1.3.3)-(1.3.4). Then in the domain $[\tau, 2\tau]$ the DDE model (1.3.1)-(1.3.2) is transformed into the IVP

$$\dot{y}(t) = f(t, y(t), \varphi_1(t - \tau)), \ t \in [\tau, 2\tau],$$ (1.3.5)

$$y(\tau) = \varphi_1(\tau),$$ (1.3.6)

which has a solution $\varphi_2(t)$.

Generally, in the sub-domain $[m\tau, (m+1)\tau]$ the DDE (1.3.1)-(1.3.2) is transformed into the IVP

$$
\begin{aligned}
\dot{y}(t) &= f(t, y(t), \varphi_{m-1}(t - \tau)),\ t \in [m\tau, (m+1)\tau], & (1.3.7) \\
y(m\tau) &= \varphi_{m-1}(m\tau), & (1.3.8)
\end{aligned}
$$

which has solution $\varphi_m(t)$.

The final solution $y(t)$ will be the union of the solutions $\varphi_m(t)$ for $m = 1, \ldots, K-1$.

Method of reduction:

The method of reduction leads to two types of problems. These are

- Reduction of DDE into PDE, and

- Reduction of DDE into a system of ODEs.

Below we describe each of these methods.

Reduction of DDE into PDE:

Consider a DDE of the form

$$
\begin{aligned}
\dot{x}(t) &= f(x(t), x(t - \tau)), t \in [0, T], & (1.3.9) \\
x(\theta) &= \varphi_0(\theta), \theta \in [-\tau, 0]. & (1.3.10)
\end{aligned}
$$

Define a function $u : [0, T] \times [-\tau, 0] \to \mathbb{R}$ as

$$
u(t, \theta) = x(t + \theta),\ t \in [0, T],\ \theta \in [-\tau, 0].
$$

Due to the symmetry of $x(t + \theta)$, it is clear that

$$
\frac{\partial u}{\partial t} = \frac{\partial u}{\partial \theta}.
$$

The function $u(t, \theta)$ satisfies

$$u(0, \theta) = x(\theta) = \varphi_0(\theta), \ \theta \in [-\tau, 0]$$

and

$$\frac{\partial u}{\partial \theta}(t, 0) = \frac{\partial u}{\partial t}(t, 0) = \dot{x}(t) = f(x(t), \varphi_0(-\tau)), \ t \in [0, T].$$

Thus solving the delay differential equation (1.3.9) with its initial data (1.3.10) is equivalent to solving the partial differential equation

$$\begin{aligned}
\frac{\partial u}{\partial t} &= \frac{\partial u}{\partial \theta}, \ t \in [0, T], \theta \in [-\tau, 0], \\
u(0, \theta) &= \varphi_0(\theta), \ \theta \in [-\tau, 0], \\
\frac{\partial u}{\partial \theta}(t, 0) &= f(x(t), \varphi_0(-\tau)), \ t \in [0, T].
\end{aligned}$$

Reduction of DDE into a system of ODEs:

Consider the delay differential equation

$$\begin{aligned}
\dot{x}(t) &= f(t, x(t), x(t - \tau)), \ t \in [0, T], & (1.3.11) \\
x(\theta) &= \varphi_0(\theta), \ \theta \in [-\tau, 0]. & (1.3.12)
\end{aligned}$$

Let N be a positive integer and $\delta = \tau/N$.

Define new variables $x_m(t)$, $m = 0, \dots, N$ by

$$x_m(t) = x(t - m\delta),$$

then $x_0(t) = x(t)$ and $x_N(t) = x(t - \tau)$.

Then

$$\dot{x}_m(t) \approx \frac{x_m(t + \delta) - x_m(t)}{\delta} = N \left(\frac{x_{m-1}(t) - x_m(t)}{\tau} \right).$$

This leads to the following system of ordinary differential equations

$$
\begin{aligned}
\dot{x}_0(t) &= f(t, x_0(t), x_N(t)),\ t \in [0, T] \\
\dot{x}_m(t) &= N\left(\frac{x_{m-1}(t) - x_m(t)}{\tau}\right),\ t \in [m\delta, T] \\
x_m(0) &= \varphi_0(-m\delta),\ m = 0, \ldots, N.
\end{aligned}
$$

By solving the above system, we obtain the solution of (1.3.11)-(1.3.12).

Method using Lambert W functions:

The Lambert W function ([30, 101]) (also referred as product log function) is the solution of the algebraic equation

$$we^w = z, \tag{1.3.13}$$

where w and z are two complex numbers. The Lambert W function has an infinite number of branches $W_m(z)$; $m = 0, \pm 1, \pm 2, \ldots$, where $W_0(z)$ is called the main branch, and hence, the algebraic equation (1.3.13) has an infinite number of solutions $W_m(z)$. This function has the property that it is symmetric with respect to the real axis. If $z = x$ is a real number, then the domain of the definition of $W(x)$ is restricted to $[-e^{-1}, \infty)$, with $W(-e^{-1}) = -1$, $W(0) = 0$ and $W(e) = 1$. Nowadays, this function is even available as an in-built function in many programming languages like Maple and Mathematica. In fact, Jarlebring stated in [70] that *"Because of its availability in software and the fair amount of applications, some argue that this (Lambert W) function should be added to the set of elementary mathematical functions"*.

The Lambert W function is related to a system of linear delay differential equations via its characteristic equation. The spectrum of a linear delay differential equation can be found through inverting the Lambert W function that gives the solution and then determine the stability of the system. Many authors used the Lambert functions for solving a system of linear delay differential equations [3, 4, 69].

To describe the procedure, let us consider the linear DDE

$$\dot{y}(t) \;=\; Ay(t) + By(t - \tau), t \in [0, T], \tag{1.3.14}$$

$$y(\theta) \;=\; \varphi_0(\theta), \; \theta \in [-\tau, 0], \tag{1.3.15}$$

where A and B are constants, and $\tau > 0$ is the delay parameter.

Plugging the solution

$$y(t) = e^{\lambda t}$$

in equation (1.3.14), we obtain the algebraic equation

$$e^{-\lambda \tau} = \frac{1}{B}\left(\lambda - A\right), \tag{1.3.16}$$

which has the solution

$$\lambda_m = A + \frac{W_m\left(B\tau e^{-A\tau}\right)}{\tau}, \; m = 0, \pm 1, \pm 2, \ldots,$$

where $W_m(x)$ are the branches of the Lambert W function.

The solution of (1.3.14) with the initial data (1.3.15) is given by

$$y(t) = \sum_{m=-\infty}^{\infty} c_m \exp\left(\left(A + \frac{W_m(B\tau e^{-A\tau})}{\tau}\right)t\right), \tag{1.3.17}$$

where the coefficients c_m, $m = 0, \pm 1, \ldots$ are to be computed in such a way that the function $y(t)$ is identical to the initial data $\varphi_0(t)$ on $[-\tau, 0]$.

Method of Laplace transformations:

The Laplace transform method ([10, 127]) provides an explicit expression of the solution and is a useful tool to study the spectral properties of a linear delay differential equation. It transforms the delay differential equation into an algebraic equation. The solution of the DDE is obtained by inverting the solution of the algebraic problem

using the inverse Laplace transformation ([36]). This approach for (1.3.14)-(1.3.15) is described as follows:

Taking the Laplace transformation on both sides of (1.3.14), we obtain
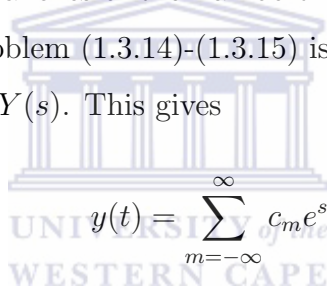
$$Y(s) = \frac{\varphi_0(0)e^{s\tau} + B \int_{-1}^{0} \varphi_0(t)e^{-st}dt}{(s-A)e^{s\tau} - B}.$$

The poles of the function $Y(s)$ are given by

$$s_m = A + \frac{W_m(B\tau e^{-A\tau})}{\tau}, \ m = 0, \pm 1, \pm 2, \ldots,$$

where the W_m's are the branches of the Lambert function.

The solution of the problem (1.3.14)-(1.3.15) is obtained by inverting the transformation using the poles of $Y(s)$. This gives

$$y(t) = \sum_{m=-\infty}^{\infty} c_m e^{s_m t}.$$

1.4   Some numerical methods and softwares for solving DDEs

Solutions of delay differential equations using Runge-Kutta methods ([21]) covers a larger class of numerical methods that are developed for solving DDEs. Such works include [9, 54, 64, 65, 75, 138].

Let us consider the following DDE

$$\dot{x}(t) = f(t, x(t), x(t-\tau)), \forall t \in [0, T],$$
$$x(\theta) = \varphi_0(\theta), \ \theta \in [-\tau, 0],$$

where $T \in \mathbb{R}^+$, $x \in \mathbb{R}$ and τ is the delay parameter. The functions

$$f : \mathbb{R}^3 \to \mathbb{R}$$

and

$$\varphi^0 : [-\tau, 0) \to \mathbb{R}$$

are continuous.

If the time space $[0, T]$ is partitioned into N subintervals through the points

$$t_0 = 0 < t_1 < \ldots < t_N = T,$$

with $h_{n+1} = t_{n+1} - t_n$, $n = 0, \ldots, N-1$, then a general s-stage continuous Runge-Kutta method for solving the above problem is given by ([9])

$$\eta(t_n + \theta h_{n+1}) = x_n + h_{n+1} \sum_{m=1}^{s} b_m(\theta) f\left(t_{n+1}, X_{n+1}^m, \eta\left(t_{n+1}^m - \tau\right)\right), \; \theta \in [0, 1], \quad (1.4.1)$$

where

$$X_{n+1}^m = x_n + h_{n+1} \sum_{\ell=1}^{s} a_{m,\ell} f\left(t_{n+1}^\ell, X_{n+1}^\ell, \eta\left(t_{n+1}^\ell - \tau\right)\right), \; m = 1, \ldots, s. \quad (1.4.2)$$

If the step-size h_{n+1} is less than τ, then $\eta(t_{n+1}^m - \tau)$ is known for all $m = 1, \ldots, s$.

Gugleilmi et al. [51] implemented RADAR5 which is based on Radau IIA ([55]) for solving stiff delay differential equations. They considered the problem

$$
\begin{aligned}
M\dot{y}(t) &= f(t, y(t), y(t - \alpha_1(t, y(t))), \ldots, y(t - \alpha_m(t, y(t)))), \\
y(t_0) &= y_0, \; y(t) = g(t), \; t < t_0,
\end{aligned}
$$

where $M \in \mathbb{R}^{d \times d}$, $y(t) \in \mathbb{R}^d$ and $\alpha_m(t, y(t)) < t$ for all $m = 1, \ldots, d$.

The application of the method based on Radau IIA leads to the approximation

$y_n \approx y(t_n)$ by solving the linear system

$$M\left(Y_m^{(n)} - y_n\right) = h_n \sum_{\ell=1}^{s} a_{m,\ell} f\left(Y_\ell^{(n)}, Z_\ell^{(n)}\right), y_{n+1} = Y_s^{(n)},$$

where $Z_m^{(n)}$, that approximates $y\left(\alpha_m^{(n)}\right) = y\left(\alpha\left(t_n + c_m h_n, Y_m^{(n)}\right)\right)$, is given by

$$Z_m^{(n)} = \begin{cases} g(\alpha_m^{(n)}), & \alpha_m^{(n)} < t_0 \\ \\ \varphi_k(\alpha_m^{(n)}), & \alpha_m^{(n)} \in [t_k, t_{k+1}]. \end{cases}$$

In the above, $\varphi_k(t)$ is a polynomial approximation of the solution $y(t)$ in $[t_k, t_{k+1}]$. It is a polynomial of degree s, that passes through the values y_k and $Y_\ell^{(k)}$ for all $\ell = 1, \dots, s$.

Explicit continuous Runge-Kutta methods can be obtained by replacing equation (1.4.2) by the equation

$$X_{n+1}^m = x_n + h_{n+1} \sum_{\ell=1}^{m-1} a_{m,\ell} f\left(t_{n+1}^\ell, X_{n+1}^\ell, \eta\left(t_{n+1}^\ell - \tau\right)\right), \ m = 1, \dots, s. \qquad (1.4.3)$$

Explicit Runge-Kutta methods have been used by several authors for solving delay differential equations. Some of the works in which the explicit continuous Runge-Kutta methods are used for delay differential equations include Shampine and Thompson [130, 131] and Paul [120].

In [130], Shampine and Thompson described the implementation of a delay differential equations solver using s-stages explicit Runge-Kutta triplet given by the equations

$$x_{n+1} = x_n + h_{n+1} \sum_{m=1}^{s} b_m f\left(t_n + m h_n, X_n^m, \varphi\left(t_n + c_m h_n - \tau\right)\right), \ \theta \in [0, 1],$$

where

$$X_n^m = x_n + h_{n+1} \sum_{\ell=1}^{s} a_{m,\ell} f\left(t_n + c_\ell h_n, X_n^\ell, \varphi\left(t_n + c_\ell h_n - \tau\right)\right), \ m = 1, \dots, s,$$

and

$$x_{n+\sigma} = x_n + h_{n+1} \sum_{m=1}^{s} b_m(\sigma) f(t_n + m h_n, X_n^m, \varphi(t_n + c_m h_n - \tau)), \ \theta \in [0,1],$$

which approximates $y(t_n + \sigma h_n), \ \sigma \in [0,1]$.

In [95], Mahmoud studied the existence, uniqueness, stability and convergence of a class of C^2-spline collocation methods for solving delay differential equations.

On the other hand, linear multi-step methods have also been used for solving delay differential equations.

Gan et al. [46] discussed error analysis of linear multistep methods and Runge-Kutta methods applied to the following classes of one-parameter stiff singularly perturbed problems with delays. The problem they considered is given by

$$\dot{x}(t) = f(t, x(t), x(t-\tau), y(t), y(t-\tau)),$$
$$\varepsilon \dot{y}(t) = g(t, x(t), x(t-\tau), y(t), y(t-\tau)).$$

Huang [60] studied the stability of the linear multistep method for the nonlinear delay differential equations:

$$\dot{x}(t) = f(t, x(t), x(t-\tau)), \ t > 0$$
$$x(t) = \varphi(t), \ t \in [-\tau, 0].$$

Verhyden et al. [141] considered the following system of linear DDEs with multiple time delays

$$\dot{y}(t) = A_0 y(t) + \sum_{j=1}^{m} A_j y(t-\tau_j), \ y(t) \in \mathbb{R}^n,$$

where $A_0, A_j \in \mathbb{R}^{n \times n}$ and $\tau_j > 0$ for $j = 1, \ldots, m$. Their aim was to find an efficient computational technique for the roots of the characteristic equation of the system, so

that the stability of the system could be determined. Their approach was based on the discretization of the integration operator by a linear multi-step method.

The characteristic equation of the linear system above is given by

$$\det(\lambda I - A_0 - \sum_{j=1}^{m} A_j e^{-\lambda \tau_j}) = 0.$$

Based on the fact that only a finite number of roots of the above characteristic equation lie on the right half of the complex plane, their problem was reduced to compute the rightmost root.

Letting h denote the length of one time step, y_m denote the value $y(mh)$, $L_j = \lceil \tau/h \rceil$ (where $\lceil x \rceil$ means the ceil number of x) and $\epsilon_j = L_j - \tau/h$, they approximated the delayed terms $y(t - \tau_j)$ at $t = t_i$ using Lagrange interpolating polynomials as

$$y(t_i - \tau_j) \approx \sum_{\ell=-s_1}^{s_2} \psi_\ell(\epsilon_j) y_{i+\ell-L_j},$$

where

$$\psi_\ell(\epsilon_j) \equiv \sum_{\sigma=-s_1}^{s_2} \frac{\epsilon_j - \sigma}{\ell - \sigma}.$$

Then their multi-step method is given by

$$\sum_{i=0}^{k} \alpha_i y_i = h \sum_{i=0}^{k} \beta_i \left(A_0 y_i + \sum_{j=1}^{m} A_j \sum_{\ell=-s_1}^{s_2} \psi_\ell(\epsilon_j) y_{i+\ell-L_j} \right),$$

where α_i and β_i are the coefficients of the linear multi-step method, s_2 is an integer such that $h \leq \tau_{min}/s_2$ and s_1 is such that $s_1 \leq s_2 \leq s_1 + 2$.

Hu et al. [59] used A-stable multi-step method for computing the numerical solution of the following neutral delay differential equation:

$$\dot{y}(t) = f(t, y(t), y(t - \tau), \dot{y}(t - \tau)), \quad t > 0$$
$$y(\theta) = \varphi(\theta), \quad \theta \in [-\tau, 0).$$

Ito et al. [66], constructed a spectral method to solve a linear system of delay differential equations:

$$\dot{x}(t) = A_0 x(t) + A_1 x(t - \tau) + f(t), \ \ t > 0$$
$$x(0) = \eta, \ x(\theta) = \varphi_0(\theta), \ \ \theta \in [-\tau, 0).$$

Their idea was to expand the solution in each delay interval $[(m - 1)\tau, m\tau]$ using a truncated Legendre series. Similarly, the functions $\varphi_0(t)$ and $f(t)$ are expanded using the truncated Legendre series. A last condition to complete the set of conditions required for a unique solution is borrowed from the τ-method ([45]).

Mead and Zubik-Kowal [98] used pseudospectral methods ([45]) based on Chebyshev pseudospectral spatial discretization and Jacobi waveform relaxation methods for time integration for solving a delay parabolic partial differential equation

$$\frac{\partial u}{\partial t} = \varepsilon \frac{\partial^2 u}{\partial x^2} + c \frac{\partial u}{\partial x} + g(x, u_{(x,t)}),$$
$$u(x, t) = f_0(x, t), \ \ t \in [-\tau, 0], -L \le x \le L,$$

where $\varepsilon \ge 0$, $c \in \mathbb{R}$, $\tau_0 \ge 0$, $L > 0$ and $T > 0$. The function $u_{(x,t)}$ is given by

$$u_{(x,t)}(\tau) = u(x, t + \tau), \ \ \tau \in [-\tau_0, 0].$$

When $\varepsilon > 0$, the problem becomes parabolic and in this case the boundary conditions are given by

$$u(\pm L, t) = f^{\pm}(t), \ \ t \in [0, T],$$

whereas when $\varepsilon = 0$ and $c \ne 0$, we have a hyperbolic problem and the boundary

conditions in this case are given by

$$
\begin{aligned}
u(L,t) &= f^+ \quad (\text{if } c > 0), \\
u(-L,t) &= f^- \quad (\text{if } c < 0),
\end{aligned}
$$

where f_0, $f^\pm$ are given.

In [67], Jackiwicz and Zubik-Kowal considered the use of Chebyshev spectral collocation and waveform relaxation methods for nonlinear delay partial differential equations:

$$
\begin{aligned}
\frac{\partial u}{\partial t} &= \varepsilon \frac{\partial^2 u}{\partial x^2} + u(x,t)(1 - u(x, t - \tau)) + f(x,t), \quad L \le x \le R, \quad t \ge 0, \\
u(x,t) &= g(x,t), \quad t \in [-\tau, 0], \quad L \le x \le R, \\
u(-1,t) &= \alpha(t), \quad t \ge 0, \\
u(1,t) &= \beta(t), \quad t \ge 0.
\end{aligned}
$$

Ansari et al. [1] developed a fitted mesh finite difference method for solving a singularly perturbed parabolic partial differential equation. The method uses a Shishkin mesh on the spatial space, whereas it uses a uniform mesh for the temporal space. The problem they considered is given by:

$$
\frac{\partial u(t,x)}{\partial t} - \varepsilon \frac{\partial^2 u(t,x)}{\partial x^2} + a(t,x)u(t,x) = f(t,x) - b(x)u(t - \tau, x),
$$

$$
(t,x) \in \overline{\Omega} \equiv [0,T] \times [0,1],
$$

with the initial data

$$
u(t,x) = u_0(t,x), \quad (t,x) \in [-\tau, 0] \times [0,1],
$$

and boundary conditions

$$u(t, x) = g_L(t), (t, x) \in [0, T] \times \{0\},$$

and

$$u(t, x) = g_R(t), (t, x) \in [0, T] \times \{1\}.$$

Besides the above-mentioned numerical methods, many of the existing software for solving delay differential equations are based on Runge-Kutta methods, see for example Corwin et al. [27], Paul [120], Shampine and Thompson [130], Shampine [131] and Thompson and Shampine [139].

Some of the other software packages for solving delay differential equations are the following:

Corwin et al. [27] developed the FORTRAN code *DKLAG6* which is based on embedded continuously fifth- and sixth-order Runge-Kutta methods.

The FORTRAN code *Archi* was developed by Paul [120] and is based on the fifth-order Dormand and Prince explicit Runge-Kutta method with a fifth-order Hermite interpolant.

Later on, Shampine and Thompson [130] developed the MATLAB routine *dde23* which is used for solving DDEs with fixed time delays. It uses the explicit Runge-Kutta method with Hermite interpolants.

Guglielmi et al. [51] developed the FORTRAN code *RADAR5* for solving stiff delay differential equations with a set of state dependent delays. The code is based on a Radau IIA method.

In 2005, Shampine [131] developed the MATLAB routine *ddesd* which is used for solving DDEs with variable time delays. This also uses the explicit Runge-Kutta methods with variable step-sizes and cubic Hermite interpolation.

Subsequent to this, Thompson and Shampine [139] developed the FORTRAN 90 code *dde_solver*. It is based on one of the earlier FORTRAN 77 codes developed by Thompson and his co-workers and is as convenient as the MATLAB dde23/ddesd

routines are.

Some other relevant softwares to solve DDEs can be found in Bocharov and Romanyukha [17], Enright and Hayashi [39], Karoui and Vaillancourt [75] and Paul [121]. Other works that may be useful for further studies in this area are [6, 8, 12, 16, 22, 26, 28, 37, 38, 40, 42, 44, 49, 50, 56, 71, 80, 89, 90, 92, 100, 109, 119, 126, 134, 135].

1.5   Summary of the thesis

We have organized the rest of this thesis as follows.

In Chapter 2, we develop fitted numerical methods for solving a single delay differential equation and a system of two delay differential equations. These methods preserve the positivity of the solution components, are convergent of first-order and are stable. Some numerical examples are considered to show the performance of these methods. Comparative numerical results show that our methods perform better than the classical fourth-order Runge-Kutta method.

In Chapter 3, we design and analyze fitted numerical method for solving a two-point BVP for a class of singularly perturbed second-order delay differential equations with a small time delay. Numerical results obtained by this method are compared with those found in literature.

Singularly perturbed delay parabolic partial differential equation (SPDPPDE) are considered in Chapter 4. Based on the method of steps, we derive formulas for the bounds on the solution and its partial derivatives. Then, we develop two fitted numerical methods for solving the SPDPPDE. The first one is a fitted mesh finite difference method, whereas the second one is a fitted operator finite difference method. We prove that the two methods are convergent and unconditionally stable. Numerical results are shown to confirm the theoretical estimates.

Ideas developed in Chapter 4 are extended in Chapter 5 where we develop a fitted numerical method for solving a system of two delay parabolic partial differential equations, describing the dynamics of two co-operative species. The proposed method

is convergent and unconditionally stable. Test examples are used to show the performance of the method and the results are compared with others found in the literature. A system of two delay parabolic partial differential equations, describing the dynamics of two competitive species is solved in Chapter 6.

Finally, in Chapter 7, we provide some concluding remarks and discuss the scope for the future research.

Chapter 2

Fitted Numerical Methods for a System of First Order Delay Differential Equations
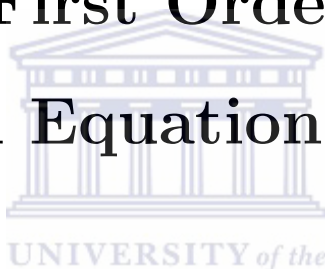
In this chapter, we design some positivity preserving methods (PPMs) to solve two delay differential equation models. We prove the stability of these methods and also show that they are convergent with order one. Three test examples have been used to confirm the efficiency of the method. Comparisons are also made with the classical fourth-order Runge-Kutta method and we found that our methods perform better than it.

2.1   Introduction

Systems of first-order delay differential equations have been used to describe many biological systems. In this chapter, our goal is to consider some population models that fall under this category. There are some analytical investigations available in the literature about these models, however, due to the fact that the state variables (such variables usually describe densities, concentrations, populations sizes, etc.) must be non-negative functions, many of the numerical methods, in particular, the standard fi-

nite difference methods are found to be inappropriate. The reason being the occurrence
of erroneous solutions in the transient states. This has motivated us to construct the
fitted numerical methods that preserve the positivity of the solutions of such biological
systems.

Positivity preserving methods (PPMs) have been used by many authors for the
solutions of ordinary or systems of ordinary differential equations that are modelling
biological systems (see, e.g., [52, 103, 104, 105]). These PPMs are based on the con-
cept of non-local discrete representations of nonlinear terms ([102]), and can give high
stability properties. However, for the biological systems described by delay differential
equations, such PPMs are not yet exploited. Hence, our purpose in this chapter is to
design PPMs with high stability properties that can solve delay differential equation
models describing the dynamics of some biological systems.

We consider two models whose dynamics are described by a single delay differential
equation and a system of two delay differential equations, respectively. The first system
is due to Cooke et al. [29] and describes the dynamics of a mature population, whereas
the second model is due to Pujo-Menjouet et al. [99] and describes the dynamics of
periodic chronic myelogenous leukemia (PCML). Further details on these two models
are provided in subsequent sections.

The rest of this chapter is organized as follows. In Section 2.2, we state the two
models and give their biological interpretations. In Section 2.3, we discuss the quali-
tative behaviour of the solutions of these models. Then, we describe the construction
of the fitted methods in Section 2.4 and analyze them for convergence in Section 2.5.
In Section 2.6, we show the performance of these methods. These results are further
discussed in Section 2.7.

2.2   The DDE models

In this section, we consider two delay differential equation models. The first model
is a single delay differential equation model considered by Cooke et al. in [29]. In

this model, it is assumed that the total population is divided into two groups: mature
and immature sub-populations. The model describes the dynamics of the mature
population only. The second model is a system of two delay differential equations
considered by Pujo-Menjouet and Mackey in [99]. It describes the dynamics of periodic
chronic myelogenous leukemia (PCML).

2.2.1 Population model with maturation delay and nonlinear birth

Cooke et al. [29] considered a population in which an individual follows m life stages
$S_j : \ j = 1, \ldots, m$ after its birth before it becomes mature. The length of each life stage
S_j is τ_j; hence, an individual spends a life time $\tau = \tau_1 + \ldots + \tau_m$ before it becomes
mature and able to produce new members. The death rate in each stage S_j before
maturation is d_j. They assumed that the individuals in the different stages before
the maturation are dying with equal death rate, that is $d_j = d_1$ for $j = 2, \ldots, m$.
Therefore, d_1 gives the death rate in the immature population. The death rate in the
mature population was considered as d. They also assumed that the birth rate in the
population is proportional to the number of the mature individuals and the individuals
in the population become mature with a rate of $B(N(t - \tau))$, where the function B
is termed as the *birth rate function* and is assumed to be nonlinear in the size of the
mature population $N(t - \tau)$. Then, the model that they considered is

$$\dot{N}(t) = B(N(t - \tau))N(t - \tau)e^{-d_1\tau} - dN(t), t \in [0, T], \qquad (2.2.1a)$$

with initial data

$$N(t) = \varphi_0(t), \text{ for } t \leq 0. \qquad (2.2.1b)$$

Equation (2.2.1a) governs the growth of the adult population. The first term
$B(N(t - \tau))N(t - \tau)$ in equation (2.2.1a) gives the number of newly born individuals in the population whereas the second term $dN(t)$ gives the ratio of the mature

population individuals from which dies every day.

The birth rate function $B(N(t))$ is assumed to satisfy the following conditions

$$B(N) > 0, \tag{2.2.2}$$

$$B(N) \text{ is continuously differentiable with } \dot{B}(N) < 0 \text{ and} \tag{2.2.3}$$

$$B(0^+) > d > B(\infty). \tag{2.2.4}$$

The conditions (2.2.3) and (2.2.4) guarantee the existence of $B^{-1}(t)$ for all $B(\infty) < t < B(0^+)$.

Cooke et al. [29] considered three different formulas for the birth function $B(N(t))$

$$B(N(t)) = B_1(N(t)) = be^{-aN(t)} \tag{2.2.5}$$

$$B(N(t)) = B_2(N(t)) = \frac{p}{q + N^n(t)}, \ p, q \text{ with } n > 0, \text{ and } \frac{p}{q} > d, \tag{2.2.6}$$

$$B(N(t)) = B_3(N(t)) = \frac{A}{N(t)} + c, \text{ with } A > 0 \text{ and } d > c > 0. \tag{2.2.7}$$

It should be noted that the model (2.2.1) with $B(N(t)) = B_1(N(t))$ has been considered in [33, 72, 112].

2.2.2 Periodic chronic myelogenous leukemia (PCML)

Chronic myelogenous leukemia (CML) is a cancer of the blood cells in which too many white blood cells are made in the bone marrow. CML is characterized by the existence of what is known as Philadelphia chromosome. The Philadelphia chromosome contains the abnormal fused gene BCR-ABL which causes the production of abnormal bcr-abl tyrosine kinase [31] that transforms the bone marrow cells into abnormal leukemic cells. The BCR-ABL fusion gene is found in over 95% of patients with CML [63]. According to Mackey et al. ([93]) and Menjouet and Mackey ([99]), it has been noticed that (in rare cases) chronic myelogenous leukemia behaves in periodic fashion. That is, white blood cells, platelets and erythrocytes all oscillate with the same period. They referred

to this case as the *periodic chronic myelogenous leukemia* (PCML).

To study the regulation of dynamics of the PCML, Pujo-Menjouet and Mackey considered a stem cell model

$$\dot{P}(t) = -\gamma P(t) + \beta(N(t))N(t) - e^{-\gamma \tau}\beta(N(t-\tau))N(t-\tau), \qquad (2.2.8a)$$

$$\dot{N}(t) = -(\beta(N(t)) + \delta)N(t) + 2e^{-\gamma \tau}\beta(N(t-\tau))N(t-\tau), \qquad (2.2.8b)$$

subject to the initial data

$$N(t) = \vartheta_0(t), \qquad (2.2.8c)$$

and the initial condition

$$P(0) = P_0. \qquad (2.2.8d)$$

In the above model, the cells are partitioned according to their functions into one of two phases: the proliferating phase (called Mitosis) and the resting phase G_0 (called interphase) ([41]). A cell in the proliferating phase undergoes cell division, giving two daughter cells. The newly born cells immediately enter the resting phase, in which they cannot divide but undergo their functions and prepare themselves for mitosis.

As far as the notations and individual terms used in the above model are concerned, the densities of the proliferating and resting cells are denoted by $P(t)$ and $N(t)$, respectively. Cells entering the proliferating phase either die with a rate γ or divide at time τ after the entry. The fraction of surviving cells about to leave the proliferating phase at a time τ earlier are given by the term $e^{-\gamma \tau}\beta(N_\tau)N_\tau$ in equation (2.2.8a), whereas the daughter cells which enter the resting phase are given by the term $2e^{-\gamma \tau}\beta(N_\tau)N_\tau$ in equation (2.2.8b). The function $\beta(N) = \beta_0\theta^n/(\theta^n + N^n(t))$ represents the mitotic re-entry rate from the resting phase into the proliferation phase with a maximal rate β_0 and θ is the size of the population of resting cells at which the rate of cell movement from the resting phase G_0 into the proliferation phase is half of its maximal value β_0.

The parameter n is a positive real number that controls the sensitivity of the mitotic re-entry rate (denoted by β) to changes in the size of G_0.

In the next section, we discuss qualitative behaviours of the above two models.

2.3   Some qualitative properties

2.3.1   Qualitative properties for the population model with maturation delay and nonlinear birth

Model (2.2.1) has a unique positive equilibrium $N^* = B^{-1}(de^{d_1\tau})$.

By considering

$$B(0^+) > de^{d_1\tau} > B(\infty), \tag{2.3.1}$$

instead of (2.2.4), Cooke et al. [29] showed that this positive equilibrium is asymptotically stable if the conditions (2.2.2) and (2.2.3)

$$\frac{dB(N)N}{dt} > 0, \tag{2.3.2}$$

hold.

For the particular case when $B(N) = B_2(N) = p/(q + N^n)$ with $p/q > de^{d_1\tau}$, $0 \le n \le 1$ or $B(N) = B_3(N) = A/N + c$ with $c \le de^{-d_1\tau}$ and positive initial functions, the unique positive equilibrium $N^* = B^{-1}(de^{d_1\tau})$ is globally asymptotically stable for all $\tau \ge 0$. They showed that if $B(N)$ satisfies the conditions (2.2.2), (2.2.3) and (2.3.1) but not the condition (2.3.2), then the dynamics of (2.2.1) is different from the one obtained by letting $\tau = 0$.

On the other hand, in the case when $B(N) = B_1(N) \left(= be^{-aN}\right)$ satisfies the conditions (2.2.2), (2.2.3) and (2.3.1) together with the conditions $a > 0$, $b > de^{d_1\tau}$ and if the initial data are positive, then it the following has been proved.

1. If $b/d < e^{k^*+1}$, then the unique positive equilibrium $N^* = (1/a)\ln b/(de^{d_1\tau})$ is

locally asymptotically stable independent of τ, where k^* is the solution of the system

$$\sin w = -\cos w \left(\frac{d_1}{d} w \cos w + k^* \sin w \right),$$

$$\frac{\sin w - w \cos w}{w - \sin w \cos w} = 2 \frac{w d_1 \cos w}{d \sin w} + k^*.$$

2. If $b/d > e^{k^*+1}$, then there exists $0 < \tau^* < \tau^{**}$ such that N^* loses its stability when τ increases to pass through τ^*, and stabilizes when τ increases further and pass through τ^{**}.

The critical delays τ^* and τ^{**} are defined by

$$\tau^* = \frac{x_1}{d} \text{ and } \tau^{**} = \frac{x_2}{d},$$

where x_1 and x_2 with $x_1 < x_2$ are the two positive solutions of the equations

$$\begin{cases} x = -\frac{v}{\tan v}, \\ \frac{v}{\sin v} = x \left(\ln \frac{b}{de} - \frac{d_1}{d} x \right). \end{cases}$$

3. For small $0 \le \tau < \tau_0$ where $\tau_0 = \min \left\{ \frac{1}{d_1} \ln \frac{b}{d}, \tau', \tau'' \right\}$, the equilibrium N^* is globally asymptotically stable, where τ' and τ'' are defined by

$$\tau' = \max \left\{ \tau \ge 0 : \tau e^{(d-d_1)\tau} \le \frac{e}{b} \right\}$$

$$\tau'' = \begin{cases} \infty, & \text{if } \frac{b}{d} < e^{k^*+1}, \\ \tau^*, & \text{if } \frac{b}{d} < e^{k^*+1}. \end{cases}$$

4. If $d + b/e^2 < d_1$, then N^* is globally asymptotically stable for all

$$\tau < \min \left\{ \left(\frac{1}{d_1} \right) \ln \left(\frac{b}{d} \right), \tau'' \right\}.$$

For the special case when $d_1 = 0$ with $a > 0$ and $b > d$ and initial values are positive, it has been proven that

1. If $b/d \leq e^2$, then $N^* = (1/a) \ln(b/d)$ is locally asymptotically stable, independent of τ.

2. If $b/d > e^2$, then there exists a $\tilde{\tau} > 0$ such that Hopf bifurcation occurs when τ increases through $\tilde{\tau}$.

3. For small $0 \leq \tau < \tau_0 = \min\{\tau', \tau''\}$, the equilibrium N^* is globally asymptotically stable.

2.3.2 Qualitative properties for the PCML model

The steady-state solution for the PCML model satisfies
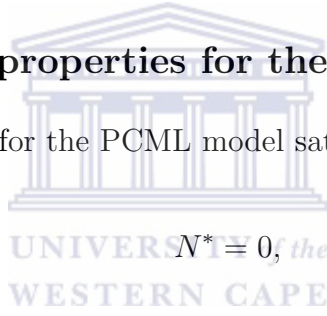
$$N^* = 0,$$

or

$$N^* = \beta^{-1}\left(\frac{\delta}{2e^{-\gamma\tau} - 1}\right) = \theta\left(\frac{\beta_0}{\beta^*} - 1\right)^{1/n},$$

where $\beta^* = \delta/(2e^{-\gamma\tau} - 1)$, and the steady-state re-entry rate can be positive only if the delay τ satisfies the inequality $0 \leq \tau \leq (1/\gamma)\ln 2$.

The non-trivial steady-state exists if $\tau \geq 0$ satisfies

$$\frac{\beta_0}{\beta^*} \geq 1 \Rightarrow \tau \leq -\frac{1}{\gamma}\ln\left(\frac{\delta + \beta_0}{2\beta_0}\right) = \tau_{max},$$

with $\delta < \beta_0$.

To determine the stability of the model, Pujo-Menjouet and Mackey ([99]) used the normalized variable $x = N/\theta$, and transformed the equation (2.2.8b) to

$$\dot{x}(t) = -(\beta(x) + \delta)x + \kappa\beta(x_\tau)x_\tau \qquad (2.3.3)$$

which has the steady-state solutions

$$x^* = 0$$
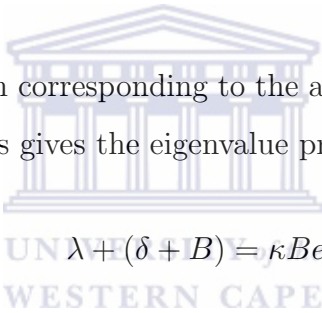
and

$$x^* = (\beta_0/\beta^* - 1)^{1/n}.$$

Linearizing equation (2.3.3) around x^*, letting $z = x - x^*$ and $B = B^* + B^{*\prime}x^*$, one
obtains the linear delay differential equation

$$\dot{z}(t) = -(B + \delta)z(t) + \kappa B z(t - \tau). \tag{2.3.4}$$

The characteristic equation corresponding to the above DDE is obtained by substitut-
ing $z = e^{\lambda\tau}$ into 2.3.4. This gives the eigenvalue problem

$$\lambda + (\delta + B) = \kappa B e^{-\lambda\tau}. \tag{2.3.5}$$

In summary:

1. if $n \in [0,1]$, then the solution is locally stable for $0 \le \tau \le \tau_{max}$,

2. if $n > 1$, then there are two subcases

    (a) if $n\delta/(n-1) \ge \beta_0$, then the solutions are locally stable for $\tau \in [0, \tau_{max}]$,

    (b) if $0 \le n\delta/(n-1) < \beta_0$ and let

$$\tau_n = -(1/\gamma) \ln \left((\delta/\beta_0)(1 + 1/(n-1)) + 1 \right)/2,$$

    then,

    i. the solution is stable iff

$$-1 \le \frac{\delta + B}{\kappa B} \le 1$$

and

$$\tau < \tau_{crit} = \frac{\cos^{-1}\left(\frac{\delta+B}{\kappa B}\right)}{\sqrt{(\kappa B)^2 - (\delta+B)^2}},$$

provided that $\tau \in [0, \tau_{max}]$, and

ii. if $0 \leq n\delta/(n-1) < \beta_0$, then the solutions are locally stable for $\tau \in [\tau_n, \tau_{max}]$.

Some of these properties will be verified by the numerical methods developed in the next section.

2.4   Construction of the numerical method

In this section we construct the numerical methods for solving the models described in Section 2.2. There are various ways to go towards designing the fitted methods for these models. However our goal is to design some positivity preserving numerical methods and therefore we put more emphasis on how to tackle the nonlinear terms in the individual models rather than looking at the particular denominator functions. We will use the nonlocal approximation (see, [102] and [52, 114] for details) for certain terms in these differential models.

To begin with, let M be a positive integer and partition the interval $[0, T]$ through the points

$$t_0 = 0 < t_1 < \ldots < t_M,$$

where $t_{j+1} - t_j = k = T/M; \; j = 0, \ldots, M-1$.

2.4.1   Numerical method for the population model with maturation delay and nonlinear birth

We approximate the model given by (2.2.1) with the difference method

$$\frac{N^{j+1} - N^j}{k} = -dN^{j+1} + B(N(t_j - \tau))N(t_j - \tau). \tag{2.4.1}$$

The difference scheme (2.4.1) can be further simplified to

$$N^{j+1} = \frac{N^j + kB(N(t_j - \tau))N(t_j - \tau)}{1 + kd}, \; j = 0, \ldots, M - 1. \tag{2.4.2}$$

Let $s = \tau/k$, be a positive integer.

For $j = 0, \ldots, s$, the history term $N(t_j - \tau)$ can be evaluated from the expression

$$N(t_j - \tau) = \varphi_0(t_j - \tau), \; \text{for } j \leq s,$$

and the difference scheme (2.4.2) becomes

$$N^{j+1} = \frac{N^j + kB(\varphi_0(t_j - \tau))\varphi_0(t_j - \tau)}{1 + kd}, \; j = 0, \ldots, s. \tag{2.4.3}$$

Now, the data
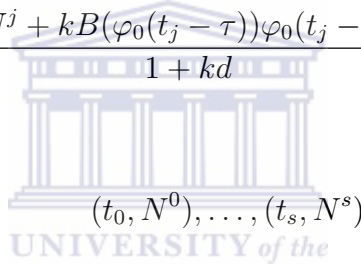
$$(t_0, N^0), \ldots, (t_s, N^s)$$

are interpolated with a cubic Hermite spline function ([128]) $\varphi^s(t)$.

For $j = s + 1, \ldots, M - 1$, when we move from t_j to t_{j+1}, the history term $N(t_j - \tau)$ is evaluated from the relation

$$N(t_j - \tau) = \varphi^j(t_j - \tau), \; \text{for } j \leq s + 1, \ldots, M - 1$$

and we evolve the solution to the point t_{j+1} using the difference scheme

$$N^{j+1} = \frac{N^j + kB(\varphi^j(t_j - \tau))\varphi^j(t_j - \tau)}{1 + kd}, \; j = s + 1, \ldots, M - 1 \tag{2.4.4}$$

and then we extend the definition of $\varphi^j(t)$ to the interval $[t_j, t_{j+1}]$ leading to a cubic Hermite spline $\varphi^{j+1}(t)$ that interpolates the data

$$(t_0, N^0), \ldots, (t_{j+1}, N^{j+1}).$$

Our finite difference method for the population model with nonlinear birth and
maturation delay is then consisting of equations (2.4.3) and (2.4.4) together with the
initial data (2.2.1b).

2.4.2 Numerical method for the PCML model

We approximate equations (2.2.8a) and (2.2.8b) with the difference method

$$\frac{P^{j+1} - P^j}{k} = -\gamma P^{j+1} + \beta(N^j)N^j - e^{-\gamma\tau}\beta(N(t_j - \tau))N(t_j - \tau), \quad (2.4.5)$$

$$\frac{N^{j+1} - N^j}{k} = -(\beta(N^j) + \delta)N^{j+1} + 2e^{-\gamma\tau}\beta(N(t_j - \tau))N(t_j - \tau). \quad (2.4.6)$$

Simplifying the above, we obtain,

$$P^{j+1} = \frac{P^j + k(\beta(N^j)N^j - e^{-\gamma\tau}\beta(N(t_j - \tau))N(t_j - \tau))}{1 + k\gamma},$$

$$N^{j+1} = \frac{N^j + k(2e^{-\gamma\tau}\beta(N(t_j - \tau))N(t_j - \tau))}{1 + k(\beta(N^j) + \delta)}.$$

On the interval $[0, \tau]$ the history term $N(t_j - \tau)$ can be evaluated from the history
function $\vartheta_0(t)$ as

$$N(t_j - \tau) = \vartheta_0(t_j - \tau),$$

and therefore, the difference method becomes

$$P^{j+1} = \frac{P^j + k(\beta(N^j)N^j - e^{-\gamma\tau}\beta(\vartheta_0(t_j - \tau))\vartheta_0(t_j - \tau))}{1 + k\gamma}, \quad (2.4.7)$$

$$N^{j+1} = \frac{N^j + k(2e^{-\gamma\tau}\beta(\vartheta_0(t_j - \tau))\vartheta_0(t_j - \tau))}{1 + k(\beta(N^j) + \delta)}, \quad (2.4.8)$$

for $j = 0, \ldots, s$.

Let $\vartheta^s(t)$ be the cubic Hermite spline that interpolates the data

$$(t_0, N^0), \ldots, (t_s, N^s).$$

For $j = s + 1, \ldots, M - 1$, when we move from t_j to t_{j+1}, we approximate the delayed term $N(t_j - \tau)$ using the cubic Hermite polynomial $\vartheta^j(t)$; that is $N(t_j - \tau) = \vartheta^j(t_j - \tau)$. Then, P^{j+1} and N^{j+1} can respectively be approximated using

$$P^{j+1} = \frac{P^j + k(\beta(N^j)N^j - e^{-\gamma\tau}\beta(\vartheta^j(t_j - \tau))\vartheta^j(t_j - \tau))}{1 + k\gamma}, \qquad (2.4.9)$$

and

$$N^{j+1} = \frac{N^j + k(2e^{-\gamma\tau}\beta(\vartheta^j(t_j - \tau))\vartheta^j(t_j - \tau))}{1 + k(\beta(N^j) + \delta)}, \qquad (2.4.10)$$

for $j = s + 1, \ldots, M - 1$, and we extend the definition of $\vartheta^j(t)$ to the interval $[t_j, t_{j+1}]$ and obtain $\vartheta^{j+1}(t)$.

2.5   Analysis of the numerical methods

In this section we prove the convergence and the stability of the numerical methods developed in the previous section.

Convergence:

Using the Taylor expansion, we have

$$\frac{N(t_{j+1}) - N(t_j)}{k} - (-dN(t_j) + B(N(t_j - \tau))N(t_j - \tau)) = Ck + \mathcal{O}(k^2). \qquad (2.5.1)$$

where C is a constant.

The local truncation error for the method (2.4.1) is given by

$$\text{LTE} = \frac{N(t_{j+1}) - N(t_j)}{k} - (-dN(t_j + k) + B(N(t_j - \tau))N(t_j - \tau)),$$

which implies that

$$
\begin{aligned}
|\text{LTE}| \;=\; & \left| \frac{N(t_{j+1}) - N(t_j)}{k} - \left(-dN(t_j + k) + B(N(t_j - \tau))N(t_j - \tau)\right) \right| \\[2ex]
\leq \; & \left| \frac{N(t_{j+1}) - N(t_j)}{k} - \left(-d(N(t_j) + k\dot{N}(\xi)) + B(N(t_j - \tau))N(t_j - \tau)\right) \right| \\[2ex]
\leq \; & \left| \frac{N(t_{j+1}) - N(t_j)}{k} - \left(-dN(t_j + k) + B(N(t_j - \tau))N(t_j - \tau)\right) \right| \\[2ex]
& + k\,|dN(\xi)| \\[2ex]
\leq \; & Ck + \mathcal{O}(k^2) + k\,|dN(\xi)| = \mathcal{O}(k) \to 0 \text{ as } k \to 0.
\end{aligned}
$$
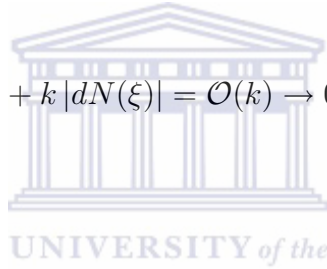
Stability:

Let $\varphi(t)$ be the spline function which approximates the history terms $N(t_j - \tau)$ at $t = t_j - \tau$. Then equation (2.4.2) can be written as

$$
N^{j+1} = \frac{1}{1 + kd}N^j + \frac{k}{1 + kd}B(\varphi(t_j - \tau))\varphi(t_j - \tau), \; j = 0, \ldots, M - 1. \qquad (2.5.2)
$$

Substituting the exact solution $N(t_j)$ instead of N^j in equation (2.5.2), we obtain

$$
N(t_{j+1}) = \frac{1}{1 + kd}N(t_j) + \frac{k}{1 + kd}B(\varphi(t_j - \tau))\varphi(t_j - \tau), \; j = 0, \ldots, M - 1.
$$

Subtracting the above equation from (2.5.2), taking the absolute values on both two sides and applying the triangle inequality, we obtain

$$
|e_{j+1}| \leq \left(\frac{1}{1 + kd} \right)|e_j| + \left(\frac{k}{1 + kd} \right)\left| B(\varphi(t_j - \tau))\varphi(t_j - \tau) - B(N(t_j - \tau))N(t_j - \tau) \right|,
$$
$$
(2.5.3)
$$

where $e_j = N^j - N(t_j)$ denotes the error at $t = t_j$.

We would like to determine how e_j behaves as $j \to \infty$.

For $j = 0, \ldots, s$, the history terms are $\varphi(t_j - \tau) = N(t_j - \tau)$ and hence, equation
(2.5.3) reduces to

$$|e_{j+1}| \leq \frac{1}{1+kd}|e_j| = \left(\frac{1}{1+kd}\right)^j |e_1|.$$

For $j = s+1, \ldots, N-1$, we first linearize the nonlinear function $B(\varphi(t_j - \tau))$
around $N(t_j - \tau)$ as

$$B(\varphi(t_j - \tau)) = B(N(t_j - \tau)) + (\varphi(t_j - \tau) - N(t_j - \tau))\dot{B}(\xi) = B(N(t_j - \tau)) + e_{j-s}\dot{B}(\xi),$$

where $\xi \in [t_{j-s}, t_{j+1-s}]$.

Substituting the above equation in (2.5.3) and simplifying, we obtain

$$|e_{j+1}| \leq \frac{1}{1+kd}|e_j| + \frac{k}{1+kd}\left|\left(B(N(t_j - \tau)) + \dot{B}(N(\xi))\right)\right||e_{j-s}|. \tag{2.5.4}$$

Equation (2.5.4) can be expressed as

$$|e_{j+1}| \leq \left(\frac{1}{1+kd}\right)^j |e_1| + \left(\frac{k}{1+kd}\right)\left|\left(B(N(t_j - \tau)) + \dot{B}(N(\xi))\right)\right|\left(\frac{1}{1+kd}\right)^{j-s}.$$

We note in the above inequality that both d and k are positive and the two terms on
right hand side go to zero, and hence $e_j \to 0$, $j \to \infty$.

This proves that the method is unconditionally stable.

Remark 2.5.1 For the PCML model (2.4.7), (2.4.8), (2.4.9), (2.4.10), we see that

$$|\text{LTE}_P| \leq Ck + \mathcal{O}(k^2) + k\,|\gamma P(\xi)| = \mathcal{O}(k) \to 0 \text{ as } k \to 0,$$
$$|\text{LTE}_N| \leq Ck + \mathcal{O}(k^2) + k\,|(\beta(N(\zeta)) + \delta)N(\zeta)| = \mathcal{O}(k) \to 0 \text{ as } k \to 0,$$

where ξ and ζ are in $[t_j, t_j + k]$. Moreover, the method is unconditionally stable.

2.6 Numerical results

In this section we provide numerical results for the models described by equations
(2.2.1) and (2.2.8).

Example 2.6.1 Consider (2.2.1) with $B(N(t)) = B_1(N(t))$. Then the model takes
the form

$$\dot{N}(t) = be^{-aN(t-\tau)}N(t-\tau)e^{d_1\tau} - dN(t)$$

with the initial data $N(t) = \vartheta_0(t) = 3.5$.

We solve the model for $a = d = 1$ and (a) $d_1 = 1$, $b = 80$, (b) $d_1 = 1$, $b = 20$, (c)
$d_1 = 0$, $b = 80$, (d) $d_1 = 0$, $b = 20$.

Results for different values of the delay parameter τ and the other parameters are
presented in Figure 2.6.1.

The comparative solutions with Runge-Kutta method are presented in Figure 2.6.2.

Example 2.6.2 By setting $B(c(t)) = B_2(c(t))$, $d_1 = 0$, where the function $c(t)$ is the
concentration of the blood cells (per mm^3), one can obtain the Mackey-Glass model
([91])

$$\dot{c}(t) = \frac{pc(t-\tau)}{q + c^n(t-\tau)} - dc(t),$$

with the initial data $c(t) = \vartheta_0(t) = 0.5$ for $t \in [-\tau, 0]$.

We solve this model for $p = 0.2$, $q = 1$, $n = 10$ and $d = 0.1$.

Results for different values of the delay parameter τ and the other parameters are
presented in Figure 2.6.3.

Example 2.6.3 Consider model (2.2.8) with $\theta = 1.98 \times 10^8$, $\delta = 0.05$, $\beta_0 = 1.77$,
$P_0 = 0.71 \times 10^8$, $\vartheta_0(t) = 6.43 \times 10^8$ for $t \in [-\tau, 0]$ and $n = 3$.

Results for different values of the delay parameter τ and the other parameters are
presented in Figure 2.6.5.

In Figure 2.6.1 we plot the solutions for the parameters values taken from [29]. In
that work, Cooke et al. used $a = d = 1$ and (a) $d_1 = 1$, $b = 80$, (b) $d_1 = 1$, $b = 20$,
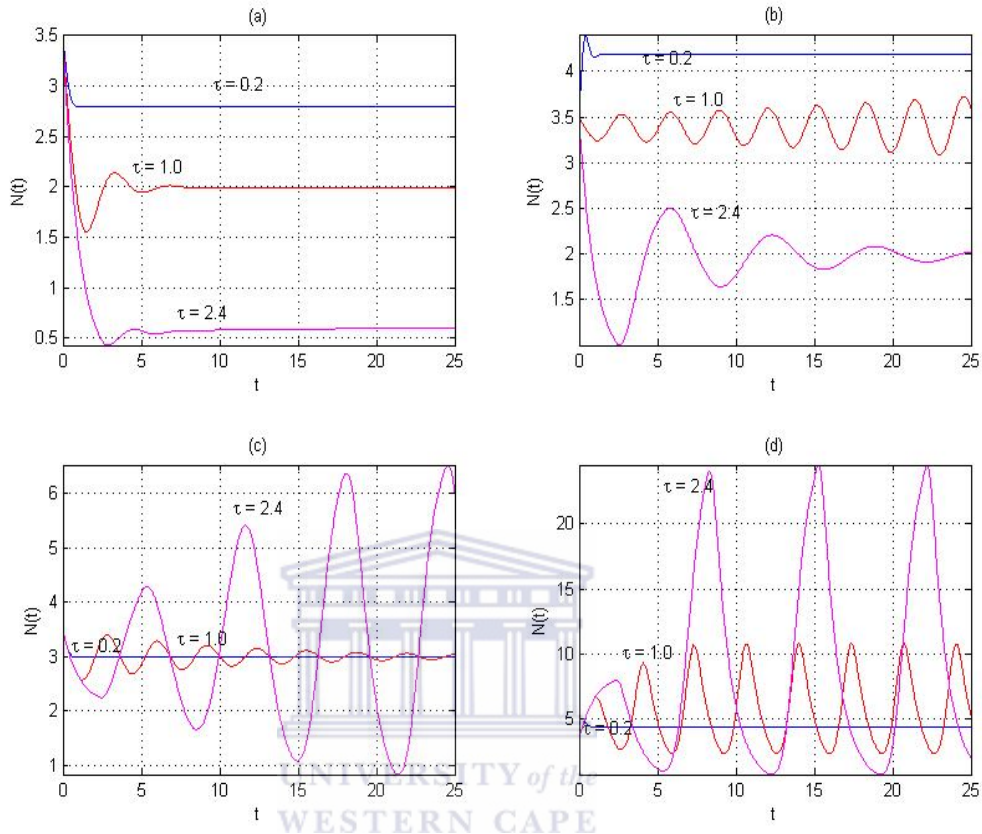
Figure 2.6.1: Solution for Example 2.6.1, with $B = B_1$, for $a = d = 1$ and (a) $d_1 = 1$, $b = 80$, (b) $d_1 = 1$, $b = 20$, (c) $d_1 = 0$, $b = 80$, (d) $d_1 = 0$, $b = 20$.

(c) $d_1 = 0$, $b = 80$, (d) $d_1 = 0$, $b = 20$. We see from Figure 2.6.1 (a) that the solution is stable for all the values of the delay parameter $\tau \in \{0.2, 1.0, 2.4\}$. Figure 2.6.1 (b) shows that the solution is stable for the delay parameters $\tau = 0.2$ and $\tau = 2.4$ whereas it is unstable for $\tau = 1$. This tells us that the solution looses its stability as τ passes through some critical value $\tau_1 \in (0.2, 1)$ and restores itself as the delay passes through another critical value $\tau_2 \in (1, 2.4)$. In Figure 2.6.1 (c), we see that the solution is stable for the delay parameters $\tau = 0.2$ and $\tau = 1.0$ whereas it is unstable for $\tau = 2.4$. This tells that the solution looses its stability as τ passes through some critical value $\tau_1 \in (1, 2.4)$. Finally, Figure 2.6.1 (d) shows that the solution is stable for the delay parameter $\tau = 0.2$ whereas it is unstable for $\tau = 1.0$ and $\tau = 2.4$. This means that the

solution looses its stability as τ passes through some critical value $\tau_1 \in (0.2, 1)$.

Figure 2.6.2: Solutions for Example 2.6.1, using the classical fourth-order Runge-Kutta
method and the PPM (2.4.1), with $B = B_1$ and step-size $k = 2$ and for parameter values
$a = d = 1$, $b = 20$ and $d_1 = 0$.

In Figure 2.6.2, we compare the performances of the classical fourth-order Runge-
Kutta method and the proposed PPM (2.4.1) for a step-size $k = 2$ with $\tau = 2.5$ in
$[0, 50]$. The fourth-order Runge-Kutta method failed to solve the problem for this step-
size, whereas PPM could solve the problem and maintained the non-negative profile of
the solution.

Figure 2.6.3 shows the dynamics of the concentration of the blood cells for different
values of the delay τ. The solution is stable for $\tau = 1$ and periodic for $\tau = 5$ and
$\tau = 10$. This means that there is a critical time delay $\tau_1^* \in (1, 5)$ such that the solution
loses its asymptotic stability when it passes through the critical delay τ_1^*. For $\tau = 15$
the solution is chaotic which indicates that there is another critical value $\tau_2^* \in (10, 15)$
for which the solution loses its stability.

In Figure 2.6.4 we compare the performance of the fourth-order Runge-Kutta
method with the proposed PPM (2.4.1). The comparison is made by taking $\tau = 60$ and
step-size $k = 24$ in $[0, 1200]$. The chosen parameter values of the model are $p = 0.2$,
$q = 1$, $n = 10$ and $d = 0.1$. The solution profile given by the fourth-order Runge-Kutta
method contains negative values for the blood concentration, whereas the one given by
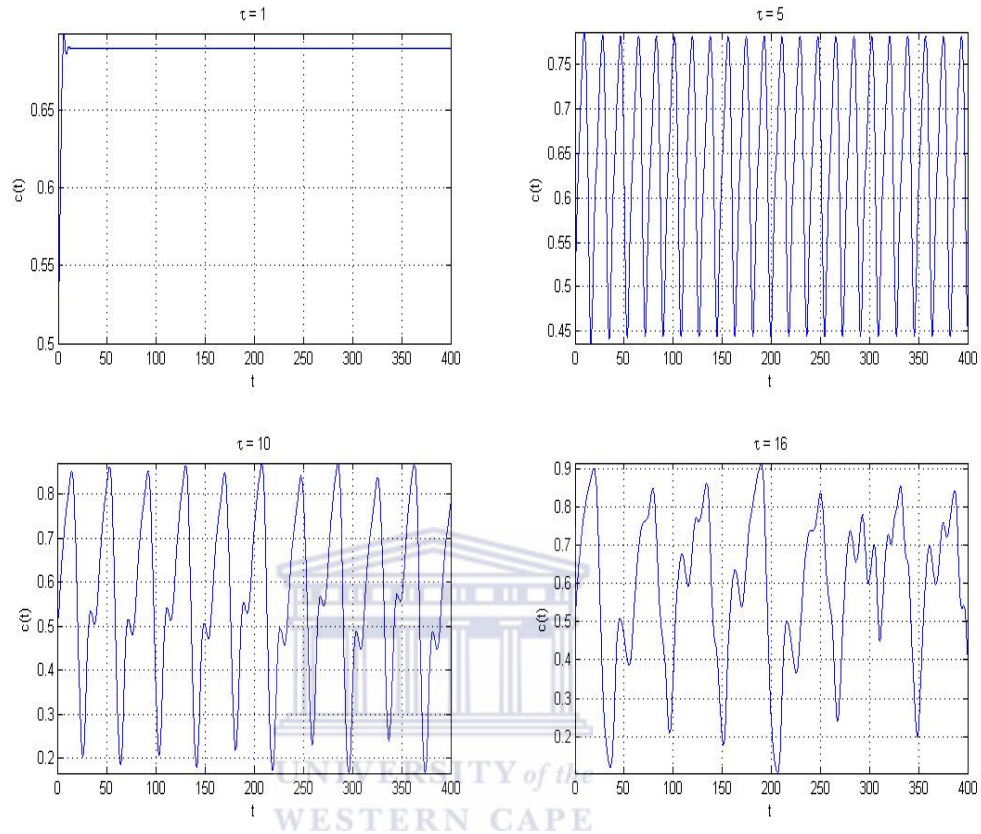
Figure 2.6.3: Solution for Example 2.6.2 in $[0, 400]$ for different values of the time delay τ, for $p = 0.2$, $q = 1$, $n = 10$ and $d = 0.1$.

our PPM is non-negative on the whole solution domain.

From Figure 2.6.5 we see that the solution of the model is stable for $\tau = 1.8, 2.1$ and $\tau = 5$, whereas it is periodic for $\tau = 2.4$. This indicates that the solution loses its asymptotic stability when the delay τ passes through some critical value $\tau_1^* \in (2.1, 2.4)$ and restores it when the delay τ passes through another critical value $\tau_2^* \in (2.4, 5)$.

In Figure 2.6.6, we compare the performance of the classical fourth-order Runge-Kutta method with the PPM (2.4.5)-(2.4.6). We fixed both the time delay τ and the step-size k to the value 10. We can see that the solution profile obtained by the Runge-Kutta method has negative values whereas the solution profile obtained by the proposed PPM is always nonnegative.
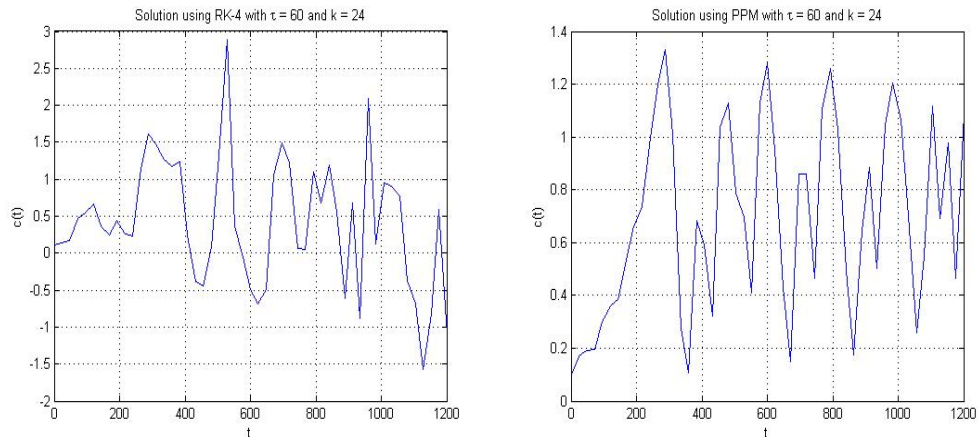
Figure 2.6.4: Solutions for Example 2.6.2 using the fourth-order Runge-Kutta method
and the PPM (2.4.1), for $\tau = 60$ and step-size $k = 24$ in $[0, 1200]$ where the parameters
of the model take the values $p = 0.2$, $q = 1$, $n = 10$ and $d = 0.1$.

2.7   Discussion

In this chapter, we designed positivity preserving methods (PPMs) for solving two
different biological models described by delay differential equations. These methods
are unconditionally stable and are first-order accurate.

To monitor the performance of the proposed PPMs, we chose two different routes:

Firstly, we fixed the step-size and varied the delay parameter to monitor the changes
in the qualitative behaviour of the solution, so that we could compare the results
obtained by these methods with the theoretical and other results found in the literature.
Figures 2.6.1, 2.6.3 and 2.6.5 show that the numerical results obtained by the PPMs
affirms the above statement.

Secondly, we have used moderately large step-sizes in the simulations for the three
test problems and compared the performances of the classical fourth-order Runge-
Kutta method to the proposed PPMs. In the first test example the fourth-order Runge-
Kutta method could not converge, and in the next two test examples it failed to give
non-negative solution profiles. On the other hand, the PPMs could solve the three test
problems and give non-negative solution profiles for these test problems. In fact, the
PPMs have been tested for many large time delays with large step-sizes maintaining
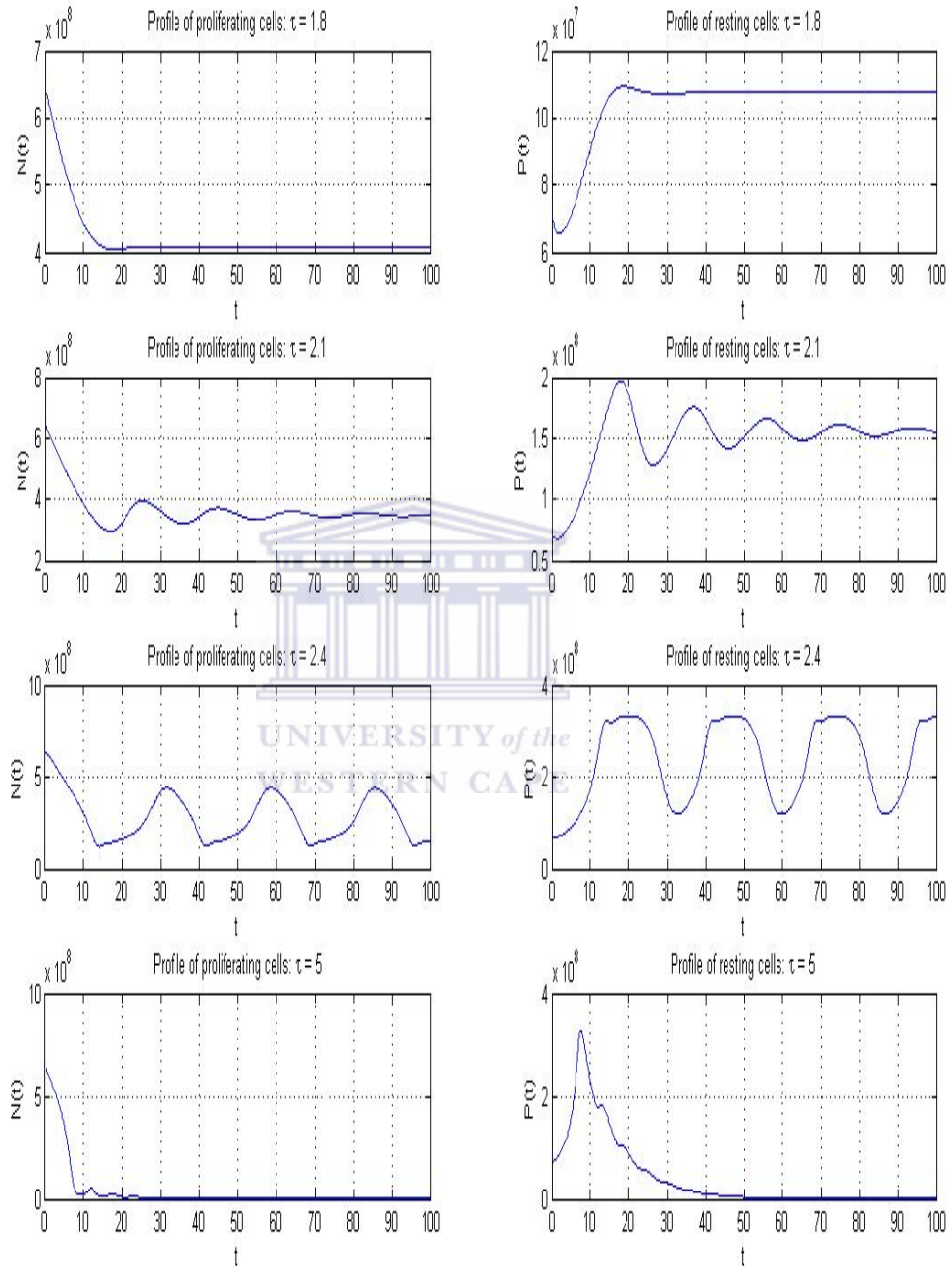
Figure 2.6.5: Solution for Example 2.6.3, for $\theta = 1.98 \times 10^8$, $\delta = 0.05$, $\beta_0 = 1.77$, $P_0 = 0.71 \times 10^8$, $\vartheta_0(t) = 6.43 \times 10^8$ for $t \in [-\tau, 0]$ and $n = 3$.
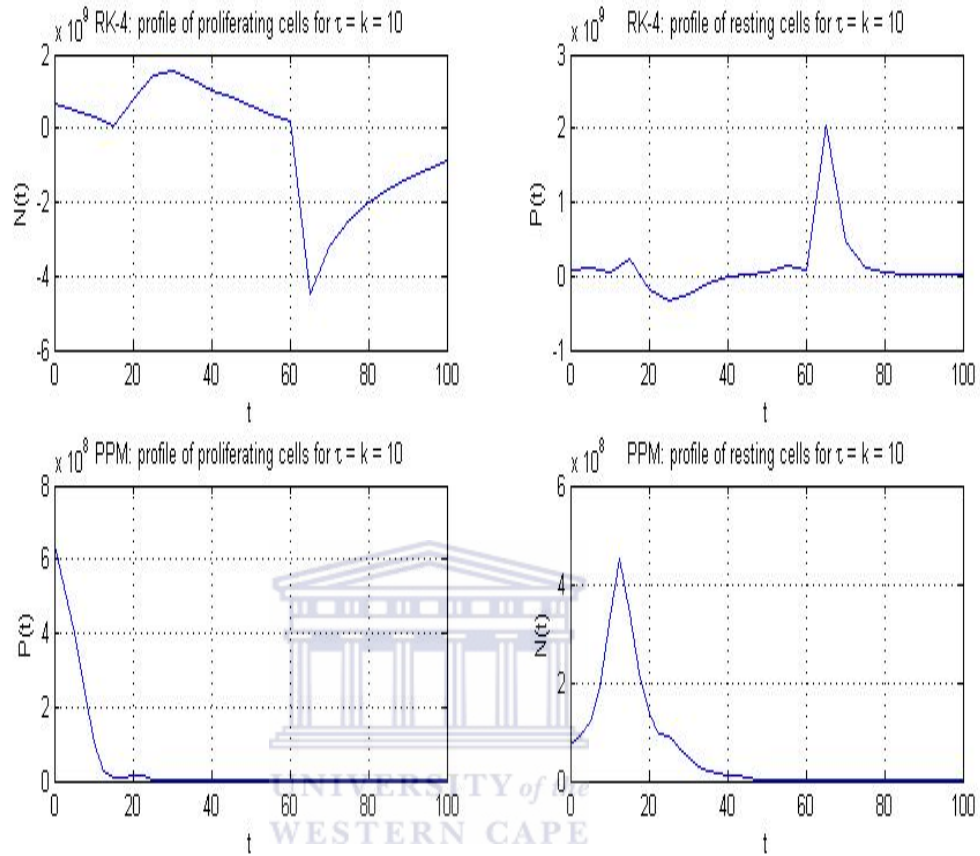
Figure 2.6.6: Solutions for Example 2.6.3 using the classical fourth-order Runge-Kutta
method and the PPM (2.4.5)-(2.4.6) on $[0, 100]$ with a delay and a step-size $\tau = k = 10$,
for $\theta = 1.98 \times 10^8$, $\delta = 0.05$, $\beta_0 = 1.77$, $P_0 = 0.71 \times 10^8$, $\vartheta_0(t) = 6.43 \times 10^8$ for $t \in [-\tau, 0]$,
$\tau = 2.5$ and $n = 3$.

the step-sizes to be bounded by the time delay τ. The PPMs have passed all these
tests giving non-negative bounded solutions. From these tests we can conclude that
the PPMs outperform the fourth-order Runge-Kutta method for large step-sizes and
large delays.

Chapter 3

An Efficient Fitted Operator Method to Solve Delayed Singularly Perturbed Differential Difference Equation
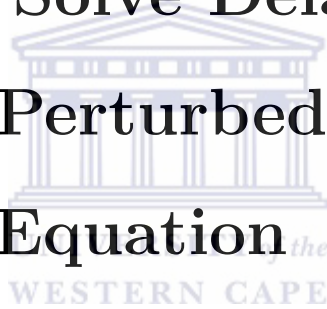
In this chapter, we develop a fitted numerical method for solving a singularly perturbed boundary-value problem for a second-order delay differential-difference equation. The delay appears in the first-order derivative term. The proposed method is first-order accurate. The results obtained are comparable with some of those available in the literature.

3.1 Introduction

Boundary-value second-order delay differential-difference equations model many biological systems. According to Lange and Miura ([81]), BVPs involving a DDE are satisfied by the moments of the time of first exit ([140]) of temporally homogeneous Markov processes ([96]) governing such phenomena as the time between impulses of a

nerve cell and the persistence times of populations with large random fluctuations.

Lange and Miura ([84]) stated that the determination of the expected time for the generation of action potentials in nerve cells (see, e.g., [5, 149]) by random synaptic inputs in the dendrites can be modelled as a first-exit time problem. They stated that under particular circumstances the problem for the expected first exit-time y, given the initial membrane potential $x \in [x_1, x_2]$, can be formulated as a general boundary-value problem for a second-order differential-difference equation of the form

$$\frac{\sigma^2}{2}\frac{d^2y}{dx^2} + (\mu - x)\frac{dy}{dx} + \lambda_E y(x + a_E) + \lambda_I y(x - a_I) - (\lambda_E + \lambda_I)y(x) = -1, \quad (3.1.1)$$

where the values $x = x_1$ and $x = x_2$ correspond to the inhibitory reversal potential and to the threshold value of the membrane potential for action potential genera-tion, respectively. The first-order term $-xy'$ corresponds to exponential decay between synaptic inputs whereas the undifferentiated terms correspond to excitatory and in-hibitory synaptic inputs modelled as Poisson processes ([79]) with mean rates λ_E and λ_I, respectively, and produce jumps in the membrane potential of amounts a_E and $-a_I$, which are small quantities and could depend on voltage.

The above general singularly perturbed second-order boundary value problem is considered by Lange and Miura in [84] and studied further by Kadalbajoo et al. in [73] and some of the references listed in [73]. Other relevant works include [81, 82, 83, 85].

The biological model stated by Lange and Miura in [84] leads us to consider a BVP for a singularly perturbed second-order differential-difference equation ([84])

$$\varepsilon\frac{d^2y}{dx^2} + a(x)y(x - \delta) + b(x)y(x) = f(x), \ x \in [0, 1], \quad (3.1.2)$$

$$y(\theta) = \varphi(\theta), \ \theta \in [-\delta, 0], \quad (3.1.3)$$

$$y(1) = \gamma, \quad (3.1.4)$$

where γ is a real constant, $0 < \varepsilon \leq 1$ is the singular perturbation parameter, the functions $a(x)$, $b(x)$ and $f(x)$ are sufficiently smooth and the initial function $\varphi(x)$ is

continuous.

If the shift parameter δ in (3.1.2) is taken to be zero (i.e., the case of no shift), then the solution of the resulting non-delayed problem can exhibit either a left or a right boundary layer depending on whether the function $a(x)$ is positive or negative in the interval $[0, 1]$. For very small values of the shift $\delta > 0$, the solution profile can still maintain the existing boundary layer. Once the shift parameter starts increasing, small oscillations start appearing in the boundary layer region. After some stage when these oscillations grow, the boundary layer is completely destroyed and oscillations dominate throughout the region. This particular feature makes this problem more interesting because such change in the overall dynamics cannot be resolved by many fitted mesh methods. We overcome this difficulty by using a fitted operator method instead.

Lange and Miura [84] reduced the DDE (3.1.2) into a system of ODEs of the form

$$\varepsilon y_n''(x) + a(x)y_n'(x) + b(x)y_n(x) = f(x) + a(x)(y_{n-1}'(x) - y_{n-1}'(x - \delta))$$

and used an iterative algorithm to solve the resulting problem. Their simulations show both boundary layer behaviour (for small shifts) and oscillatory dynamics (for large shifts).

Patidar and Sharma ([117]) considered problem (3.1.2) with small shifts. They used a two term Taylor expansion to approximate problem (3.1.2) through a non-delayed singularly perturbed second-order differential equation. They separated the cases of left and right boundary layers and constructed ε-uniformly convergent fitted operator finite difference methods for solving the approximate problem.

Rather than solving an approximate problem (the one obtained by using Taylor expansions) as in Patidar and Sharma ([117]), we develop a numerical method that can solve the problem (3.1.2)-(3.1.4) directly.

The rest of this chapter is organized as follows. In Section 3.2, we discuss some of the qualitative properties of the solution of (3.1.2)-(3.1.4). The fitted operator finite

difference method is constructed in Section 3.3. In Section 3.4, we analyze this method.
Numerical examples are presented in Section 3.5. Finally, in Section 3.6, we discuss
these numerical results.

3.2   Qualitative behaviour of the solution

In this section we review the qualitative behaviour of the solution of (3.1.2)-(3.1.4)
based on the work found in [84].

If the shift δ is taken to be zero in (3.1.2)-(3.1.4), then the resulting ordinary
differential equation will have either a boundary layer at the left side ($x = 0$) or a
boundary layer at the right side ($x = 1$), depending on whether $a(x) > 0$ or $a(x) < 0$,
respectively.

Letting the delay parameter δ taking very small values will not affect the boundary
layer initially. Then increasing the value of δ leads to the appearance of oscillations
within the boundary layer without destroying its structure. Increasing the value of δ
further, oscillations (starting from the layer side) begin to dominate until the boundary
layer is destroyed completely and they simultaneously move towards the other end.
These features have been shown via some figures in [84]. Their simulations indicate
significant effects of the delay on the first-order derivative.

Some notable observations from [84] are as follows:

1. In the case of no delay (i.e., when $\delta = 0$) with $a(x) > 0$, there is a boundary layer
   at $x = 0$, and the outer solution is given by

$$y(x) = \gamma e^{\int_x^1 b(t)/a(t)dt} + \mathcal{O}(\varepsilon).$$

   The analytical solution in this case is then given by

$$y(x) = \Gamma + (\phi(0) - \Gamma)e^{-a(0)x/\varepsilon} + \mathcal{O}(\varepsilon),$$

where $\Gamma = \gamma e^{\int_x^1 b(t)/a(t)dt}$.
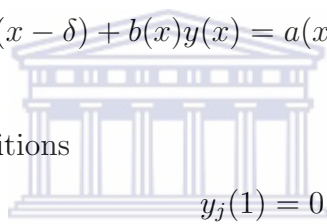
2. For $\delta = \tau\varepsilon$ where τ is a positive parameter of $\mathcal{O}(1)$, they assumed an outer
solution of the form

$$y(x) = \sum_{j=0}^{\infty} y_j(x)\varepsilon^j,$$

as $\varepsilon \to 0$, where y_0 satisfies the reduced problem obtained by setting $\varepsilon = 0$, with
boundary condition $y_0(1) = \gamma$, whereas the functions $y_j(x), j = 1, 2, \ldots$ satisfy
equations of the form

$$\varepsilon y_j''(x) + a(x)y'(x - \delta) + b(x)y(x) = a(x)\sum_{k=1}^{j}(-1)^k\frac{\tau^k}{k!}y_{j-k}^{(k+1)}(x) - y''(x),$$

with boundary conditions

$$y_j(1) = 0.$$

Using the change in the variables $\tilde{x} = x/\varepsilon$ and $\tilde{y}(\tilde{x}) = y(\varepsilon x)$, the solution of the
transformed problem

$$\tilde{y}'' + a(\varepsilon\tilde{x})\tilde{y}'(\tilde{x} - \tau) + \varepsilon b(\varepsilon\tilde{x})\tilde{y}(\tilde{x}) = 0, \ 0 \le \tilde{x} \le \infty,$$

can be written as

$$\tilde{y}(\tilde{x}) = \sum_{j=1}^{\infty} \tilde{y}_j(\tilde{x})\varepsilon^j,$$

where the smooth component $\tilde{y}_0(\tilde{x})$ satisfies the problem

$$\tilde{y}_0''(\tilde{x}) + \tilde{y}_0'(\tilde{x} - \tau) = 0, \ \tilde{y}_0(\tilde{x}) = 1 \text{ on } [-\tau, 0].$$

Integrating the above with respect to x, we obtain

$$\tilde{y}'(\tilde{x}) + \tilde{y}(\tilde{x} - \tau) = \tilde{y}'(0) + 1 = \Gamma,$$

assuming that $a(0) = 1$.

The solution of the above problem is obtained by first applying the Laplace transform, which yields

$$\widetilde{Y}_0(s) = \frac{1}{s} + \frac{\Gamma - 1}{s(s + e^{-\tau s})}$$

and then one uses the inverse Laplace transform.

The transformed problem has infinite number of poles. One of the poles is $s = 0$ and the other poles are obtained by determining the roots of

$$P(s, \tau) = s + e^{-s\tau} = 0.$$

The results about the poles of $P(s, \tau)$ are summarized as follows:

(a) For $\tau \in (0, e^{-1})$, there are two distinct real roots $s_0 \in (-\infty, -e)$ and $s_1 \in (-e, -1)$. When $\tau \to 0^+$, then $s_0 \to -\infty$ and $s_1 \to -1$, whereas when $\tau > 0$, all the other roots occur in complex conjugate pairs with $Re(s_n) \approx (1/\tau) \ln (2\tau/(4n - 3)\pi)$ as $n \to \infty$.

(b) For $\tau = e^{-1}$, the two negative roots coalesce at $s_1 = -e$.

(c) For $\tau > e^{-1}$, the roots split into complex conjugate pairs, and at $\tau = \pi/2$, $Re(s_1) = 0$.

(d) For $\tau > \pi/2$, s_1 and $\bar{s}_1$ cross the imaginary axis to the right half plane.

Then the solution obtained by the inversion of $\widetilde{Y}_0(s)$ is given by

$$\widetilde{y}_0(\widetilde{x}) = \Gamma + c_0 e^{s_0 \widetilde{x}} + c_1 e^{s_1 \widetilde{x}} + \sum_{n=2}^{\infty} (c_n e^{s_n \widetilde{x}} + \bar{c}_n e^{s_n \widetilde{x}}),$$

where

$$c_n = \frac{\Gamma - 1}{s_n(1 + \tau s_n)}, \quad n = 0, 1, \dots.$$

From the natures of the poles of the transformed problem, Lange and Miura [84] concluded that

(a) for $\tau \in (0, e^{-1})$, the roots s_0 and s_1 are real and distinct, and

$$\widetilde{y}_0(\widetilde{x}) \approx \Gamma + c_0 e^{s_0 \widetilde{x}} + c_1 e^{s_1 \widetilde{x}}, \; \widetilde{x} \to \infty, \; \varepsilon \to 0,$$

is an accurate numerical approximation for the boundary layer solution $\widetilde{y}(\widetilde{x})$.

(b) for $\tau > e^{-1}$, s_0 and s_1 are complex conjugates, and c_0 and s_0 are replaced by $\bar{c}_1$ and $\bar{s}_1$.

(c) the leading order layer solution neither depends on the function $b(x)$ nor on the function $f(x)$, except through Γ.

The qualitative information described above will be useful for verification of the numerical results that we obtain by the fitted method presented in next section.

3.3 Construction of the numerical method

In this section we design a fitted numerical method to solve the problem (3.1.2)-(3.1.4).

To begin with, we partition the interval $[0, 1]$ through the points

$$x_0 = 0 < x_1 < \ldots < x_N = 1,$$

where N is a positive integer and $x_{m+1} - x_m = h = 1/N$ for $m = 0, \ldots, N-1$.
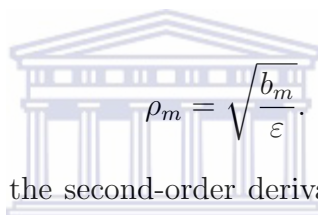
The value of N is chosen in such a way that $\delta = sh$ for some positive integer s. This will make it possible for the shift parameter δ to coincide with the grid point x_s. This in line with most of the works seen in the literature (see, e.g., [29, 32, 133]) for this kind of problem where either the length of the interval is considered as the multiple of the delay parameter or both the interval length and the delay are integer multiples of the step-size h.

Using the theory of difference equations (see, e.g., [87, 116]), the appropriate de-

nominator function (ϕ_m^2) in the discretization of (3.1.2)-(3.1.4) can be considered as
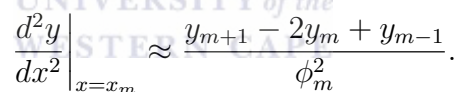
$$
\phi_m^2 =
\begin{cases}
\dfrac{h\varepsilon}{a_m}\left(e^{\frac{ha_m}{\varepsilon}} - 1\right), & \text{if } a_m < 0, \\[3ex]
\dfrac{h\varepsilon}{a_m}\left(1 - e^{-\frac{ha_m}{\varepsilon}}\right), & \text{if } a_m > 0, \\[3ex]
\dfrac{4}{\rho_m^2}\sinh^2\frac{\rho_m h}{2}, & \text{if } a_m = 0 \text{ and } b_m > 0, \\[3ex]
\dfrac{4}{\rho_m^2}\sin^2\frac{\rho_m h}{2}, & \text{if } a_m = 0 \text{ and } b_m < 0,
\end{cases}
\tag{3.3.1}
$$

where

$$
\rho_m = \sqrt{\frac{b_m}{\varepsilon}}.
$$

At the grid points x_m, the second-order derivative term in equation (3.1.2) is approximated as

$$
\frac{d^2 y}{dx^2}\bigg|_{x=x_m} \approx \frac{y_{m+1} - 2y_m + y_{m-1}}{\phi_m^2}.
$$

Similarly, the first-order term involving delay is approximated at $x_m - \delta$ as

$$
\frac{dy}{dx}\bigg|_{x=x_m-\delta} \approx \frac{y(x_{m+1} - \delta) - y(x_m - \delta)}{h}.
$$

Using the above approximations, we obtain the following difference method for (3.1.2):

$$
\varepsilon\frac{y_{m+1} - 2y_m + y_{m-1}}{\phi_m^2} + a_m\frac{y(x_{m+1} - \delta) - y(x_m - \delta)}{h} + b_m y_m = f_m,
\tag{3.3.2}
$$

$m = 1, \ldots, N - 1$.

Equation (3.3.2) can be further simplified to

$$
\frac{\varepsilon}{\phi_m^2}y_{m-1} - \frac{2\varepsilon}{\phi_m^2}y_m + \frac{\varepsilon}{\phi_m^2}y_{m+1} + \frac{a_m}{h}y(x_{m+1} - x_s) - \frac{a_m}{h}y(x_m - x_s) = f_m,
\tag{3.3.3}
$$

$m = 1, \ldots, N-1$

For $m \leq s$, the delayed term $y(x_m - \delta)$ is evaluated from the history function as

$$y(x_m - \delta) = \varphi(x_m - \delta) = \varphi(x_m - x_s),$$

and therefore, equation (3.3.3) becomes

$$\frac{\varepsilon}{\phi_m^2} y_{m-1} - \frac{2\varepsilon}{\phi_m^2} y_m + \frac{\varepsilon}{\phi_m^2} y_{m+1} = f_m - \frac{a_m}{h} \varphi(x_{m+1} - x_s) - \frac{a_m}{h} \varphi(x_m - x_s), \qquad (3.3.4)$$

when $m < s$, whereas when $m = s$, we have

$$\frac{\varepsilon}{\phi_s^2} y_{s-1} - \frac{2\varepsilon}{\phi_s^2} y_s + \frac{\varepsilon}{\phi_s^2} y_{s+1} + \frac{a_{s+1}}{h} y_1 = f_s - \frac{a_s}{h} \varphi(0). \qquad (3.3.5)$$

For $m = s + 1, \ldots, N - 1$, equation (3.3.3) takes the form

$$\frac{\varepsilon}{\phi_m^2} y_{m-1} - \frac{2\varepsilon}{\phi_m^2} y_m + \frac{\varepsilon}{\phi_m^2} y_{m+1} + \frac{a_m}{h} y(x_{m+1-s}) - \frac{a_m}{h} y(x_{m-s}) = f(x_m). \qquad (3.3.6)$$

Our fitted operator finite difference method consists of equation (3.3.3) along with the initial data (3.1.3) and the boundary condition (3.1.4).

Combining (3.3.4), (3.3.5) and (3.3.6), we obtain a linear system

$$AY = F,$$

where A is the $(N-1) \times (N-1)$ matrix

$$
A_{j,k} = \begin{cases}
-\frac{2\varepsilon}{\phi_m^2} + b_m, & \text{if } j = k = m, \ m = 1, \ldots, N-1 \\[2ex]
\frac{\varepsilon}{\phi_{m-1}^2} & \text{if } j = m-1, \ k = m, \ m = 2, \ldots, N-1 \\[2ex]
\frac{\varepsilon}{\phi_m^2}, & \text{if } j = m, \ k = m-1, \ m = 2, \ldots, N-1 \\[2ex]
\frac{a_s}{h}, & \text{if } j = s \text{ and } k = 1 \\[2ex]
-\frac{a_m}{h}, & \text{if } j = m-s, \ k = m, \ m > s \\[2ex]
\frac{a_m}{h}, & \text{if } j = m-s+1, \ k = m, \ m > s \\[2ex]
0, & \text{otherwise.}
\end{cases}
$$

The $N-1$ entries of the right hand side vector F are given by

$$
F_m = \begin{cases}
f(x_1) - \frac{\varepsilon}{\phi_1^2} y(x_0) - \frac{a_1}{h}(\varphi(x_2 - \delta) - \varphi(x_1 - \delta)), & \text{if } m = 1, \\[2ex]
f_m - \frac{a_m}{h}(\varphi(x_{m+1} - \delta) - \varphi(x_m - \delta)) & \text{if } 1 < m < s, \\[2ex]
f_s + \frac{a_s}{h} y_0, & \text{if } m = s, \\[2ex]
f_m, & \text{if } s < m < N-1, \\[2ex]
f_{N-1} - \frac{\varepsilon}{\phi_{N-1}^2}\gamma, & \text{if } m = N-1,
\end{cases}
$$

and Y denotes the vector $[y_1, \ldots, y_{N-1}]^T$ of unknowns.

3.4 Analysis of the numerical method

In this section we analyze the proposed fitted method. We will consider the case of large delays that are sufficient to destroy the boundary layer. In this case, highly oscillatory solutions will be obtained. Therefore, we assume that the solution function $y(x)$ and its derivatives up to order three are bounded by a constant C, which is independent of ε. On the other hand, the cases of the small delays have already been analyzed by other researchers in the past, see, e.g., [73], where due to the smallness of the delay, the differential equation (obtained via Taylor approximations) was still a very good approximation to the problem (3.1.2)-(3.1.4).

Convergence of the method:

The local truncation error of the method at $x = x_m$ is given by

$$
\begin{aligned}
\text{LTE} \;=\; & \varepsilon \left(y''(x_m) - \frac{y(x_{m+1}) - 2y(x_m) + y(x_{m-1})}{\phi_m^2} \right) \\
& + a_m \left(y'(x_m - \delta) - \frac{y(x_{m+1} - \delta) - y(x_m - \delta)}{h} \right),
\end{aligned}
\qquad (3.4.1)
$$

which implies that

$$
\begin{aligned}
|\text{LTE}| \;\leq\; & \varepsilon \left| y''(x_m) - \frac{y(x_m + h) - 2y(x_m) + y(x_m - h)}{\phi_m^2} \right| \\
& + |a_m| \left| y'(x_m - \delta) - \frac{y(x_{m+1} - \delta) - y(x_m - \delta)}{h} \right|.
\end{aligned}
\qquad (3.4.2)
$$

The first term on the right hand side of the inequality (3.4.2) can be replaced by

$$
\begin{aligned}
& \varepsilon \left(y''(x_m) - \frac{y(x_{m+1}) - 2y(x_m) + y(x_{m-1})}{h^2} \right) \\
& + \varepsilon \left(\frac{y(x_{m+1}) - 2y(x_m) + y(x_{m-1})}{h^2} - \frac{y(x_{m+1}) - 2y(x_m) + y(x_{m-1})}{\phi_m^2} \right).
\end{aligned}
\qquad (3.4.3)
$$

This gives

$$\varepsilon \left| y''(x_m) - \frac{y(x_{m+1}) - 2y(x_m) + y(x_{m-1})}{h^2} \right| = \mathcal{O}(h^2) \to 0 \text{ as } h \to 0$$

Moreover, by expanding ϕ_m^2, we see that

$$\varepsilon \left| \frac{y(x_{m+1}) - 2y(x_m) + y(x_{m-1})}{h^2} - \frac{y(x_{m+1}) - 2y(x_m) + y(x_{m-1})}{\phi_m^2} \right|$$

$$\leq \frac{\varepsilon \mathcal{O}(\frac{h}{\varepsilon})}{1 + \mathcal{O}(\frac{h}{\varepsilon})} \to 0 \text{ as } h \to 0,$$

provided that $h \leq C\delta$, where $C \in (0, 1]$ is a constant.

The second term on the right hand side of the inequality (3.4.2) satisfies

$$|a_m| \left| y'(x_m - \delta) - \frac{y(x_{m+1} - \delta) - y(x_m - \delta)}{h} \right| \leq |a_m| \mathcal{O}(h) \to 0 \text{ as } h \to 0.$$

Hence, the LTE is $\mathcal{O}(h)$ and it tends to zero as $h \to 0$ and $h \leq C\delta$, which proves that the method is convergent of order 1.

Remark 3.4.1 In order to accommodate all the delays, it is reasonable to choose the step-size to be of the magnitude of δ. Hence, the condition $h \leq C\delta$ for the convergence is logically very appropriate.

Stability of the method:

The stability of the fitted method depends on the eigenvalues of the matrix A denoted by λ_m, $m = 1, \ldots, N - 1$. If for all $m = 1, \ldots, N - 1$, the eigenvalues of A^{-1} denoted by λ_m^{-1} satisfy

$$|\lambda_m^{-1}| < 1,$$

then the method will be stable. We would like to determine the conditions on the step-size h, under which the proposed fitted method is stable.

To do so, we make use of the Gershgorin's disk theorem ([61]), which states that

each eigenvalue λ_m of the matrix A should lie in a Gershgorin's disk (denoted by D_m), which is centered at $b_m - 2\varepsilon/\phi_m^2$ and has a radius equals to the magnitude of the summation of the non-diagonal elements in row m. Our strategy here is to consider each Gershgorin's disk D_m, and let the whole disk lies in $(-\infty, -1)$ one time and lies in $(1, \infty)$ another time and for each of the two cases we determine the range for the step-size h which allow the disk to lie in the corresponding region. This is done by allowing both the left and right bounds of the disk to lie together either in $(-\infty, -1)$ or in $(1, \infty)$.

For $m = 1, \ldots, s - 1$, each Gershgorin's disk is centered at $b_m - 2\varepsilon/\phi_m^2$ and has a radius $2\varepsilon/\phi_m^2$, that is

$$D_m = \left[b_m - \frac{4\varepsilon}{\phi_m^2}, b_m \right].$$

Then, $|\lambda_m^{-1}| < 1$ if $|\lambda_m| > 1$ and this will happen only if both the limits of D_m are below -1 or both are above 1.

If we solve the two inequalities

$$b_m \quad < \quad -1$$

and

$$b_m - \frac{4\varepsilon}{\phi_m^2} \quad < \quad -1,$$

we obtain

$$h \quad < \quad \frac{\varepsilon}{a_m} W \left(\frac{4a_m^2}{b_m + 1} \right), \text{ for } a_m > 0$$

and

$$h \quad < \quad \frac{2a_m^2}{b_m + 1}, \text{ for } a_m < 0,$$

where $W(x)$ denotes the Lambert W function evaluated at x.

On the other hand, if we solve the two inequalities

$$b_m \quad > \quad 1$$

and

$$b_m - \frac{4\varepsilon}{\phi_m^2} \quad > \quad 1,$$

we obtain

$$h \quad < \quad \frac{\varepsilon}{a_m} W\left(\frac{4a_m^2}{b_m - 1}\right), \text{ for } a_m > 0$$

and

$$h < \frac{2a_m^2}{b_m - 1}, \text{ for } a_m < 0.$$

The Gershgorin's disk D_s is given by

$$D_s = \left[b_s - \frac{4\varepsilon}{\phi_m^2} - \frac{a_{s+1}}{h}, b_m + \frac{a_{s+1}}{h}\right]$$

and again $|\lambda_s| > 1$ only if both the limits of D_s are below -1 or both are above 1.

The solution of the inequalities

$$b_s - \frac{4\varepsilon}{\phi_m^2} - \frac{a_{s+1}}{h} \quad < \quad -1$$

and
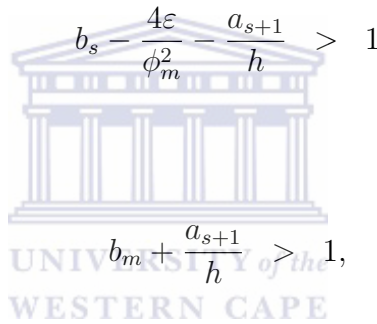
$$b_m + \frac{a_{s+1}}{h} \quad < \quad -1,$$

leads to

$$h \; < \; \frac{\varepsilon}{a_s} W \left(\frac{4a_s^2}{b_s + 1} \right), \; \text{for } a_s > 0$$

and

$$h \; < \; \frac{2a_s^2}{b_s + 1}, \; \text{for } a_s < 0,$$

whereas the solution of the inequalities

$$b_s - \frac{4\varepsilon}{\phi_m^2} - \frac{a_{s+1}}{h} \; > \; 1$$

and

$$b_m + \frac{a_{s+1}}{h} \; > \; 1,$$

leads to

$$h \; < \; \frac{\varepsilon}{a_s} W \left(\frac{4a_s^2}{b_s - 1} \right), \; \text{for } a_s > 0$$

and

$$h \; < \; \frac{2a_s^2}{b_s - 1}, \; \text{for } a_s < 0.$$

Similarly, for $m = s + 1, \ldots, N - 1$, the Gershgorin's disks are given by

$$D_m = \left[b_m - \frac{4\varepsilon}{\phi_m^2} - \left(\frac{a_{m+1}}{h} - \frac{a_m}{h} \right), b_m + \left(\frac{a_{m+1}}{h} - \frac{a_m}{h} \right) \right],$$

and the eigenvalues λ_m in this case satisfy $|\lambda_m| > 1$ only if both the limits of D_m are

below -1 or both are above 1.

By solving the inequalities

$$b_m - \frac{4\varepsilon}{\phi_m^2} - \left(\frac{a_{m+1}}{h} - \frac{a_m}{h}\right) \quad < \quad -1$$

and

$$b_m + \left(\frac{a_{m+1}}{h} - \frac{a_m}{h}\right) \quad < \quad -1,$$

we obtain

$$h \quad < \quad \frac{\varepsilon}{a_m} W\left(\frac{4a_m^2}{b_m+1}\right), \quad \text{for } a_m > 0$$

and

$$h < \frac{2a_m^2}{b_m+1}, \quad \text{for } a_m < 0.$$

On the other hand, if we solve the two inequalities

$$b_m - \frac{4\varepsilon}{\phi_m^2} - \left(\frac{a_{m+1}}{h} - \frac{a_m}{h}\right) \quad > \quad 1$$

and

$$b_m + \left(\frac{a_{m+1}}{h} - \frac{a_m}{h}\right) \quad > \quad 1,$$

we obtain

$$h \quad < \quad \frac{\varepsilon}{a_m} W\left(\frac{4a_m^2}{b_m-1}\right), \quad \text{for } a_m > 0$$

and

$$h \quad < \quad \frac{2a_m^2}{b_m-1}, \quad \text{for } a_m < 0.$$

The above condition on h guarantee the stability of the method. It should be noted
that due to the nature of the coefficients, none of the above conditions seem to be
severe.

3.5   Numerical results

Example 3.5.1 [84] We consider (3.1.2)-(3.1.4) with $a(x) = b(x) = \varphi(x) = \gamma = 1$,
$f(x) = 0$. and $\varepsilon = 0.01$.

Example 3.5.2 [84] We consider (3.1.2)-(3.1.4) with $\varphi(x) = 1$, $a(x) = b(x) = \gamma = -1$
and $f(x) = 0$.

In Figure 3.5.1 we plot the solutions for Example 3.5.1 corresponding to different
values of the delay. These plots show different dynamics: left boundary layers, oscilla-
tions on the layer side and movement of the oscillations to the other side. In Figure
3.5.2 we plot the solutions for Example 3.5.2 for different values of δ. These plots also
show different behaviour for the solution of the system, including smooth and oscilla-
tory behaviour. These numerical results confirm the observations made earlier about
the qualitative behaviour of the solution.

3.6   Discussion

In this chapter, we have developed a fitted numerical method for solving a second-order
delay differential equation with a delay involved in the first-order derivative term. The
method is shown to be stable and convergent of order 1.

By applying the fitted method to Example 3.5.1 we noticed that for very small
values of the delay δ (up to $\delta = 0.5\varepsilon$), the left boundary layer is maintained. When the
delay is more than 0.5ε but remains below $\delta = 1.1\varepsilon$, oscillations within the boundary
layer are seen while the layer structure is still being maintained. For delays that are
greater than 1.1ε, oscillations begin to dominate in the boundary layer region and
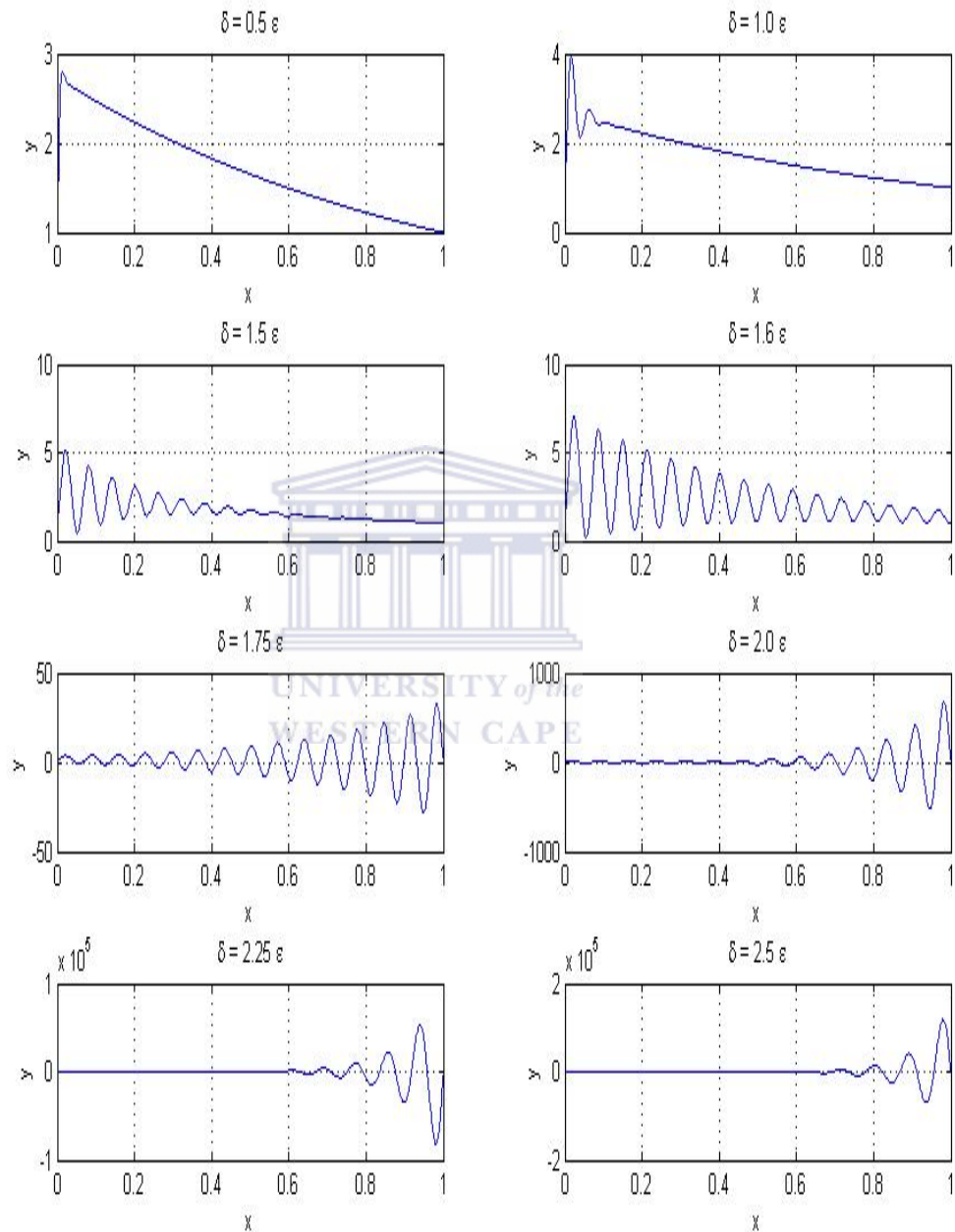
Figure 3.5.1: Solution for Example 3.5.1, with $a(x) = b(x) = \varphi(x) = \gamma = 1$ and $f(x) = 0$.
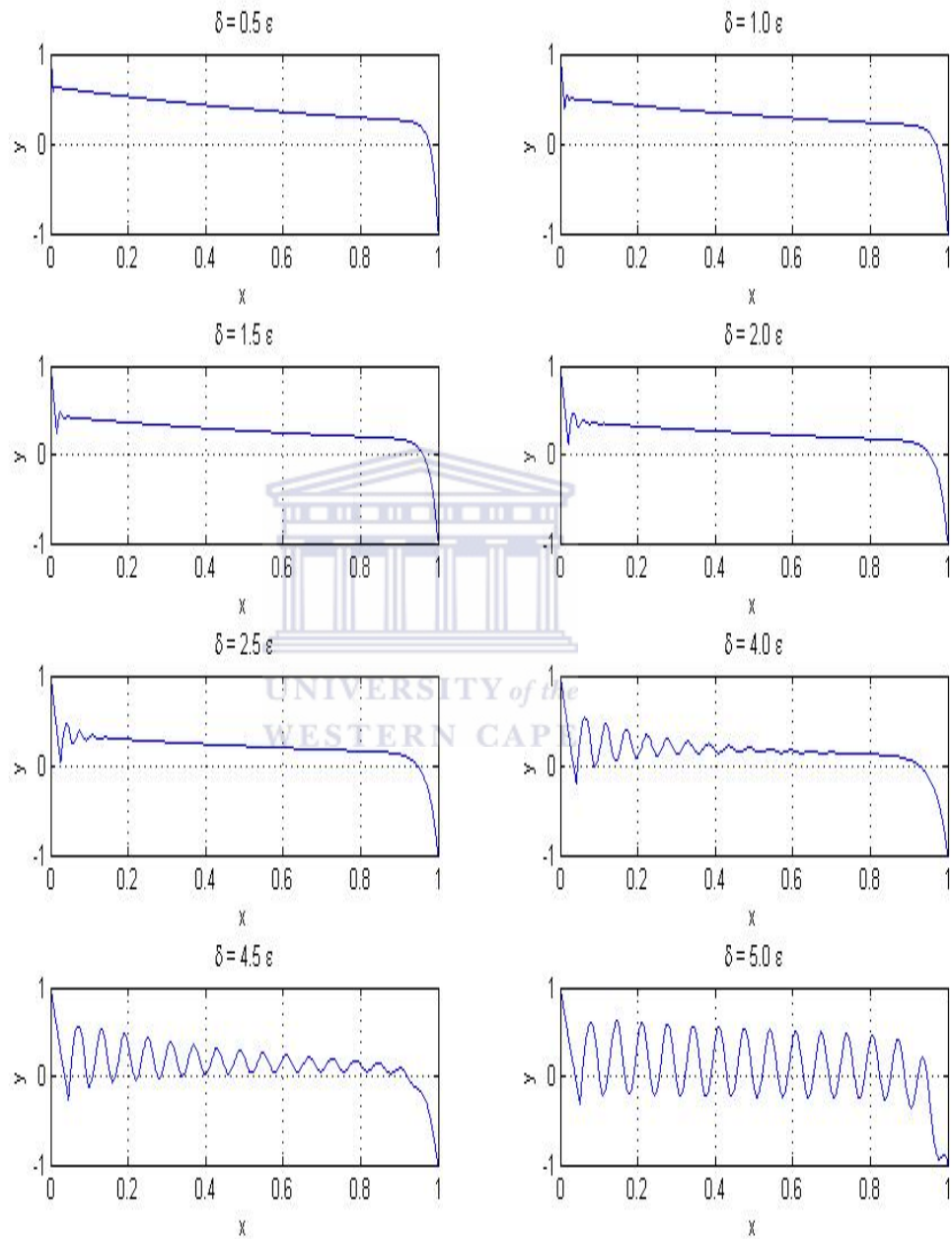
Figure 3.5.2: Solution for Example 3.5.2, $\varphi(x) = 1$, $a(x) = b(x) = \gamma = -1$ and $f(x) = 0$.

the shape of the boundary layer is completely destroyed when the value of the delay parameter reaches 1.5ε. At around $\delta = 1.6\varepsilon$ oscillations profile is the same on the left and right sides. After that the oscillations become weaker on the left side compared to the right side, their magnitudes on the right side grow rapidly by increasing the value of the delay. The profile remains like that for the rest of the values of the delay. It should be noted that the results which we obtain by our fitted numerical method for this example agree with those found in [84].

The solutions for Example 3.5.2 are explained in Figure 3.5.2. Again we see the movement from very smooth profiles corresponding to very small delays to oscillatory profiles with small oscillations to oscillatory dynamics.

The condition that the step-size must be below the singular perturbation parameter looks very severe, but the fact that the delay and the singular perturbation parameter are of similar order shows that this condition is reasonable. This is not surprising since even the MATLAB *dde23* solver has been designed to include the time delay δ, 2δ and 3δ on the mesh in order for *dde23* to not avoid step-sizes smaller than or equal to δ.

Chapter 4

Fitted Methods for Singularly Perturbed Delay Parabolic Partial Differential Equations

In this chapter, we develop reliable numerical methods for solving a class of singularly perturbed delay parabolic partial differential equation (SPDPPDE). We consider both fitted mesh and fitted operator numerical methods for solving these problems.

4.1 Introduction

We consider a singularly perturbed delay parabolic partial differential equation (SPDP-PDE) of the form

$$\frac{\partial u(t,x)}{\partial t} - \varepsilon \frac{\partial^2 u(t,x)}{\partial x^2} + a(t,x)u(t,x) = f(t,x) - b(x)u(t-\tau, x), \qquad (4.1.1)$$

$$(t,x) \in \overline{\Omega} \equiv [0,T] \times [0,1],$$

with the initial data

$$u(t,x) = u_0(t,x), \ (t,x) \in [-\tau, 0] \times (0,1) \qquad (4.1.2)$$

69

and boundary conditions

$$u(t,x) = \Gamma_L(t), (t,x) \in \Pi_L \tag{4.1.3}$$

and

$$u(t,x) = \Gamma_R(t), (t,x) \in \Pi_R, \tag{4.1.4}$$

where $0 < \varepsilon \leq 1$ is the singular perturbation parameter and $\tau > 0$ is the delay parameter. The functions $a(t,x) \geq 0$, $b(t,x) \geq \beta \geq 0$, $f(t,x)$, $u_0(t,x)$, $\Gamma_L(t)$ and $\Gamma_R(t)$ are bounded and sufficiently smooth functions and Π_L and Π_R denote $[0,T] \times \{0\}$ and $[0,T] \times \{1\}$, respectively, are the left and right boundaries of the domain $\overline{\Omega}$. The terminal time $T > 0$ is assumed to satisfy $T = K\tau$ where K is a positive integer, whereas the initial function $u_0(t,x)$ is assumed to satisfy the compatibility conditions [122]:

$$
\begin{aligned}
u_0(0,0) &= \Gamma_L(0), \\
u_0(0,1) &= \Gamma_R(0), \\
\frac{\partial u_0(0,0)}{\partial t} &= \varepsilon\frac{\partial^2 u_0(0,0)}{\partial x^2} - b(0)u(-\tau,0) + f(0,0),
\end{aligned}
$$

and

$$\frac{\partial u_0(0,1)}{\partial t} = \varepsilon\frac{\partial^2 u_0(0,1)}{\partial x^2} - b(1)u(-\tau,1) + f(0,1).$$

Under the above assumptions and conditions, problem (4.1.1) with the initial data (4.1.2) and the boundary conditions (4.1.3) and (4.1.4) has a unique solution [1].

Singularly perturbed parabolic partial differential equations (SPPPDEs) model a wide range of real life phenomena. In biology many singularly perturbed diffusive models have been established to describe the dynamics of some biological systems. The smallness of the diffusion parameter is found in many real life applications, see, for example, Murray [110], in which he pointed out that in blood, haemoglobin molecules have a diffusion coefficient of the order of $10^{-7}cm^2sec^{-1}$ while that for oxygen in blood is of the order of $10^{-5}cm^2sec^{-1}$. As indicated in [1], the dynamics of the solutions of these SPPPDEs are far different than those of the solutions of the SPDPPDEs. A lot

of work exists regarding singularly perturbed partial differential equations (SPPDEs), see, e.g., Cheng and Jia-qi [25], Burie et al. [18], Murray [110], Roos et al. [124] and the references therein. However, to the best of our knowledge, except the work of Ansari et al. [1] not much work has been done to solve SPDPPDE.

Nowadays, both fitted operator finite difference methods (FOFDMs) and fitted mesh finite difference methods (FMFDMs) are widely being used for singularly perturbed problems.

The basic idea behind the FOFDMs is to replace the denominator functions of the classical derivatives with positive functions derived in such a way that they capture some notable properties of the governing differential equation and hence provide reliable numerical results [116]. FOFDMs thus obtained are very stable for all the finite values of step-sizes [114].

While FOFDMs can provide a difference operator that reflects the dynamics of the solution on a uniform mesh, they sometimes suffer from the drawback that their construction is not always straightforward. In fact not many FOFDMs which are constructed for singularly perturbed two-point boundary value problems can easily be extended for singularly perturbed PDEs. The FMFDMs on the other hand are getting popularity because of their ease in the construction for multi-dimensional problems. Therefore, in this chapter, we design and analyze a FMFDM for a SPDPPDE described in (4.1.1)-(4.1.4). This problem has been solved earlier by Ansari et al. in [1]. Unlike the work in [1], the proposed approach has better convergence properties. Moreover, by adding some novel proofs for the *a priori* estimates, we strengthen the mathematical theory related to such problems.

The rest of the chapter is organized as follows. In Section 4.2, we derive estimates for the bounds on the solution $u(t, x)$ and its derivatives. Section 4.3 deals with the construction and analysis of the FMFDM whereas the same for the FOFDM is given in Section 4.4. In Section 4.5, we illustrate the performance of these methods through a test example. These results are discussed in Section 4.6 where we also provide some concluding remarks and scope for future work.

4.2   Qualitative properties of the solution

In this section we find estimates for the bounds on the solution $u(t, x)$ and its partial
derivatives using the method of steps [9].

Let us assume that the function $u(t, x) \in C^{3+\alpha, 4+\beta}(\overline{\Omega})$ where $0 < \alpha, \beta < 1$.

Let $T_\ell = [(\ell - 1)\tau, \ell\tau]$ and let $\Omega_\ell = T_\ell \times (0, 1)$ for $\ell = 0, \ldots, K$. Also, let $u_\ell(t, x)$ be
the restriction of $u(t, x)$ on Ω_ℓ, that is,

$$u_\ell(t, x) = u(t, x)|_{(t,x)\in\overline{\Omega}_\ell}, \ \ell = 1, \ldots, K.$$

Let $(\Pi_L)_\ell$ and $(\Pi_R)_\ell$ be the sets $T_\ell \times \{0\}$ and $T_\ell \times \{1\}$, respectively, and let $\partial\Omega_\ell = \{(\ell - 1)\tau\} \times [0, 1]$.

In Ω_ℓ problem (4.1.1)-(4.1.4) is transformed to a sequence of K singularly-perturbed
parabolic partial differential equations given by

$$\frac{\partial u_\ell(t, x)}{\partial t} - \varepsilon\frac{\partial^2 u_\ell(t, x)}{\partial x^2} + a_\ell(t, x)u_\ell(t, x) = f_\ell(t, x) - b(x)u_{\tau,\ell}(t, x), \ (t, x) \in \overline{\Omega}_\ell, \quad (4.2.1)$$

with the initial condition

$$u_\ell((\ell - 1)\tau, x) = u_{\ell-1}((\ell - 1)\tau, x), x \in [0, 1] \quad\quad\quad (4.2.2)$$

and boundary conditions

$$u_\ell(t, 0) = \Gamma_L(t), t \in T_\ell \quad\quad\quad (4.2.3)$$

and

$$u_\ell(t, 1) = \Gamma_R(t), t \in T_\ell, \quad\quad\quad (4.2.4)$$

for $\ell = 1, \ldots, K$.

The function $u_{\tau,\ell}(t, x)$ is given by

$$u_{\tau,\ell}(t, x) = u_{\ell-1}(t - \tau, x), \ \text{for } (t, x) \in \overline{\Omega}_\ell.$$

In the presentation below, C_ℓ and C will denote positive constants that are always independent of ε (and the mesh step sizes used in the later sections).

The following lemma presents bounds on the solution function $u(t, x)$:

Lemma 4.2.1 *If the initial function $u_0(t, x)$ is bounded by a constant at $t = 0$, then there exists a positive constant C such that $|u(t, x)| \leq C$ for all $(t, x) \in \overline{\Omega}$.*

Proof. The solution function $u(t, x)$ satisfies the compatibility conditions at the two corners $(0, 0)$ and $(0, 1)$, so does the function $u_1(t, x)$. This guarantees that

$$|u_1(t, x) - u_0(0, x)| \leq M_1 t,$$

where M_1 is a positive constant that is independent of ε. Hence,

$$|u_1(t, x)| - |u_0(0, x)| \leq |u_1(t, x) - u_0(0, x)| \leq M_1 t \leq M_1 \tau \Rightarrow |u_1(t, x)| \leq C_1,$$

where C_1 is a constant. This proves that $u_1(t, x)$ is bounded by C_1 in Ω_1.

In Ω_ℓ, $\ell = 2, \ldots, K$, the continuity of $u(t, x)$ implies that

$$u_\ell((\ell - 1)\tau, x) = u_{\ell-1}((\ell - 1)\tau, x), \ \ x \in [0, 1].$$

Then by using a similar argument as the above, we have

$$|u_\ell(t, x)| \leq C_\ell, \ \ \ell = 1, \ldots, K.$$

Let $C = \max_\ell \{C_\ell\}$, $\ell = 1, \ldots, K$, then

$$|u(t, x)| \leq C,$$

which completes the proof.

$\square$

Now, we prove that problem (4.1.1)-(4.1.4) satisfies a continuous maximum principle.

Lemma 4.2.2 *(Continuous Maximum principle) Let $\Phi(t, x)$ be a sufficiently smooth function satisfying $\Phi(t, x) \geq 0$ on $\partial\Omega$, then $L_\varepsilon \Phi(t, x) \geq 0$ in $\overline{\Omega}$ implies $\Phi(t, x) \geq 0$ for all $(t, x) \in \overline{\Omega}$.*

Proof. To begin with, let us define the differential operator L_ε in (4.1.1) by

$$L_\varepsilon \equiv \frac{\partial}{\partial t} - \varepsilon \frac{\partial^2}{\partial x^2} + a(t, x).$$

First we prove that the lemma is satisfied in Ω_1 and then we generalize the proof for Ω_ℓ.

In Ω_1, we assume that the function $\Phi(t, x)$ takes its minimum value at a point (t_1^*, x_1^*) and this minimum is negative, i.e.,

$$\Phi(t_1^*, x_1^*) = \min_{(t,x) \in \overline{\Omega}_1} \Phi(t, x) < 0,$$

then

$$\frac{\partial \Phi(t_1^*, x_1^*)}{\partial t} = \frac{\partial \Phi(t_1^*, x_1^*)}{\partial x} = 0 \text{ and } \frac{\partial^2 \Phi(t_1^*, x_1^*)}{\partial x^2} > 0.$$

Hence,

$$L_\varepsilon \Phi(t_1^*, x_1^*) = -\varepsilon \Phi_{xx}(t_1^*, x_1^*) + a(t_1^*, x_1^*)\Phi(t_1^*, x_1^*) < 0,$$

which is a contradiction and therefore,

$$\Phi(t, x) \geq 0 \text{ for all } (t, x) \in \overline{\Omega}_1.$$

This implies that $\Phi(\tau, x) \geq 0$.

Similarly, by using the result $\Phi(\tau, x) \geq 0$ along with $\Phi(t, 0) \geq 0$, $\Phi(t, 1) \geq 0$, $t \in T_2$ and $L_\varepsilon \Phi(t, x) \geq 0 \in \overline{\Omega}_2$ we obtain

$$\Phi(t, x) \geq 0 \text{ for all } (t, x) \in \overline{\Omega}_2,$$

and in general, given that $\Phi((\ell-1)\tau, x) \geq 0$ along with $\Phi(t, 0) \geq 0$, $\Phi(t, 1) \geq 0$, $t \in T_\ell$ and $L_\varepsilon \Phi(t, x) \geq 0$ in $\overline{\Omega}_\ell$ gives the result that

$$\Phi(t, x) \geq 0 \text{ for all } (t, x) \in \overline{\Omega}_\ell.$$

Proceeding in this manner, finally we get that

$$\Phi(t, x) \geq 0 \text{ for all } (t, x) \in \cup_{\ell=1}^{K} \overline{\Omega}_\ell = \overline{\Omega}.$$

$\square$

The following theorem gives the bounds on the derivatives of the solution.

Theorem 4.2.1 *Let* $b(x) \in C^{4+\beta}([0,1])$, $f(t,x) \in C^{3+\alpha,4+\beta}(\overline{\Omega})$, $u_0(t,x) \in C^{3+\alpha,4+\beta}(\overline{\Omega})$, Γ_L, $\Gamma_R \in C^{3+\alpha}([0,T])$ *and* $u(t,x) \in C^{3,4}(\overline{\Omega})$, *where* $\alpha, \beta \in (0,1)$. *Then, we have*

$$\left| \frac{\partial^{i+j} u(t,x)}{\partial t^i \partial x^j} \right| \leq C \left(1 + \varepsilon^{1-j/2} + \varepsilon^{-j/2} \left(e^{-x/\sqrt{\varepsilon}} + e^{-(1-x)/\sqrt{\varepsilon}} \right) \right), \tag{4.2.5}$$

for all the integers i *and* j *such that* $0 \leq 2i + j \leq 6$.

Proof. To find estimates for the bounds on the solution function $u(t, x)$ and its partial derivatives, we consider the stretched variable $\tilde{x} = x/\sqrt{\varepsilon}$ which transforms problem (4.1.1)-(4.1.4) into the following delayed parabolic partial differential equation

$$\frac{\partial \tilde{u}}{\partial t} - \frac{\partial \tilde{u}}{\partial \tilde{x}^2} + \tilde{a}(t, \tilde{x})\tilde{u} = \tilde{f} - \tilde{b}(\tilde{x})\tilde{u}(t - \tau, \tilde{x}) \tag{4.2.6}$$
$$(t, \tilde{x}) \in \widetilde{\Omega} = [0, T] \times [0, 1/\sqrt{\varepsilon}],$$

with the initial data

$$\tilde{u}(t, \tilde{x}) = u_0(t, \tilde{x}), \ (t, \tilde{x}) \in [-\tau, 0] \times \left[0, \frac{1}{\sqrt{\varepsilon}} \right] \tag{4.2.7}$$

and boundary conditions

$$\tilde{u}(t, 0) = \Gamma_L(t) \tag{4.2.8}$$

and

$$\tilde{u}\left(t, \frac{1}{\sqrt{\varepsilon}}\right) = \Gamma_R(t) \tag{4.2.9}$$

which by the method of steps can be transformed to a sequence of K parabolic partial differential equations of the form

$$\frac{\partial \tilde{u}_\ell}{\partial t} - \frac{\partial \tilde{u}_\ell}{\partial \tilde{x}^2} + \tilde{a}(t, \tilde{x})\tilde{u}_\ell = \tilde{f}_\ell - \tilde{b}(\tilde{x})\tilde{u}_\ell(t - \tau, \tilde{x}) \tag{4.2.10}$$

$$(t, \tilde{x}) \in \widetilde{\Omega}_\ell \equiv T_\ell \times \left[0, \frac{1}{\sqrt{\varepsilon}}\right],$$

with the initial data

$$\tilde{u}_\ell(t - \tau, \tilde{x}) = \tilde{u}_{\ell-1}(t - \tau, \tilde{x}), \ (t, \tilde{x}) \in T_\ell \times \left[0, \frac{1}{\sqrt{\varepsilon}}\right] \tag{4.2.11}$$

and boundary conditions

$$\tilde{u}_\ell(t, 0) = \Gamma_L(t), \ t \in T_\ell \tag{4.2.12}$$

and

$$\tilde{u}_\ell\left(t, \frac{1}{\sqrt{\varepsilon}}\right) = \Gamma_R(t), t \in T_\ell, \tag{4.2.13}$$

for $\ell = 1, \ldots, K$.

As is mentioned in [107] that problem (4.2.10)-(4.2.13) defined on $\widetilde{\Omega}_\ell$ is independent of ε, hence, the solution $\tilde{u}_\ell(t, \tilde{x})$ and its partial derivatives with respect to both t and $\tilde{x}$ must satisfy

$$\left| \frac{\partial^{i+j} \tilde{u}_\ell(t, \tilde{x})}{\partial t^i \partial \tilde{x}^j} \right| \le \widetilde{C}_\ell, \tag{4.2.14}$$

for all the non-negative integers i and j such that $2i+j \le 6$. In terms of the upstretched variable, (4.2.14) is reduced to

$$\left| \frac{\partial^{i+j} u_\ell(t, x)}{\partial t^i \partial x^j} \right| \le C_\ell \varepsilon^{-j/2}, \ 0 \le 2i + j \le 6. \tag{4.2.15}$$

This implies that

$$\left| \frac{\partial^{i+j} u(t, \tilde{x})}{\partial t^i \partial x^j} \right| \leq C \varepsilon^{-j/2},$$

for all the non-negative integers i and j such that $2i + j \leq 6$.

The above bounds do not show the explicit dependence on the boundary layer solutions. Therefore, to obtain stronger estimates for the bounds on the solution function $u(t, x)$ and its partial derivatives, we use the standard approaches, e.g., those given in [106, 107] for singular perturbation problems.

We decompose the solution $u(t, x)$ into its smooth and singular components $v(t, x)$ and $w(t, x)$ respectively, that is,

$$u(t, x) = v(t, x) + w(t, x),$$

where the function $v(t, x)$ satisfies

$$\frac{\partial v(t, x)}{\partial t} - \varepsilon \frac{\partial^2 v(t, x)}{\partial x^2} = f(t, x) - b(x) v(t - \tau, x), \ (t, x) \in \Omega, \qquad (4.2.16)$$

$$v(0, x) = u_0(0, x), \ x \in (0, 1), \qquad (4.2.17)$$

and the values of the function $v(t, x)$ at $x = 0$ and $x = 1$ are to be specified later such that the bounds on the first two partial derivatives of v with respect to x are independent of ε. The two terms asymptotic expansion for the smooth component $v(t, x)$ is

$$v(t, x) = v_0(t, x) + \varepsilon v_1(t, x),$$

where the function $v_0(t, x)$ satisfies the reduced problem

$$\frac{\partial v_0(t, x)}{\partial t} = f(t, x) - b(x) v_0(t - \tau, x), \ (t, x) \in \overline{\Omega}, \qquad (4.2.18)$$

$$v_0(0, x) = u_0(0, x), \ x \in (0, 1), \qquad (4.2.19)$$

whereas the function $v_1(t, x)$ satisfies

$$\frac{\partial v_1(t, x)}{\partial t} \quad - \quad \varepsilon \frac{\partial^2 v_1(t, x)}{\partial x^2} = -b(x)v_1(t - \tau, x) + \frac{\partial^2 v_0(t, x)}{\partial x^2}, \ (t, x) \in \overline{\Omega}$$

$$v_1(t, x) \quad = \quad 0, \ \ \text{for} \ (t, x) \in \partial \Omega.$$

On the other hand, the singular component $w(t, x)$ solves the problem

$$\frac{\partial w(t, x)}{\partial t} \quad - \quad \varepsilon \frac{\partial^2 w(t, x)}{\partial x^2} = -b(x)w(t - \tau, x), \ (t, x) \in \Omega \tag{4.2.20}$$

$$w(0, x) \quad = \quad 0, \tag{4.2.21}$$

$$w(t, 0) \quad = \quad u(t, 0) - v(t, 0), \tag{4.2.22}$$

$$w(t, 1) \quad = \quad u(t, 1) - v(t, 1) \tag{4.2.23}$$

and is further decomposed into the left boundary layer solution $w_L(t, x)$ and the right
boundary layer solution $w_R(t, x)$ respectively. The component w_L satisfies

$$\frac{\partial w_L(t, x)}{\partial t} \quad - \quad \varepsilon \frac{\partial^2 w_L(t, x)}{\partial x^2} = -b(x)w_L(t - \tau, x), \ (t, x) \in \overline{\Omega}, \tag{4.2.24}$$

$$w_L(t, x) \quad = \quad 0, \ \text{for} \ (t, x) \in [-\tau, 0] \times [0, 1], \tag{4.2.25}$$

$$w_L(t, 0) \quad = \quad \Gamma_L(t) - v_0(t, 0), \ \ \text{for} \ (t, x) \in [0, T] \times \{0\}, \tag{4.2.26}$$

$$w_L(t, 1) \quad = \quad 0, \ \ \text{for} \ t \in ([0, T] \tag{4.2.27}$$

and the component w_R satisfies

$$\frac{\partial w_R(t, x)}{\partial t} \quad - \quad \varepsilon \frac{\partial^2 w_R(t, x)}{\partial x^2} = -b(x)w_R(t - \tau, x), \ (t, x) \in \overline{\Omega}, \tag{4.2.28}$$

$$w_R(t, x) \quad = \quad 0, \ \text{for} \ (t, x) \in [-\tau, 0] \times [0, 1], \tag{4.2.29}$$

$$w_R(t, 0) \quad = \quad 0, \ \ \text{for} \ (t, x) \in ([0, T], \tag{4.2.30}$$

$$w_R(t, 1) \quad = \quad \Gamma_R(t) - v_0(t, 1), \ \ \text{for} \ (t, x) \in [0, T] \times \{1\}. \tag{4.2.31}$$

We find estimates for each component that belongs to either the smooth component
v or the singular component w.

The method of steps applied in this case, suggests that the function $v_0(t, x)$ should
be written as a union of functions $(v_0)_\ell(t, x)$ each defined on $\overline{\Omega}_\ell$ and satisfies a problem
of the form

$$\frac{\partial (v_0)_\ell(t, x)}{\partial t} = f_\ell(t, x) - b(x)(v_0)_\ell(t - \tau, x), \ \ (v_0)_0(0, x) = u_0(0, x), \ \ (t, x) \in \Omega_\ell.$$

Since each function $(v_0)_\ell$ is independent of ε, then for some constant C_ℓ the following
estimate is satisfied

$$\left| \frac{\partial^{i+j}(v_0)_\ell}{\partial t^i \partial x^j} \right| \leq C_\ell.$$

By taking $C = \max_\ell \{C_\ell\}, \ \ell = 1, \ldots, K$, the following estimates for the bounds on
$v_0(t, x)$ and its partial derivatives are obtained

$$\left| \frac{\partial^{i+j} v_0}{\partial t^i \partial x^j} \right| \leq C, \tag{4.2.32}$$

for all the integers i and j such that $0 \leq 2i + j \leq 6$.

Using the above procedure and the fact that the equation in $v_1(t, x)$ has the same
form as that for $u(t, x)$, we obtain

$$\left| \frac{\partial^{i+j} v_1}{\partial t^i \partial x^j} \right| \leq C \varepsilon^{-\frac{j}{2}}. \tag{4.2.33}$$

By using the estimates (4.2.32) and (4.2.33), we prove the following lemma.

Lemma 4.2.3 *The partial derivatives of $v(t, x)$ satisfy*

$$\left| \frac{\partial^{i+j} v}{\partial t^i \partial x^j} \right| \ \leq \ C \left(1 + \varepsilon^{1 - \frac{j}{2}} \right). \tag{4.2.34}$$

for all the integers i and j such that $0 \leq 2i + j \leq 6$.

In the following two lemmas we give bounds on $w_L(t, x)$ and $w_R(t, x)$. Proof of
which follows the barrier function approach described in [13] and [77].

□

Lemma 4.2.4 *The partial derivatives of $w_L(t, x)$ satisfy*

$$\left| \frac{\partial^{i+j} w_L}{\partial t^i \partial x^j} \right| \leq C\varepsilon^{-\frac{j}{2}} e^{-\frac{x}{\sqrt{\varepsilon}}}, \ (t, x) \in \overline{\Omega}. \tag{4.2.35}$$

for all the integers i and j such that $0 \leq 2i + j \leq 6$.

Proof. We transform problem (4.2.24)-(4.2.27) to a sequence of K singularly perturbed
parabolic partial differential equations of the form

$$\frac{\partial (w_L)_\ell(t, x)}{\partial t} - \varepsilon \frac{\partial^2 (w_L)_\ell(t, x)}{\partial x^2} = -b(x)(w_L)_\ell(t - \tau, x), \ (t, x) \in \overline{\Omega}_\ell, \tag{4.2.36}$$

$$(w_L)_\ell(t, 0) = \Gamma_L(t) - (v_0)_\ell(t, 0), \quad \text{for } (t, x) \in T_\ell \times \{0\}, \tag{4.2.37}$$

$$(w_L)_\ell(t, x) = 0, \quad \text{for } (t, x) \in (T_\ell \times \{1\}) \cup (\{0\} \times [0, 1]). \tag{4.2.38}$$

In each Ω_ℓ we define a barrier function

$$\Phi_\ell^\pm(t, x) = C_\ell e^{-\frac{x}{\sqrt{\varepsilon}}} \pm (w_L)_\ell(t, x).$$

It is clear that $\Phi_\ell^\pm(t, x) \geq 0$ for all $(t, x) \in \partial \Omega_\ell$ and is satisfying

$$L_\varepsilon \Phi_\ell^\pm(t, x) \geq 0,$$

for all $(t, x) \in \overline{\Omega}_\ell$. Then by Lemma 4.2.2, we have

$$\Phi_\ell^\pm(t, x) \geq 0, \quad \text{for all } (t, x) \in \overline{\Omega}_\ell,$$

which implies that

$$|(w_L)_\ell(t, x)| \leq C_\ell e^{-\frac{x}{\sqrt{\varepsilon}}}, \ (t, x) \in \overline{\Omega}_\ell.$$

By taking $C = \max\limits_{\ell}\{C_\ell\}, \ \ell = 1, \ldots, K$ we obtain the estimates

$$|w_L(t, x)| \ \leq \ Ce^{-\frac{x}{\sqrt{\varepsilon}}}, \ (t, x) \in \overline{\Omega}. \tag{4.2.39}$$

Now the problem in w_L also satisfies a continuous maximum principle and therefore, by using the transformation $\tilde{x} = x/\sqrt{\varepsilon}$ for problem (4.2.36)-(4.2.38) and the same technique that was used for finding bounds on the transformed problem (4.2.6)-(4.2.9), we obtain

$$\left|\frac{\partial^{i+j} w_L}{\partial t^i \partial x^j}\right| \leq C\, |w_L(t, x)| \leq C\varepsilon^{-\frac{j}{2}} e^{-\frac{x}{\sqrt{\varepsilon}}}. \tag{4.2.40}$$

$\square$

Lemma 4.2.5 *The partial derivatives of $w_L(t, x)$ satisfy*

$$\left|\frac{\partial^{i+j} w_R}{\partial t^i \partial x^j}\right| \leq C\varepsilon^{-\frac{j}{2}} e^{-\frac{1-x}{\sqrt{\varepsilon}}}, \ (t, x) \in \overline{\Omega}, \tag{4.2.41}$$

for all the integers i and j such that $0 \leq 2i + j \leq 6$.

Proof. Analogous to the proof of Lemma 4.2.4.

From the two lemmas 4.2.4 and 4.2.5 we see that

Lemma 4.2.6 *The partial derivatives of $w(t, x)$ satisfy*

$$\left|\frac{\partial^{i+j} w}{\partial t^i \partial x^j}\right| \leq C\varepsilon^{-\frac{j}{2}} \left(e^{-\frac{x}{\sqrt{\varepsilon}}} + e^{-\frac{1-x}{\sqrt{\varepsilon}}}\right), \ (t, x) \in \overline{\Omega}. \tag{4.2.42}$$

for all the integers i and j such that $0 \leq 2i + j \leq 6$.

Proof. The proof is accomplished by using the decomposition $w = w_L + w_R$ and the estimates (4.2.35) and (4.2.41).

Finally, the proof of the theorem is completed by using the estimates in Lemma 4.2.3 and 4.2.6.

$\square$

The above bounds on the solution will be used later in the analysis of the numerical
method.

4.3 A fitted mesh finite difference method

In this section we develop a numerical method for solving a singularly perturbed de-
lay parabolic partial differential equation. The proposed method consists of Crank-
Nicolson finite difference method constructed on a mesh of Shishkin type and hence
referred to as a fitted mesh finite difference method. We analyse the method for sta-
bility and convergence and found that it is unconditionally stable and converges with
order $\mathcal{O}\left(N_t^{-2} + N_x^{-2} \ln^2 N_x\right)$ where N_t and N_x are the numbers of subintervals in the t
and x directions, respectively.
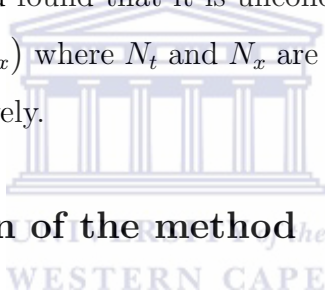
4.3.1 Construction of the method

Let N_x be a positive integer and let

$$\sigma = \min\{0.25, 2\sqrt{\varepsilon}\ln N_x\}$$

be the transition point. Let $N_x^\sigma = N_x/4$. To generate the Shishkin mesh we divide
each of the subintervals $[0, \sigma]$ and $[1 - \sigma, 1]$ into N_x^σ subintervals through the points
$x_0, \ldots, x_{N_x^\sigma}$ and $x_{3N_x^\sigma}, \ldots, x_{N_x}$, respectively, whereas the subinterval $[\sigma, 1-\sigma]$ is divided
into $2N_x^\sigma$ subintervals through the points $x_{N_x^\sigma}, \ldots, x_{3N_x^\sigma}$. The associated step-size $h_m =$
$x_{m+1} - x_m$ is then given by

$$
h_m = \begin{cases}
4\sigma/Nx, & \text{if } m \in \{0, \ldots, N_x^\sigma - 1\} \\[2em]
2(1 - 2\sigma)/N_x, & \text{if } m \in \{N_x^\sigma, \ldots, 3N_x^\sigma\} \\[2em]
4\sigma/Nx, & \text{if } m \in \{3N_x^\sigma + 1, \ldots, N_x\}.
\end{cases}
$$

Let N_t be any positive integer and $k = T/N_t$. We divide the interval $[0, T]$ into N_t subintervals through the points $t_0 = 0, \ldots, t_{N_t} = T$ where $t_{n+1} = t_n + k$. We assume that $T = K\tau$ for some positive integer K and that N_t is chosen in such a way that $\tau = t_s = sk$ for some positive integer s.

Let Ω^{N_t} denote $\{t_n : n = 0, \ldots, N_t\}$, $\Omega_\sigma^{N_x}$ denote $\{x_m : m = 0, \ldots, N_x\}$, where $N_x \geq 4$ and N denotes (N_t, N_x), then the fitted piecewise uniform mesh Ω_σ^N is given by the following tensor product grid

$$\Omega_\sigma^N = \Omega^{N_t} \times \Omega_\sigma^{N_x}.$$

Let U_m^n be the numerical approximation of $u(t_n, x_m)$, $D_x^+ U_m^n$, $D_x^- U_m^n$ and δ_x^2 be the forward, backward and central difference operators defined as

$$D_x^+ U_m^n = \frac{U_{m+1}^n - U_m^n}{x_{m+1} - x_m},$$

$$D_x^- U_m^n = \frac{U_m^n - U_{m-1}^n}{x_m - x_{m-1}}$$

and

$$\delta_x^2 U_m^n = \frac{(D_x^+ - D_x^-) U_m^n}{x_{m+1} - x_{m-1}}.$$

Furthermore, the approximations of the functions $a(t, x)$ and $f(t, x)$ at a local grid point (t_n, x_m) are denoted by a_m^n and f_m^n, respectively, whereas the value of the function $b(x)$ at x_m is denoted by b_m.

Our fitted mesh finite difference method (FMFDM) then consists of the Crank-Nicolson discretization for problem (4.1.1)-(4.1.4) on the Shishkin mesh (described above) and reads as

$$D_t^+ U_m^n - \frac{\varepsilon}{2} \left(\delta_x^2 U_m^n + \delta_x^2 U_m^{n+1} \right) + \frac{1}{2} (a_m^n U_m^n + a_m^{n+1} U_m^{n+1}) = \frac{1}{2} \left(f_m^n + f_m^{n+1} \right)$$

$$- \frac{1}{2} \left(b_m H_m^n + b_m H_m^{n+1} \right), \quad (4.3.1)$$

along with the initial data

$$U_m^0 = u_0(0, x_m) \tag{4.3.2}$$

and boundary conditions

$$U_0^n = \Gamma_L(t_n, 0) \tag{4.3.3}$$

and

$$U_{N_x}^n = \Gamma_R(t_n, 1). \tag{4.3.4}$$

The term H_m^n in (4.3.1) is called the history term and is given by

$$H_m^n = \begin{cases} u_0(t_n - \tau, x_m), & \text{if } t_n < \tau, \\ \\ U_m^{n-s}, & \text{if } t_n \geq \tau. \end{cases} \tag{4.3.5}$$

Expanding (4.3.1), we obtain

$$\frac{U_m^{n+1} - U_m^n}{k} - \frac{\varepsilon}{2} \frac{\frac{U_{m+1}^{n+1} - U_m^{n+1}}{h_m} - \frac{U_m^{n+1} - U_{m-1}^{n+1}}{h_{m-1}} + \frac{U_{m+1}^n - U_m^n}{h_m} - \frac{U_m^n - U_{m-1}^n}{h_{m-1}}}{\frac{h_m + h_{m-1}}{2}}$$

$$+ \frac{1}{2}\left(a_m^n U_m^n + a_m^{n+1} U_m^{n+1}\right) = \frac{1}{2}\left(\left(f_m^n + f_m^{n+1}\right) - b_m(H_m^n + H_m^{n+1})\right)$$

$$m = 1, \ldots, N_x - 1; \ n = 0, \ldots, N_t - 1,$$

which can be simplified to

$$-\frac{\varepsilon}{h_{m-1}(h_m + h_{m-1})} U_{m-1}^{n+1} + \left(\frac{1}{k} + \frac{\varepsilon}{h_m h_{m-1}} + \frac{a_m^{n+1}}{2}\right) U_m^{n+1} - \frac{\varepsilon}{h_m(h_m + h_{m-1})} U_{m+1}^{n+1}$$

$$= \frac{\varepsilon}{h_{m-1}(h_m + h_{m-1})} U_{m-1}^n + \left(\frac{1}{k} - \frac{\varepsilon}{h_m h_{m-1}} - \frac{a_m^n}{2}\right) U_m^n + \frac{\varepsilon}{h_m(h_m + h_{m-1})} U_{m+1}^n$$

$$+ \frac{1}{2}\left(\left(f_m^n + f_m^{n+1}\right) - b_m\left(H_m^n + H_m^{n+1}\right)\right). \tag{4.3.6}$$

Equation (4.3.6) can further be written as a linear system of the form

$$T_L U^{n+1} = T_R U^n + \frac{1}{2} \left(\left(f^n + f^{n+1} \right) - b \star \left(H^n + H^{n+1} \right) + \left(g^n + g^{n+1} \right) \right), \qquad (4.3.7)$$

for $n = 1, \ldots, N_t - 1$, where $\star$ denotes the componentwise multiplication of the two vectors and T_L and T_R are two tridiagonal matrices given by

$$T_L = \text{Tri} \left(-\frac{\varepsilon}{h_{m-1}(h_m + h_{m-1})}, \frac{1}{k} + \frac{\varepsilon}{h_m h_{m-1}} + \frac{a_m^{n+1}}{2}, -\frac{\varepsilon}{h_m(h_m + h_{m-1})} \right),$$

and

$$T_R = \text{Tri} \left(\frac{\varepsilon}{h_{m-1}(h_m + h_{m-1})}, \frac{1}{k} - \frac{\varepsilon}{h_m h_{m-1}} - \frac{a_m^n}{2}, \frac{\varepsilon}{h_m(h_m + h_{m-1})} \right)$$

$$m = 1, \ldots, N_x.$$

Furthermore, the vector g^n is given by

$$g^n = \left[\frac{\varepsilon(U_0^n + U_0^{n+1})}{h_0(h_1 + h_0)}, 0, \ldots, 0, \frac{\varepsilon(U_{N_x}^n + U_{N_x}^{n+1})}{h_{N_x-1}(h_{N_x-2} + h_{N_x-1})} \right]^T \in \mathbb{R}^{N_x-1}.$$

The numerical solution is obtained by solving equation (4.3.7) along with equations (4.3.2)-(4.3.5).

4.3.2 Convergence of the method

The convergence analysis presented in this section is based on some of the approaches used in [107].

Let Φ_m^n be any mesh function on Ω_σ^N and from (4.3.1) we define the discrete operator L_ε^N at (t_n, x_m) as

$$L_\varepsilon^N \Phi_m^n \equiv D^+ \Phi_m^n - \frac{\varepsilon}{2} \left(\delta_x^2 \Phi_m^n + \delta_x^2 \Phi_m^{n+1} \right) + \frac{1}{2} \left(a_m^n \Phi_m^n + a_m^{n+1} \Phi_m^{n+1} \right).$$

We show that the following discrete maximum principle is satisfied.

Lemma 4.3.1 *Assume that $\Phi_m^n \geq 0$ on the boundaries of Ω_σ^N. Then $L_\varepsilon^N \Phi_m^n \geq 0$ on Ω_σ^N implies that $\Phi_m^n \geq 0$ on Ω_σ^N.*

Proof. Assume that $\Phi_m^n < 0$ for some n, m, and its minimum denoted by Φ^* is achieved at a point (t_{n^*}, x_{m^*}). Then $D^+ \Phi^* = 0$ and $\delta_x^2 \Phi^* > 0$.

Now we can choose N_t big enough in order to have either $\Phi_{m^*}^{n^*+1} < 0$ or $\left| \Phi_{m^*}^{n^*} \right| > \left| \Phi_{m^*}^{n^*+1} \right|$ and $\delta_x^2 \Phi_{m^*}^{n^*+1} \geq 0$. Then

$$L_\varepsilon^N \Phi_{m^*}^{n^*} < 0,$$

which is a contradiction. Thus $\Phi_m^n \geq 0$ at any mesh point (t_n, x_m).

We also note that the above mesh function satisfies the stability estimate provided in the following lemma.

Lemma 4.3.2 *Let Φ be any mesh function satisfying $\Phi_m^n = 0$ on $\partial\Omega_\sigma^N$ and $\bar{a} = \min\limits_{m,n}\{a_m^n\}$, $m = 0, \ldots, N_x$ and $n = 0, \ldots, N_t$. Then*

$$\begin{cases} |\Phi_m^n| \leq (1+T) \max \left| L_\varepsilon^N \Phi_m^n \right|, & \text{if } \bar{a} = 0 \\[3mm] |\Phi_m^n| \leq \frac{1+T}{\bar{a}} \max \left| L_\varepsilon^N \Phi_m^n \right|, & \text{if } \bar{a} > 0 \end{cases}$$

Proof. Let $\widetilde{M}$ denotes $\max\limits_{m,n} \left| L_\varepsilon^N \Phi_m^n \right|$. We define a barrier function $(\Psi_m^n)^{\pm}$ as

$$(\Psi_m^n)^{\pm} = \begin{cases} (1+t)\widetilde{M} \pm \Phi_m^n, & \text{if } \bar{a} = 0 \\[3mm] \frac{1+T}{\bar{a}}\widetilde{M} \pm \Phi_m^n, & \text{if } \bar{a} > 0 \end{cases}$$

Since $\Phi_m^n = 0$ on $\partial\Omega_\sigma^N$ and $\widetilde{M} > 0$ on $\partial\Omega_\sigma^N$, then on $\partial\Omega_\sigma^N$ we have

$$(\Psi_m^n)^{\pm} = \begin{cases} (1+t)\widetilde{M}, & \text{if } \bar{a} = 0 \\[3mm] \frac{1+T}{\bar{a}}\widetilde{M}, & \text{if } \bar{a} > 0 \end{cases} \geq \begin{cases} \widetilde{M}, & \text{if } \bar{a} = 0 \\[3mm] \frac{1+T}{\bar{a}}\widetilde{M}, & \text{if } \bar{a} > 0 \end{cases} \geq \quad 0.$$

Now,

$$
L_\varepsilon^N \left(\Psi_m^n\right)^\pm =
\begin{cases}
\widetilde{M} \pm L_\varepsilon^N \Phi_m^n, & \text{if } \bar{a} = 0 \\[3ex]
\frac{(1+T)}{2\bar{a}} \widetilde{M} \left(a_m^n + a_m^{n+1}\right) \pm L_\varepsilon^N \Phi_m^n \geq (1+T)\widetilde{M} \pm L_\varepsilon \Phi_m^n & \text{if } \bar{a} > 0
\end{cases}
$$
$$
\geq \quad 0
$$

on Ω_σ^N.

Using the discrete maximum principle, we have $(\Psi_m^n)^\pm \geq 0$ on Ω_σ^N. The proof is then completed by noticing that $0 \leq t \leq T$.

Now, we find an error estimate in approximating the exact solution $u(t_n, x_m)$ by the numerical solution U_m^n using the FMFDM. To simplify the notations, we denote the quantity $f(t_n, x_m) - b_m H_m^n$ by G_m^n and the values of a mesh function Φ at the boundaries of Ω by $\Phi(\partial\Omega_\sigma^N)$. That is,

$$
\Phi(\partial\Omega_\sigma^N) = \Phi(t_n, x_m), \quad (t_n, x_m) \in \partial\Omega_\sigma^N.
$$

We decompose the numerical solution U into its smooth and singular components V and W respectively, that is,

$$
U = V + W,
$$

where the smooth component V satisfies

$$
L_\varepsilon V_m^n = \frac{1}{2} \left(G_m^n + G_m^{n+1}\right), \; V\left(\partial\Omega_\sigma^N\right) = v\left(\partial\Omega_\sigma^N\right)
$$

and the singular component W satisfies

$$
L_\varepsilon W_m^n = 0, \; W\left(\partial\Omega_\sigma^N\right) = u\left(\partial\Omega_\sigma^N\right) - v\left(\partial\Omega_\sigma^N\right).
$$

The error at the point (t_n, x_m) is then given by

$$u(t_n, x_m) - U_m^n = v(t_n, x_m) - V_m^n + w(t_n, x_m) - W_m^n,$$

which by the triangle inequality implies that

$$|u(t_n, x_m) - U_m^n| = |v(t_n, x_m) - V_m^n| + |w(t_n, x_m) - W_m^n|. \tag{4.3.8}$$

Thus,

$$
\begin{aligned}
L_\varepsilon^N & (V_m^n - v(t_n, x_m)) \\
&= L_\varepsilon^N V_m^n - L_\varepsilon^N v(t_n, x_m) \\
&= \frac{1}{2}\left(G_m^n + G_m^{n+1}\right) - L_\varepsilon^N(v(t_n, x_m)) \\
&= \frac{1}{2}\left(G_m^n + G_m^{n+1}\right) - \left(D^+ - \frac{\partial}{\partial t}\right)v(t_n, x_m) \\
&\quad + \varepsilon\left(\frac{\delta_x^2 v(t_n, x_m) + \delta_x^2 v(t_{n+1}, x_m)}{2} - \frac{\partial^2}{\partial x^2}v(t_n, x_m)\right) \\
&= \frac{1}{2}\left(G_m^n + G_m^{n+1}\right) - \frac{N_t^{-2}}{12}\left(\varepsilon v_{xxttt}(\xi, x_m) + (av)_{ttt}(\xi, x_m) + f_{ttt}(\xi, x_m)\right) \\
&\quad + \begin{cases} \varepsilon\frac{h_{m+1} - h_m}{3} v_{xxx}(t_n, \zeta), & \text{if } x_m = \sigma \text{ or } x_m = 1 - \sigma \\[2ex] -\varepsilon\frac{h_{m+1}^2 - h_m h_{m+1} + h_m^2}{12} v_{xxxx}(t_n, \zeta), & \text{otherwise} \end{cases}
\end{aligned}
$$

which implies that

$$
|L_\varepsilon^N(V_m^n - v(t_n, x_m))| \tag{4.3.9}
$$

$$
\leq \quad \frac{N_t^{-2}}{12} \left(\varepsilon |v_{xxttt}| + |a_{ttt}| |v| + |a(t_n, x_m)| |v_{ttt}| + |f_{ttt}| \right) (\xi, x_m)
$$

$$
+ \begin{cases}
\varepsilon \left| \frac{h_m - h_{m-1}}{3} \right| |v_{xxx}(t_n, \zeta)|, & \text{if } x_m = \sigma \text{ or } x_m = 1 - \sigma \\[2ex]
\varepsilon \left| \frac{h_m^2 - h_m h_{m+1} + h_{m+1}^2}{12} \right| |v_{xxxx}(t_n, \zeta)| & \text{otherwise,}
\end{cases}
$$

$$
\leq \begin{cases}
\varepsilon \left| \frac{h_m - h_{m-1}}{3} \right| |v_{xxx}(t_n, \zeta)|, & \text{if } x_m = \sigma \text{ or } x_m = 1 - \sigma \\[2ex]
\varepsilon \left| \frac{h_m^2 - h_m h_{m+1} + h_{m+1}^2}{12} \right| |v_{xxxx}(t_n, \zeta)| & \text{otherwise,}
\end{cases}
$$

$$
\leq \begin{cases}
C \left(N_t^{-2} + N_x^{-1} \ln N_x \right), & \text{if } x_m = \sigma \text{ or } x_m = 1 - \sigma \\[2ex]
C \left(N_t^{-2} + N_x^{-2} \right), & \text{otherwise.}
\end{cases} \tag{4.3.10}
$$

Defining a barrier function

$$
\phi(t_n, x_m) = C \left(\frac{\sigma}{\varepsilon} N_x^{-2} \theta(x_m) + (1 + t_n) N_x^{-2} + t_n N_t^{-2} \right)
$$

where

$$
\theta(x) = \begin{cases}
\frac{x}{\sigma}, & \text{if } 0 \leq x \leq \sigma \\[2ex]
1, & \text{if } \sigma \leq x \leq 1 - \sigma \\[2ex]
\frac{1-x}{\sigma}, & \text{if } 1 - \sigma \leq x \leq 1
\end{cases}
$$

and applying the discrete maximum principle (Lemma 4.3.2), we have

$$
|V_m^n - v(t_n, x_m)| \leq \begin{cases}
C \left(N_t^{-2} + N_x^{-2} \ln^2 N_x \right), & \text{if } x_m = \sigma \text{ or } x_m = 1 - \sigma \\[2ex]
C \left(N_t^{-2} + N_x^{-2} \right), & \text{otherwise.}
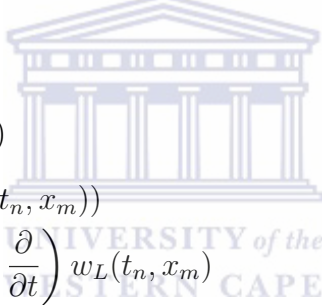\end{cases} \tag{4.3.11}
$$

On the otherhand, the singular component W is decomposed into its left boundary solution W_L and right boundary solution W_R, that is,

$$W = W_L + W_R$$

and hence the error can be written as

$$W_m^n - w(t_n, x_m) = (W_L)_m^n - w_L(t_n, x_m) + (W_R)_m^n - w_R(t_n, x_m).$$

We estimate the errors $(W_L)_m^n - w_L(t_n, x_m)$ and $(W_R)_m^n - w_R(t_n, x_m)$, separately. We have

$$
\begin{aligned}
L_\varepsilon^N ((W_L)_m^n &- w_L(t_n, x_m)) \\
&= -L_\varepsilon^N (w_L(t_n, x_m)) \\
&\leq -\left(D^+ - \frac{\partial}{\partial t} \right) w_L(t_n, x_m) \\
&\quad + \varepsilon \left(\frac{\delta_x^2 w_L(t_n, x_m) + \delta_x^2 w_L(t_{n+1}, x_m)}{2} - \frac{\partial^2}{\partial x^2} w_L(t_n, x_m) \right) \\
&= \frac{N_t^{-2}}{12} \left((w_L)_{xxttt} + (aw_L)_{ttt} \right) (\xi, x_m) \\
&\quad - \begin{cases} \varepsilon \frac{h_{m+1} - h_m}{3} (w_L)_{xxx}(t_n, \zeta), & \text{if } x_m = \sigma \text{ or } x_m = 1 - \sigma \\[2ex] -\varepsilon \frac{h_{m+1}^2 - h_m h_{m+1} + h_m^2}{12} (w_L)_{xxxx}(t_n, \zeta), & \text{otherwise.} \end{cases}
\end{aligned}
$$

By taking the absolute values of the two sides, applying the triangle inequality, using the estimates of the bounds on w_L from Lemma 4.2.4 and simplifying further, we obtain

$$\left| L_\varepsilon^N ((W_L)_m^n - w_L(t_n, x_m)) \right| \leq C \left(N_t^{-2} + \left(N_x^{-1} \ln N_x \right)^2 \right).$$

Finally, applying Lemma 4.3.2, we obtain

$$|(W_L)_m^n - w_L(t_n, x_m)| \leq C\left(N_t^{-2} + \left(N_x^{-1}\ln N_x\right)^2\right). \tag{4.3.12}$$

Similarly, we can prove that

$$|(W_R)_m^n - w_R(t_n, x_m)| \leq C\left(N_t^{-2} + \left(N_x^{-1}\ln N_x\right)^2\right). \tag{4.3.13}$$

Combining equation (4.3.8) and equations (4.3.11)-(4.3.13), we have the following theorem.

Theorem 4.3.1 *The FMFDM (4.3.1)-(4.3.4) is convergent with the order $\mathcal{O}(N_t^{-2} + N_x^{-2}\ln^2 N_x)$ in the sense that*

$$\sup_{0<\varepsilon\leq 1}\max_{1\leq m,n\leq N-1}|u(t_n, x_m) - U_m^n| \leq C(N_t^{-2} + N_x^{-2}\ln^2 N_x).$$

where U is the numerical solution obtained by the FMFDM (4.3.1)-(4.3.4) and N is the total number of subintervals taken in either directions.

In the next section we develop a fitted operator finite difference method for solving the problem under consideration.

4.4   A fitted operator finite difference method

This method is constructed by replacing the classical differential operator with a fitted operator based on Crank-Nicolson's discretization. The proposed method is analyzed for stability and convergence and it is found that this method is unconditionally stable and is convergent with order $\mathcal{O}(k^2 + h^2)$, where k and h are respectively the time and space step-sizes.

4.4.1 Construction of method

We partition the domain $\overline{\Omega} = [0, T] \times [0, 1]$ through the grid points (t_n, x_m) where $t_n = n\Delta t$, $x_m = m\Delta x$; $\Delta t = k = T/N_t$, $\Delta x = h = 1/N_x$, $n = 0, \ldots, N_t$, $m = 0, \ldots, N_x$ and N_t and N_x are the total number of subintervals in time and spatial directions respectively. Assume that N_t has been chosen such that $\tau = s\Delta t = sk$ where s is any positive integer.

We discretize the SPDPPDE (4.1.1)-(4.1.4) by the fitted Crank-Nicolson's scheme which reads as

$$\frac{U_m^{n+1} - U_m^n}{k} - \frac{\varepsilon}{2} \frac{U_{m-1}^{n+1} - 2U_m^{n+1} + U_{m+1}^{n+1} + U_{m-1}^n - 2U_m^n + U_{m+1}^n}{\phi_m^2} =$$
$$\frac{1}{2} \left(f(t_n, x_m) + f(t_{n+1}, x_m) \right) - \frac{b(x_m)e^{-\tau}}{2} \left(H_m^n + H_m^{n+1} \right), \tag{4.4.1}$$

where
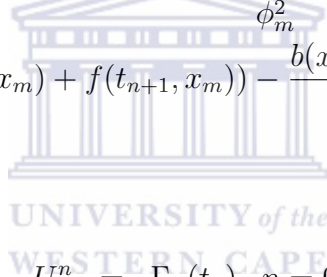
$$U_0^n = \Gamma_L(t_n), \ n = 0, \ldots, N_t, \tag{4.4.2}$$

$$U_{N_x-1}^n = \Gamma_R(t_n), \ n = 0, \ldots, N_t, \tag{4.4.3}$$

and H_m^n denotes the delayed term $u(t_n - \tau)$ which is evaluated as

$$H_m^n = \begin{cases} \theta(t_n - \tau, x_m), & \text{if } t_n < \tau, \ m = 0, \ldots, N_x \\ \\ U_m^{n-s}, & \text{if } t_n \geq \tau, \ m = 0, \ldots, N_x. \end{cases} \tag{4.4.4}$$

The function ϕ_m^2 in (4.4.1) above is called the denominator function ([102]) and it replaces the classical denominator h^2 with a function of h and ε. A suitable expression for this function for the problem under consideration is

$$\phi_m(h) = \frac{2}{\rho_m} \sinh \frac{\rho_m h}{2} \tag{4.4.5}$$

where $\rho_m = \sqrt{b(x_m)e^{-\tau}/\varepsilon} : \ m = 0, \ldots, N_x$.

Method (4.4.1)-(4.4.3) can be written as a linear system of the form

$$T_L v^{n+1} = T_R v^n + \frac{1}{2}\left(F^n + F^{n+1}\right) + \frac{1}{2}\left(g^n + g^{n+1}\right), \tag{4.4.6}$$

where $v^\ell = [U_1^\ell, \dots, U_{N_x-1}^\ell]^T$ and T_L and T_R are tri-diagonal matrices whose entries are given by

$$T_L(n,m) = \begin{cases} -\frac{\varepsilon}{2\phi_{m+1}^2}, & \text{if } n = m-1 \\[2mm] \frac{1}{k} + \frac{\varepsilon}{\phi_m^2}, & \text{if } n = m \\[2mm] -\frac{\varepsilon}{2\phi_m^2}, & \text{if } n = m+1 \\[2mm] 0, & \text{otherwise,} \end{cases} \tag{4.4.7}$$

and

$$T_R(n,m) = \begin{cases} \frac{\varepsilon}{2\phi_{m+1}^2}, & \text{if } n = m-1 \\[2mm] \frac{1}{k} - \frac{\varepsilon}{\phi_m^2}, & \text{if } n = m \\[2mm] \frac{\varepsilon}{2\phi_m^2}, & \text{if } n = m+1 \\[2mm] 0, & \text{otherwise,} \end{cases} \tag{4.4.8}$$

for all $m = 1, \dots, N_x - 1$.

The entries of the vectors g^ℓ and F^ℓ are given by

$$
g_m^\ell = \begin{cases}
\frac{\varepsilon}{2\phi_1^2}U_0^\ell, & \text{if } m = 0 \\[2ex]
0, & \text{if } 1 \leq m \leq N_x - 3 \\[2ex]
\frac{\varepsilon}{2\phi_{N_x-1}^2}U_{N_x}^\ell, & \text{if } m = N_x - 2
\end{cases}
$$

and

$$
F^\ell = \left[f_1^\ell - b \star H_1^\ell, \ldots, f_{N_x-1}^\ell - b \star H_{N_x-1}^\ell \right]^T,
$$

where $\star$ denotes the componentwise multiplication of the components of vectors b and $H_{N_x-1}^{n+1}$.

Method consisting of (4.4.1)-(4.4.4) is termed as the fitted operator finite difference method (FOFDM). The numerical solution with this method is then obtained by solving the linear system (4.4.6) for all the levels $n = 1, 2, \ldots, N_t$.

4.4.2   Analysis of the numerical method

In this section we discuss the consistency and stability of the proposed method which will then imply the convergence through the equivalence theorem of Lax [108, 125].

Consistency

The local truncation error (LTE) at the grid point (t_n, x_m) is given by

$$
\begin{aligned}
\text{LTE} &= -\frac{\varepsilon k^2}{12}u_{tttxx}(\xi, x_m) + \frac{\varepsilon k^2}{12}f_{ttt}(\xi, x_m) - \varepsilon\frac{h^2}{12}u_{xxxx}(t_n, \zeta) \\
&\quad + \frac{\varepsilon}{2}\left(\frac{1}{h^2} - \frac{1}{\phi_m^2}\right)\left(U_{m+1}^n - 2U_m^n + U_{m-1}^n + U_{m+1}^{n+1} - 2U_m^{n+1} + U_{m-1}^{n+1}\right), \quad (4.4.9)
\end{aligned}
$$

where $\xi \in [t_n, t_n + k]$ and $\zeta \in [x_m - h, x_m + h]$.

From (4.2.5) we have

$$|u_{tttxx}(t,x)| \leq C\left(1 + \varepsilon + \varepsilon^{2-1} + \varepsilon^{-1}\left(e^{-x/\sqrt{\varepsilon}} + e^{(1-x)/\sqrt{\varepsilon}}\right)\right).$$

Thus the first term on the right hand side of (4.4.9) satisfies

$$
\begin{aligned}
\left|-\frac{\varepsilon k^2}{12}u_{tttxx}(\xi, x_m)\right| &\leq \frac{k^2 C}{12}\left(\varepsilon + 2\varepsilon^2 + \left(e^{-x/\sqrt{\varepsilon}} + e^{(1-x)/\sqrt{\varepsilon}}\right)\right) \\
&\leq Ck^2 \to 0 \text{ as } k \to 0. \quad\quad (4.4.10)
\end{aligned}
$$

Since the function $f(t,x)$ and its partial derivatives with respect to both t and x are assumed to be continuous, $\partial^{i+j} f/\partial t^i x^j$ is bounded by a constant $\widetilde{M}$ for all $i \geq 0$ and $j \geq 0$. Therefore, the second term on the right hand side of (4.4.9) satisfies

$$\left|\frac{\varepsilon k^2}{12}f_{ttt}(\xi, x_m)\right| \leq \frac{\varepsilon k^2 \widetilde{M}}{12} \leq \widetilde{M}k^2 \to 0 \text{ as } k \to 0. \quad\quad (4.4.11)$$

Also, from (4.2.5), we have

$$|u_{xxxx}(t,x)| \leq C\left(1 + \varepsilon + \varepsilon^0 + \varepsilon^{-2}\left(e^{-x/\sqrt{\varepsilon}} + e^{(1-x)/\sqrt{\varepsilon}}\right)\right)$$

yielding that the second term on the right hand side of (4.4.9) is bounded by

$$\left|\varepsilon\frac{h^2}{12}u_{xxxx}(t_n, \zeta)\right| \leq C\frac{h^2}{12}\left(2\varepsilon + \varepsilon^2 + \varepsilon^{-1}\left(e^{-x/\sqrt{\varepsilon}} + e^{(1-x)/\sqrt{\varepsilon}}\right)\right).$$

Then, using Lemma 4.2 of [115] on the exponential behaviour of the solution, we have

$$\left|\varepsilon\frac{h^2}{12}u_{xxxx}(t, \zeta)\right| \leq \frac{Ch^2}{12}\left(2\varepsilon + \varepsilon^2\right) \leq Ch^2 \to 0 \text{ as } h \to 0. \quad\quad (4.4.12)$$

Furthermore, we have

$$\phi_m^2 = \frac{4}{\rho_m^2}\sinh^2\frac{\rho_m h}{2} = h^2\left(1 + \left(\frac{\rho_m h}{2}\right)^2 + \ldots\right) = h^2\left(1 + \mathcal{O}\left(\frac{h^2}{\varepsilon}\right)\right),$$

we find

$$\varepsilon\left(\frac{1}{h^2} - \frac{1}{\phi_m^2}\right) = \frac{\varepsilon\mathcal{O}(h^4/\varepsilon)}{h^2(1 + (\rho_m h/2)^2 + \ldots)} = \frac{\mathcal{O}(h^2)}{(1 + (\rho_m h/2)^2 + \ldots)} \qquad (4.4.13)$$

and we conclude that the fourth term on the right hand side of (4.4.9) tends to 0 as $h \to 0$.

Combining all the above information, we conclude that $|\text{LTE}| \to 0$ as $k \to 0$ and $h \to 0$ which proves the consistency of the method.

Stability

We use the matrix method [132] to analyze the stability of our method.

We rewrite the linear system (4.4.6) as

$$
\begin{aligned}
T_L U^{n+1} &= T_R U^n + \frac{1}{2}\left(f^n + f^{n+1} - \left(b^n \star H^n + b^{n+1} \star H^{n+1}\right)\right) + \left(g^n + g^{n+1}\right) \\
&= T_R U^n + \frac{1}{2}\left(F^n + F^{n+1}\right), \qquad\qquad\qquad\qquad\qquad\qquad (4.4.14)
\end{aligned}
$$

where $F^n = f^n - b^n \star H^n + g^n$.

Let $v^n = [u(t_n, x_1), \ldots, u(t_n, x_{N_x - 1})]^T$ and let $e^n = U^n - v^n$ be the difference between the approximate and exact solutions at level n.

If we insert the exact solution instead of the numerical solution in equation (4.4.6), we obtain an equation of the form

$$T_L v^{n+1} = T_R v^n + \frac{1}{2}\left(F^n + F^{n+1}\right). \qquad (4.4.15)$$

Multiplying both equations (4.4.14) and (4.4.15) by k and subtracting the latter from the former, we obtain the linear system

$$T_L' e^{n+1} = T_R' e^n - \frac{k}{2}\left(G^n + G^{n+1}\right), \qquad (4.4.16)$$

where $T_L' = kT_L$, $T_R' = kT_R$ and $G^n = -b^n \star H^n + g^n$.

Since the two matrices T'_L and T'_R are strictly diagonally dominant matrices, therefore, by Levy-Desplanques theorem [61, 145], they are nonsingular. By Gershgorin's disk theorem ([61]), each eigenvalue λ_m of the matrix T'_L should lie in one of the Gershgorin's disks $D_L^{\phi_m}\left(1 + \frac{2k\varepsilon}{\phi_m^2}, \frac{2k\varepsilon}{\phi_m^2}\right)$. Hence, all the eigenvalues of the matrix T'_L lie in $\bigcup_{m=1}^{N_x-1} D_L^{\phi_m}$, yielding that $\lambda_m > 1$ for all $m = 1, 2, \ldots, N_x - 1$.

We rearrange all the eigenvalues of T'_L such that

$$0 < \lambda_1 \leq \ldots \leq \lambda_{N_x-1}.$$

Similarly, we find that all the eigenvalues μ_m; $m = 1, \ldots, \mu_{N_x-1}$ of T'_R lie in the union of the Gershgorin disks

$$\bigcup_{m=1}^{N_x-1} D_R^{\phi_m}\left(1 - \frac{2k\varepsilon}{\phi_m^2}, \frac{2k\varepsilon}{\phi_m^2}\right).$$

It is obvious that each eigenvalue μ_m of T'_R satisfies $0 < \mu_m \leq 1$. If we rearrange the eigenvalues of T'_R such that $\mu_j \leq \mu_m$ for $j < m$, then, the eigenvalues of the two matrices T'_L and T'_R satisfy the relation

$$0 < \mu_1 \leq \ldots \leq \mu_{N_x-1} \leq 1 \leq \lambda_1 \leq \ldots \leq \lambda_{N_x-1}.$$

Let $B = T'^{-1}_L$ and $A = BT'_R$, then the solution of system (4.4.16) can be written as

$$
\begin{aligned}
e^{n+1} &= A\left(e^n + \frac{k}{2}\left(b^n \star (H^n - v_\tau^n) + b^{n+1} \star \left(H^{n+1} - v_\tau^{n+1}\right)\right)\right), \\
&= Ae^n + \frac{k}{2}B\left(b^n \star (H^n - v_\tau^n) + b^{n+1} \star \left(H^{n+1} - v_\tau^{n+1}\right)\right). \quad (4.4.17)
\end{aligned}
$$

We would like to show that the defect vector e which propagates over time, does not increase indefinitely. To this end, we note that the eigenvalues of A which are given by $\gamma_m = \mu_m/\lambda_m$ satisfy $0 < \gamma_m < 1$ while the eigenvalues of $B = T'^{-1}$ (which are given by $\nu_m = 1/\lambda_m$)) also satisfy the relation $0 < \nu_m < 1$ for all $m = 1, \ldots, N_x - 1$.

Since A is nonsingular (as neither of its eigenvalues γ_m is zero), it has a complete set of linearly independent eigenvectors φ_m corresponding to the eigenvalues γ_m, $m = 1, \ldots, N_x{-}1$. Then, the set ω_m is a basis for $\mathbb{R}^{N_x-1}$. Also, B has a complete set of linearly independent eigenvectors ϑ_m, $m = 1, \ldots, N_x - 1$ corresponding to the eigenvalues ν_m which form a basis for $\mathbb{R}^{N_x-1}$.

Using the two different bases φ_m and ϑ_m, the vector e^0 can have two different representations of the forms

$$e^0 = \sum_{m=1}^{N_x-1} \omega_m \varphi_m = \sum_{m=1}^{N_x-1} \delta_m \vartheta_m, \tag{4.4.18}$$

where ω_m and δ_m are constants, $m = 1, \ldots, N_x - 1$.

We consider (4.4.16) in two separate intervals, namely $[0, \tau]$ and $(\tau, T]$. In $[0, \tau]$ where $n \leq s$, the history terms H^n are evaluated exactly from the given history function $\theta(t, x)$. Therefore, the difference $H^{n+1} - v_\tau^{n+1}$ vanishes and hence (4.4.17) reduces to

$$e^n = A e^{n-1}. \tag{4.4.19}$$

Iterations on equation (4.4.19) imply

$$e^n = A^n e^0 = \sum_{m=1}^{N_x-1} \omega_m \gamma^n \varphi_m. \tag{4.4.20}$$

On the other hand, in $(\tau, T]$, where n is strictly greater than s, the history term H^n is equal to U^{n-s} and equation (4.4.16) takes the form

$$e^n = A e^{n-1} + \frac{k}{2} B \left(b^n \star e^{n-s} + b^{n+1} \star e^{n+1-s} \right), \tag{4.4.21}$$

Using (4.4.17) and (4.4.20) we can prove by mathematical induction that equation

(4.4.21) can be expressed as

$$e^n = A^n e^0 + \frac{k}{2} \sum_{j=1}^{n-s} \left(A^{n-s-j} B \left(b^{s+j} \star B^{j-1} e^0 + b^{s+j+1} \star B^j e^0 \right) \right). \tag{4.4.22}$$

Further simplifications to equation (4.4.22) lead to

$$
\begin{aligned}
e^n &= \sum_{m=1}^{N_x-1} \left(\omega_m \gamma^n \varphi_m \right) \\
&+ \frac{k}{2} \sum_{j=1}^{n-s} A^{n-s-j} B \left(\sum_{m=1}^{N_x-1} \delta_m \left(\nu_m \right)^{j-1} \left(b^{s+j} \star \vartheta_m + \left(\nu_m \right) b^{s+j+1} \star \vartheta_m \right) \right)
\end{aligned}
$$

and finally we obtain

$$e^n = \sum_{m=1}^{N_x-1} \left(\omega_m \gamma^n + \left(\frac{k}{2} \sum_{j=1}^{n-s} \left(\tilde{\alpha}_m + \tilde{\beta}_m \gamma_m \right) \left(\nu_m \right)^j \gamma^{n-s-j} \right) \right) \varphi_m, \tag{4.4.23}$$

where $\tilde{\alpha}_m$ and $\tilde{\beta}_m$ are constants. It should be noted that in equation (4.4.23), each basis vector ϑ_m is written as a linear combination of the basis vectors φ_m.

Now, since $0 < \gamma_m < 1$ and $0 < \nu_m < 1$, we have $\gamma_m^n \to 0$, $m = 1, \ldots, N_x-1$ as $n \to \infty$, and $\nu_m^j \gamma^{n-s-j} \to 0$, $m = 1, \ldots, N_x-1$ as $n \to \infty$.

Hence, we conclude that

$$e^n \to 0 \quad \text{as} \quad n \to \infty.$$

This proves that the proposed FOFDM is unconditionally stable.

Using (4.4.10)-(4.4.13) and the Lax equivalence theorem [108, 125], we have the following main result:

Theorem 4.4.1 *The FOFDM (4.4.1)-(4.4.4) is convergent of order $\mathcal{O}(k^2 + h^2)$ in the sense that*

$$\sup_{0 < \varepsilon \leq 1} \max_{1 \leq m,n \leq N-1} |u(t_n, x_m) - U_m^n| \leq C(k^2 + h^2),$$

where U is the numerical solution obtained by this method and N is the total number of subintervals taken in either direction.

4.5   Numerical results

In this section we provide numerical results obtained by the fitted mesh and the fitted operator methods. We also compare these results with those obtained by applying the Crank-Nicolson's method on a uniform mesh throughout the region. The latter is referred to as a standard finite difference method (SFDM).

Example 4.5.1 Consider

$$
\frac{\partial u(t,x)}{\partial t} - \varepsilon \frac{\partial^2 u(t,x)}{\partial x^2} = \frac{1}{2}\left(\left(2x\sqrt{\varepsilon} - \varepsilon\right)e^{-\left(t+x/\sqrt{\varepsilon}\right)} - \left(2x\sqrt{\varepsilon} + \varepsilon\right)e^{-\left(t+(1-x)/\sqrt{\varepsilon}\right)}\right)
$$
$$
-2e^{-1}u(t-1,x),\ (t,x)\in[0,2]\times[0,1],
$$

with the initial data

$$
u(t,x) = (2+x^2)(e^{-(t+x/\sqrt{\varepsilon})} + e^{-(t+(1-x)/\sqrt{\varepsilon})}),\ (t,x)\in[-\tau,0]\times[0,1],
$$

and boundary conditions

$$
u(t,0) = e^{-t} + e^{-t-1/\sqrt{\varepsilon}},\ t\in[0,2]
$$

and

$$
u(t,1) = \frac{3}{2}(e^{-t} + e^{-t-1/\sqrt{\varepsilon}}),\ t\in[0,2].
$$

The exact solution of the above problem is

$$
u(t,x) = \left(2+x^2\right)\left(e^{-\left(t+x/\sqrt{\varepsilon}\right)} + e^{-\left(t+(1-x)/\sqrt{\varepsilon}\right)}\right).
$$

By taking $N_t = N_x = N$, the maximum errors (denoted by $E_{N,\varepsilon}$) at all grid points are evaluated using the formula

$$
E_{N,\varepsilon} := \max_{0\le m,\,n\le N}|u(t_n,x_m) - U_m^n|.
$$

We tabulate the errors

$$E_N = \max_{0 < \varepsilon \leq 1} E_{N,\varepsilon}.$$

The errors obtained by applying the SFDM, FMFDM and FOFDM are presented in tables 4.5.1, 4.5.2 and 4.5.4. The acronym SFDM in the caption of Table 4.5.1 stands for the standard finite difference method which is defined by (4.3.1)-(4.3.4) by setting $\sigma = 0.25$ or by replacing ϕ_m^2 in (4.4.1) with h^2.

The numerical rates of convergence are computed using the formula [35]:

$$r_i \equiv r_{i,\varepsilon} := \log_2\left(E_{N_i,\varepsilon}/E_{2N_i,\varepsilon}\right), \quad i = 1, 2, \cdots$$

whereas those of uniform convergence are computed using

$$R_N := \log_2\left(E_N/E_{2N}\right).$$

These convergence rates of the FMFDM and FOFDM are presented in tables 4.5.3 and 4.5.5, respectively.

Table 4.5.1: Maximum Errors obtained by SFDM for Example 4.5.1 using $N_x = N_t = N$

ε	$N = 64$	$N = 128$	$N = 256$	$N = 512$	$N = 1024$	$N = 2048$
1	6.64E-06	1.66E-06	4.15E-07	1.04E-07	2.59E-08	6.40E-09
10^{-2}	4.64E-04	1.16E-04	2.91E-05	7.26E-06	1.82E-06	4.54E-07
10^{-4}	3.09E-02	9.10E-03	2.48E-03	6.25E-04	1.57E-04	3.93E-05
10^{-6}	4.28E-03	1.63E-02	4.05E-02	3.83E-02	1.42E-02	3.76E-03
10^{-8}	4.31E-05	1.72E-04	6.89E-04	2.76E-03	1.08E-02	3.30E-02
10^{-10}	4.31E-07	1.72E-06	6.90E-06	2.76E-05	1.10E-04	4.41E-04
10^{-12}	4.31E-09	1.72E-08	6.90E-08	2.76E-07	1.10E-06	4.42E-06
10^{-14}	4.31E-11	1.72E-10	6.90E-10	2.76E-09	1.10E-08	4.42E-08
10^{-16}	4.31E-12	1.72E-11	6.90E-11	2.76E-10	1.10E-09	4.42E-10

Table 4.5.2: Maximum Errors obtained by FMFDM for Example 4.5.1 using $N_x = N_t = N$

ε	$N = 64$	$N = 128$	$N = 256$	$N = 512$	$N = 1024$	$N = 2048$
1	6.64e-06	1.66e-06	4.15e-07	1.04e-07	2.59e-08	6.44e-09
10^{-1}	7.00e-05	1.75e-05	4.38e-06	1.09e-06	2.74e-07	6.84e-08
10^{-3}	4.08e-03	1.04e-03	2.61e-04	6.53e-05	1.63e-05	4.08e-06
10^{-4}	4.34e-03	1.49e-03	4.92e-04	1.56e-04	4.82e-05	1.46e-05
10^{-5}	4.28e-03	1.47e-03	4.85e-04	1.54e-04	4.76e-05	1.44e-05
10^{-6}	4.26e-03	1.47e-03	4.83e-04	1.53e-04	4.74e-05	1.43e-05
10^{-7}	4.25e-03	1.47e-03	4.82e-04	1.53e-04	4.73e-05	1.43e-05
10^{-8}	4.25e-03	1.46e-03	4.82e-04	1.53e-04	4.73e-05	1.43e-05
10^{-12}	4.25e-03	1.46e-03	4.82e-04	1.53e-04	4.73e-05	1.43e-05
10^{-13}	4.25e-03	1.46e-03	4.82e-04	1.53e-04	4.73e-05	1.43e-05
10^{-16}	4.25e-03	1.46e-03	4.82e-04	1.53e-04	4.73e-05	1.43e-05
E_N	4.25e-03	1.46e-03	4.82e-04	1.53e-04	4.73e-05	1.43e-05

Table 4.5.3: Rates of Convergence obtained by FMFDM for Example 4.5.1 using $N_x = N_t = N = 2^i$, $i = 6(1)10$

ε	r_1	r_2	r_3	r_4	r_5
1	2.00	2.00	2.00	2.00	2.01
10^{-1}	2.00	2.00	2.00	2.00	2.00
10^{-3}	1.98	1.99	2.00	2.00	2.00
10^{-4}	1.54	1.60	1.66	1.69	1.72
10^{-5}	1.54	1.60	1.66	1.69	1.72
10^{-6}	1.54	1.60	1.66	1.69	1.73
10^{-7}	1.54	1.60	1.66	1.69	1.73
10^{-8}	1.54	1.60	1.66	1.69	1.73
10^{-12}	1.54	1.60	1.66	1.69	1.73
10^{-13}	1.54	1.60	1.66	1.69	1.73
10^{-16}	1.54	1.60	1.66	1.69	1.73
R_N	1.54	1.60	1.66	1.69	1.73

Table 4.5.4: Maximum Errors obtained by FOFDM for Example 4.5.1 using $N_x = N_t = N$

ε	$N = 8$	$N = 16$	$N = 32$	$N = 64$	$N = 128$	$N = 256$
1	1.02e-03	8.85e-05	1.33e-05	2.81e-06	6.73e-07	1.66e-07
10^{-1}	9.14e-03	8.52e-04	1.25e-04	2.57e-05	6.08e-06	1.50e-06
10^{-2}	5.82e-02	5.50e-03	8.12e-04	1.68e-04	3.98e-05	9.82e-06
10^{-3}	1.58e-01	3.41e-02	6.33e-03	1.31e-03	3.10e-04	7.67e-05
10^{-4}	1.63e-01	4.23e-02	1.77e-02	9.18e-03	2.56e-03	6.82e-04
10^{-5}	1.63e-01	4.11e-02	1.04e-02	6.28e-03	1.05e-02	5.77e-03
10^{-7}	1.63e-01	4.11e-02	1.03e-02	2.57e-03	6.42e-04	1.75e-04
10^{-8}	1.63e-01	4.11e-02	1.03e-02	2.57e-03	6.42e-04	1.61e-04
10^{-10}	1.63e-01	4.11e-02	1.03e-02	2.57e-03	6.42e-04	1.61e-04
10^{-12}	1.63e-01	4.11e-02	1.03e-02	2.57e-03	6.42e-04	1.61e-04
10^{-13}	1.63e-01	4.11e-02	1.03e-02	2.57e-03	6.42e-04	1.61e-04
10^{-14}	1.63e-01	4.11e-02	1.03e-02	2.57e-03	6.42e-04	1.61e-04
10^{-15}	1.63e-01	4.11e-02	1.03e-02	2.57e-03	6.42e-04	1.61e-04
E_N	1.63e-01	4.11e-02	1.03e-02	2.57e-03	6.42e-04	1.61e-04

Table 4.5.5: Rates of Convergence obtained by FOFDM for Example 4.5.1 using $N_x = N_t = N = 2^i$, $i = 3(1)8$

ε	r_1	r_2	r_3	r_4	r_5
1	3.52	2.74	2.24	2.06	2.02
10^{-1}	3.42	2.77	2.28	2.08	2.02
10^{-2}	3.40	2.76	2.27	2.08	2.02
10^{-3}	2.21	2.43	2.28	2.08	2.01
10^{-4}	1.94	1.26	0.95	1.84	1.91
10^{-5}	1.99	1.98	0.73	-0.74	0.86
10^{-7}	1.99	2.00	2.00	2.00	1.87
10^{-8}	1.99	2.00	2.00	2.00	2.00
10^{-10}	1.99	2.00	2.00	2.00	2.00
10^{-12}	1.99	2.00	2.00	2.00	2.00
10^{-13}	1.99	2.00	2.00	2.00	2.00
10^{-14}	1.99	2.00	2.00	2.00	2.00
10^{-15}	1.99	2.00	2.00	2.00	2.00
R_N	1.99	2.00	2.00	2.00	2.00

4.6   Discussion

In this chapter we constructed two fitted numerical methods, namely, fitted mesh and
fitted operator finite difference methods, for solving a class of singularly perturbed
delay parabolic partial differential equations. Both of these methods are based on
the Crank-Nicolson's discretization. These methods are analyzed for stability and
convergence.

The FMFDM is unconditionally stable and converges with order $\mathcal{O}(N_t^{-2} + N_x^{-2} \ln^2 N_x)$
and which is an improvement over the estimate presented in Ansari et al. [1] for the
very same problem. These improved results can be seen from the results presented in
tables 4.5.2-4.5.3. For the sake of comparison, the results obtained by the corresponding
standard finite difference method (the Crank-Nicolson's method on a uniform mesh)
are presented in Table 4.5.1.

The FOFDM converges appropriately, is unconditionally stable and is converging
with the order $\mathcal{O}(N_t^{-2} + N_x^{-2})$. The method is robust with respect to the singular
perturbation parameter (see Table 4.5.4). Moreover, the numerical results presented
in Table 4.5.5 justify the theoretical estimates given in Theorem 4.4.1.

Chapter 5

A Fitted Numerical Method for a Delayed Model of Two Co-operating Species

In this chapter we consider a system of two coupled partial delay differential equations (PDDEs) describing the dynamics of two co-operative species. The original system is reduced to a system of ordinary delay differential equations (DDEs) obtained by applying the method of lines. Then we construct a fitted operator finite difference method (FOFDM) to solve this resulting system. The model considered in this chapter is very sensitive to small changes in the parameters associated with it. Depending on the values of these parameters, the solution can be stable, periodic and/or aperiodic. Such behaviour of the solution is exploited via the proposed FOFDM. This FOFDM is analyzed for convergence and it is seen that this method is unconditionally stable and has accuracy of $\mathcal{O}(k+h^2)$, where k and h denote time and space step-sizes, respectively. Some numerical results confirming theoretical observations are also presented. These results are comparable with those obtained in the literature.

5.1 Introduction

We consider the following system of two coupled PDDEs describing the dynamics of
two co-operative species with densities $u(t, x)$ and $v(t, x)$:

$$\frac{\partial u}{\partial t}(t, x) = \lambda_1 \frac{\partial^2 u}{\partial x^2}(t, x) + \kappa u(t, x) \left(r_1 - a_{11} u(t - \tau, x) + a_{12} v(t - \tau, x) \right) \quad (5.1.1)$$

$$\frac{\partial v}{\partial t}(t, x) = \lambda_2 \frac{\partial^2 v}{\partial x^2}(t, x) + \kappa v(t, x) \left(r_2 + a_{21} u(t - \tau, x) - a_{22} v(t - \tau, x) \right) \quad (5.1.2)$$

where $0 < x < \pi$ and $t > 0$, subject to the initial data

$$u(t, x) = u^0(t, x), \quad v(t, x) = v^0(t, x), \quad t \in [-\tau, 0], \quad (5.1.3)$$

and Dirichlet boundary conditions

$$u(t, 0) = u(t, \pi) = v(t, 0) = v(t, \pi) = 0, \ t \geq 0. \quad (5.1.4)$$

The constants $\lambda_1 > 0$ and $\lambda_2 > 0$ in the above represent the diffusivity of the two
species whereas the constants $r_1 > 0$ and $r_2 > 0$ are the growth rates of these species.
The coefficients a_{11}, a_{12}, a_{21}, a_{22} and κ are positive constants. Finally, $\tau \, (> 0)$ is a time
delay parameter.

Many biological phenomena can be described by diffusion equations such as the
system above. Some examples include the dynamics of a single species in time and
space [151], the spread of an advantageous gene in a population [110], the competition
between the gray and red squirrels in Britain which led to the decline and subsequent
disappearance of the red squirrels [111], the spread of powdery mildew disease caused
by the fungus Uncinula necator over the grapevines [34], the modified Lotka-Volterra
system with logistic growth of the prey and with both predator and prey dispersing by
diffusion [111].

The literature on the use of diffusive delay differential equations for modelling
biological systems is very rich, see for example [94, 113, 142] and the references therein.

When a time delay is involved, it indicates the non-immediate effect of some factor that inhibits the dynamics of the model, for instance, in a predator-prey model, the density of the prey is affected by hunting mature prey members that happened some time in the past. Also, in a model that describes the spread of an epidemic disease, a virus or a bacterium takes some time before it becomes mature and will be able to attack some organism. In a biological system, delay models are more realistic for describing the dynamics of the various parts of the system than the ordinary differential equations.

Under the assumption that the two species have the same diffusivity (*i.e.*, $\lambda_1 = \lambda_2 = \lambda$) and same growth rates (*i.e.*, $r_1 = r_2 = r$), Li et. al [86] used a transformation of variables to reduce the system (5.1.1)-(5.1.2) to the form

$$\frac{\partial u}{\partial t}(t,x) = \lambda \frac{\partial^2 u}{\partial x^2}(t,x) + \kappa u(t,x)\left(1 - u(t-\tau,x) + a_{12}v(t-\tau,x)\right), \quad (5.1.5)$$

$$\frac{\partial v}{\partial t}(t,x) = \lambda \frac{\partial^2 v}{\partial x^2}(t,x) + \kappa v(t,x)\left(1 + a_{21}u(t-\tau,x) - v(t-\tau,x)\right), \quad (5.1.6)$$

with $t > 0$, $0 < x < \pi$ and subject to the initial data (5.1.3) and the boundary conditions (5.1.4).

In this chapter, we design a new fitted operator finite difference method (FOFDM) which is constructed for a system of DDEs obtained by applying the method of lines [58, 97] to the system of PDDEs. These FOFDMs, which are based on the philosophy of non-standard finite difference methods of Mickens [105, 114], are widely used for singularly perturbed two-point boundary value problems. See for instance [116, 117, 118]. However, their extensions for coupled PDEs whose solutions possess oscillatory dynamics, have not been seen in the literature.

The rest of this chapter is organized as follows. In Section 5.2, we discuss the existence and stability of equilibria for the model under consideration. Section 5.3 deals with the construction of the fitted operator finite difference method which is analyzed for convergence in Section 5.4. Illustrative numerical results are presented in Section 5.5. Finally, we discuss these results in Section 5.6.

5.2   Existence and stability of equilibria

In many of the delay differential equation models, the time delay τ acts as a bifurcation parameter. As the delay τ passes through some critical value $\tau^\star$, a couple of complex conjugating eigenvalues of the system cross the imaginary axis at some pure imaginary points and stable periodic Hopf bifurcating solutions occur. Then when $\tau > \tau^\star$, the real parts of these eigenvalues cross to the positive real axis causing the solution to lose its stability. We look at these features of the solution via the existence and stability of a positive equilibrium following the works in [19, 86, 151].

Any equilibrium solution for problem (5.1.5)-(5.1.6) must solve the system

$$
\begin{aligned}
\frac{d^2u}{dx^2} + \tilde{\kappa}u(x)(1 - u(x) + a_{12}v(x)) &= 0, \\[2mm]
\frac{d^2v}{dx^2} + \tilde{\kappa}v(x)(1 + a_{21}u(x) - v(x)) &= 0,
\end{aligned}
\tag{5.2.1}
$$

with

$$
u(0) = u(\pi) = v(0) = v(\pi) = 0,
\tag{5.2.2}
$$

where the parameter $\tilde{\kappa}$ corresponds to the ratio κ/λ.

It is obvious that the trivial solution $(0,0)$ satisfies (5.2.1)-(5.2.2) and it also satisfies (5.1.5)-(5.1.6). If $\tilde{\kappa} < 1$, the trivial solution $(0,0)$ is asymptotically stable and it is the only global attractor for all non-negative solutions. Therefore, the increase in the time delay τ do not have an effect on the stability of the trivial equilibria. On the other hand, when $\tilde{\kappa} > 1$ the trivial solution is unstable. The question arising at this stage is what will happen if $\tilde{\kappa}$ becomes greater than 1 while the time delay τ is strictly positive. In the following two subsections we show that when $\tilde{\kappa} > 1$ while $\tau > 0$, a positive equilibrium $(U_{\tilde{\kappa}}(x), V_{\tilde{\kappa}}(x))$ will bifurcate from the trivial solution at $\tilde{\kappa} = 1$.

Existence of equilibria

Let D^2 denote the differential operator $\frac{d^2}{dx^2}$, and $\mathcal{N}(D^2 + 1)$ and $\mathcal{R}(D^2 + 1)$ denote the null and range spaces of the differential operator $D^2 + 1$ respectively, then

$$L^2[0, \pi] = \mathcal{N}(D^2 + 1) \oplus \mathcal{R}(D^2 + 1),$$

where

$$\mathcal{N}(D^2 + 1) = \text{span}\{\sin x\}$$

and

$$\mathcal{R}(D^2 + 1) = \{y(x) \in L^2[0, \pi] : \, <\sin x, y(x)>= \int_0^\pi (\sin x)y(x)dx = 0\}.$$

Assume that the pair of functions $(U_{\tilde{\kappa}}(x), V_{\tilde{\kappa}}(x))$ is an equilibrium solution of the system (5.1.3)-(5.1.5) and that they can be expressed as

$$U_{\tilde{\kappa}}(x) \;=\; \alpha_{\tilde{\kappa}}(\tilde{\kappa} - 1)\left(\sin x + (\tilde{\kappa} - 1)\xi_{\tilde{\kappa}}\right) \tag{5.2.3}$$

and

$$V_{\tilde{\kappa}}(x) \;=\; \beta_{\tilde{\kappa}}(\tilde{\kappa} - 1)\left(\sin x + (\tilde{\kappa} - 1)\eta_{\tilde{\kappa}}\right), \tag{5.2.4}$$

where $\xi_{\tilde{\kappa}}, \eta_{\tilde{\kappa}} \in \mathcal{R}(D^2 + 1)$ and $\alpha_{\tilde{\kappa}}$ and $\beta_{\tilde{\kappa}}$ are real numbers.

Using (5.2.1) along with equations (5.2.3)-(5.2.4), we obtain

$$(D^2 + 1)\xi_{\tilde{\kappa}} + \sin x + (\tilde{\kappa} - 1)\xi_{\tilde{\kappa}} - \tilde{\kappa}\left((\alpha_{\tilde{\kappa}} \sin x + (\tilde{\kappa} - 1)\xi_{\tilde{\kappa}})^2\right.$$
$$\left. -a_{12}\beta_{\tilde{\kappa}}(\sin x + (\tilde{\kappa} - 1)\xi_{\tilde{\kappa}})(\sin x + (\tilde{\kappa} - 1)\eta_{\tilde{\kappa}})\right) = 0 \tag{5.2.5}$$

and

$$(D^2 + 1)\eta_{\tilde{\kappa}} + \sin x + (\tilde{\kappa} - 1)\eta_{\tilde{\kappa}} - \tilde{\kappa}\left(-a_{21}\alpha_{\tilde{\kappa}}(\sin x + (\tilde{\kappa} - 1)\xi_{\tilde{\kappa}})\right.$$

$$\left.(\sin x + (\tilde{\kappa} - 1)\eta_{\tilde{\kappa}}) - \beta_{\tilde{\kappa}}(\sin x + (\tilde{\kappa} - 1)\eta)^2\right) = 0. \qquad (5.2.6)$$

For $\tilde{\kappa} = 1$, we get

$$\alpha_1 = \alpha^\star \frac{1 + a_{12}}{1 - a_{12}a_{21}} \text{ and } \beta_1 = \alpha^\star \frac{1 + a_{21}}{1 - a_{12}a_{21}},$$

provided that $a_{12}a_{21} < 1$ where

$$\alpha^\star = \frac{\int_0^\pi \sin^2 x dx}{\int_0^\pi \sin^3 x dx} = \frac{3}{8}$$

and hence, according to Li et al. [86] the unique solution of system (5.2.5)-(5.2.6) is
then given by

$$\xi_1 = \eta_1 = \frac{1}{2}\sin x + \left(\frac{x}{2} - \frac{2\alpha^\star}{3}\right)\cos x + \frac{\alpha_0^\star}{6}\cos 2x + \frac{\alpha_0^\star}{2}. \qquad (5.2.7)$$

For the general $\tilde{\kappa} \geq 1$, the following theorem is proved in [151]:

Theorem 5.2.1 *There is a constant $\tilde{\kappa}^\star$ and a continuously differentiable mapping*

$$\tilde{\kappa} \to (\xi_{\tilde{\kappa}}, \beta_{\tilde{\kappa}}, \alpha_{\tilde{\kappa}}, \beta_{\tilde{\kappa}})$$

*from $[1, \tilde{\kappa}^\star] \to H^2 \times H^2 \times \mathbb{R} \times \mathbb{R}$ such that equations (5.2.5) and (5.2.6) hold and
$<\sin x, \xi_{\tilde{\kappa}}> = <\sin x, \eta_{\tilde{\kappa}}> = 0$.*

Finally, the existence of the positive equilibrium $(U_{\tilde{\kappa}}, V_{\tilde{\kappa}})$ follows from the existence
and uniqueness of the couple $(\xi_{\tilde{\kappa}}, \eta_{\tilde{\kappa}})$ in the interval $(1, \tilde{\kappa}^\star]$.

Stability of the equilibria

To study the stability of the positive equilibrium $(U_{\tilde{\kappa}}, V_{\tilde{\kappa}})$, let $0 < \tilde{\kappa} \leq \tilde{\kappa}^{\star}$ and consider
the linearized version of the system (5.1.5)-(5.1.6) around this equilibrium, i.e.,

$$
\frac{d}{dt}\begin{pmatrix} u(t) \\ v(t) \end{pmatrix} = (D^2 + \tilde{\kappa})I_2 \begin{pmatrix} u(t) \\ v(t) \end{pmatrix} + \tilde{\kappa} \begin{pmatrix} -U_{\tilde{\kappa}} & a_{12}U_{\tilde{\kappa}} \\ a_{21}V_{\tilde{\kappa}} & -V_{\tilde{\kappa}} \end{pmatrix} \begin{pmatrix} u(t-\tau) \\ v(t-\tau) \end{pmatrix}, \quad (5.2.8)
$$

$$
\begin{pmatrix} u(t) \\ v(t) \end{pmatrix} = \begin{pmatrix} u^0(t, \cdot) \\ v^0(t, \cdot) \end{pmatrix}, \quad t \in [-\tau, 0],
$$

where $u(t) = u(t, \cdot)$ and $v(t) = v(t, \cdot)$.

By writing

$$
Y(t) = [u(t), v(t)]^T, \quad Y_0(t) = [u^0(t, \cdot), v^0(t, \cdot)]^T,
$$

$$
A(\tilde{\kappa}) = (D^2 + \tilde{\kappa})I_2
$$

and

$$
B(\tilde{\kappa}) = \begin{pmatrix} -U_{\tilde{\kappa}} & a_{12}U_{\tilde{\kappa}} \\ a_{21}V_{\tilde{\kappa}} & -V_{\tilde{\kappa}} \end{pmatrix},
$$

the stability of $(U_{\tilde{\kappa}}, V_{\tilde{\kappa}})$ is determined through solving the eigenvalue problem

$$
\left[A(\tilde{\kappa}) + \tilde{\kappa}B(\tilde{\kappa})e^{-\lambda\tau} - \lambda I_2 \right] Y = \mathbf{0}. \quad (5.2.9)
$$

An infinitesimal generator $A_\tau(\tilde{\kappa})$ of the semi-group ([136]) induced by the solutions
of the linearized system (5.2.8) is defined by

$$
A_\tau(\tilde{\kappa})Y_0(t) = dY_0(t)/dt, \quad t \in [-\tau, 0],
$$

with

$$
\mathcal{D}(A_\tau(\tilde{\kappa})) = \{v^0 \in C : \frac{dv^0}{dt} \in C, v^0(0) \in \mathbb{H}^2, \frac{dv^0}{dt} = A_\tau(\tilde{\kappa})v^0(0) + \tilde{\kappa}B(\tilde{\kappa})v^0(-\tau)\}.
$$

When $\tilde{\kappa} > 1$ the stability of the equilibrium $(U_{\tilde{\kappa}}, V_{\tilde{\kappa}})$ is determined by the eigenvalues of $A_\tau(\tilde{\kappa})$ which depend continuously on τ. For $\tau = 0$ all the eigenvalues of A_τ have negative real parts. By increasing the time delay τ, the eigenvalues of $A_\tau(\tilde{\kappa})$ may move towards the positive real part of the complex plane and the problem is then to find whether there exists a delay $\tau^\star$ for which $A_{\tau^\star}(\tilde{\kappa})$ has a pure imaginary eigenvalue $\lambda = i\nu$. However, $\lambda = i\nu$ is a pure imaginary eigenvalue of $A_\tau(\tilde{\kappa})$ if and only if the equation

$$\left[A(\tilde{\kappa}) + \tilde{\kappa} B(\tilde{\kappa}) e^{-i\theta} - i\nu I_2 \right] Y = \mathbf{0}, \tag{5.2.10}$$

is solvable for the pair $\nu > 0$ and $\theta \in [0, 2\pi]$. Then equation (5.2.10) is satisfied for all $\tau_n = (\theta + 2n\pi)/\nu, \; n = 0, 1, \dots$

It has been proved in [19] that if the triplet (ν, θ, Y) solves the eigenvalue problem (5.2.9) with $Y \neq 0$ and $\tilde{\kappa} \in (1, \tilde{\kappa}^\star]$, then $\varrho = \nu/(\tilde{\kappa} - 1)$ is uniformly bounded and

$$Y = [\sin x + (\tilde{\kappa} - 1)\gamma(x), (a + ib) \sin x + (\tilde{\kappa} - 1)\delta(x)]^T,$$

where $\gamma(x)$ and $\delta(x)$ are two smooth functions such that $< \sin x, \gamma(x) > \; = \; 0$ and $< \sin x, \delta(x) > \; = 0$.

Zhou et al. [151] proved that solving the eigenvalue problem (5.2.9) is equivalent

to solve the following system of equations:

$$
\begin{aligned}
g_1(\gamma, \delta, \varrho, \theta, a, b) &= (D^2 + 1)\gamma + (1 - i\varrho)[\sin x + (\tilde{\kappa} - 1)\gamma] + \tilde{\kappa}(-\alpha_{\tilde{\kappa}}(\sin x + (\tilde{\kappa} - 1)\xi_{\tilde{\kappa}}) \\
&\quad + a_{12}\beta_{\tilde{\kappa}}(\sin x + (\tilde{\kappa} - 1)\eta_{\tilde{\kappa}}))(\sin x + (\tilde{\kappa} - 1)\gamma) \\
&\quad + \tilde{\kappa}e^{-i\theta}\alpha_{\tilde{\kappa}}[\sin x + (\tilde{\kappa} - 1)\xi_{\tilde{\kappa}}](-(\sin x + (\tilde{\kappa} - 1)\gamma) \\
&\quad + a_{12}((a + ib)\sin x + (\tilde{\kappa} - 1)\delta)), \\
g_2(\gamma, \delta, \varrho, \theta, a, b) &= (D^2 + 1)\delta + (1 - i\varrho)[(a + ib)\sin x + (\tilde{\kappa} - 1)\delta] \\
&\quad + \tilde{\kappa}(a_{21}\alpha_{\tilde{\kappa}}(\sin x + (\tilde{\kappa} - 1)\xi_{\tilde{\kappa}}) - \beta_{\tilde{\kappa}}(\sin x + (\tilde{\kappa} - 1)\eta_{\tilde{\kappa}})) \\
&\quad ((a + ib)\sin x + (\tilde{\kappa} - 1)\delta) + \tilde{\kappa}e^{-i\theta}\beta_{\tilde{\kappa}}[\sin x + (\tilde{\kappa} - 1)\eta_{\tilde{\kappa}}] \\
&\quad (a_{21}(\sin x + (\tilde{\kappa} - 1)\gamma) - ((a + ib)\sin x + (\tilde{\kappa} - 1)\delta)), \qquad (5.2.11) \\
g_3(\gamma, \delta, \varrho, \theta, a, b) &= Re < \sin x, \gamma >= 0, \\
g_4(\gamma, \delta, \varrho, \theta, a, b) &= Im < \sin x, \gamma >= 0, \\
g_5(\gamma, \delta, \varrho, \theta, a, b) &= Re < \sin x, \delta >= 0, \\
g_6(\gamma, \delta, \varrho, \theta, a, b) &= Im < \sin x, \delta >= 0.
\end{aligned}
$$

We state the following result from [86], proved in [151]:

Theorem 5.2.2 *If $0 < \tilde{\kappa}^\star - 1 \ll 1$, then there is a continuously differentiable mapping $\tilde{\kappa} \to (\gamma_{\tilde{\kappa}}, \delta_{\tilde{\kappa}}, \varrho_{\tilde{\kappa}}, \theta_{\tilde{\kappa}}, a_{\tilde{\kappa}}, b_{\tilde{\kappa}})$ from $[1, \tilde{\kappa}^\star]$ to $(H^2)^2 \times (\mathbb{R})^4$ such that $\gamma_1 = (1 - i)\xi_1$, $\delta_1 = (1-i)a_1\xi_1$, $\theta_1 = \pi/2$, $a_1 = (1+a_{12})/(1+a_{21})$, $b_1 = 0$ and $\varrho_1 = 1$ and $(\gamma_{\tilde{\kappa}}, \delta_{\tilde{\kappa}}, \varrho_{\tilde{\kappa}}, \theta_{\tilde{\kappa}}, a_{\tilde{\kappa}}, b_{\tilde{\kappa}})$ solves problem (5.2.11) for $\tilde{\kappa} \in [1, \tilde{\kappa}^\star]$ with ξ_1 being the unique solution of the system (5.2.5)-(5.2.6) given by equation (5.2.7).*

Li et al. [86] concluded that the positive equilibrium $(U_{\tilde{\kappa}}, V_{\tilde{\kappa}})$ is asymptotically stable for $\tau < \tau_{\tilde{\kappa}_0}$ and unstable for $\tau > \tau_{\tilde{\kappa}_0}$. Moreover, the bifurcating solutions which occur from the Hopf bifurcation point $\tau = \tau_{\tilde{\kappa}_0}$ are stable while those occurring from the Hopf bifurcation points $\tau = \tau_{\tilde{\kappa}_n}$, $n = 1, 2, \ldots$ are unstable.

In summary,

- If $\tilde{\kappa} \le 1$, then the zero solution is stable and is the only global attractor of all

non-negative solutions.

- If $\tilde{\kappa} > 1$, a unique positive equilibrium $(U_{\tilde{\kappa}}, V_{\tilde{\kappa}})$ bifurcates from $\tilde{\kappa} = 1$ and $(u, v) = (0, 0)$ while the zero solution is unstable.

- For each fixed $0 < \tilde{\kappa} - 1 \ll 1$ there exists a sequence $\{\tau_{\tilde{\kappa}_n}\}_{n=0}^{\infty}$ such that the positive equilibrium $(U_{\tilde{\kappa}}, V_{\tilde{\kappa}})$ is asymptotically stable if $0 \le \tau < \tau_{\tilde{\kappa}_0}$ and unstable if $\tau > \tau_{\tilde{\kappa}_0}$.

- A Hopf bifurcation will occur as the delay τ increasingly passes through each point $\tau_{\tilde{\kappa}_n}$, $n = 1, 2, \dots$.

5.3   Construction of the numerical method

In this section, we describe the construction of the fitted numerical method for solving the system (5.1.5)-(5.1.6) with the initial data (5.1.3) and boundary conditions (5.1.4) respectively. Following the method of lines, we find an approximation to the derivatives of the functions $u(t, x)$ and $v(t, x)$ with respect to the spatial variable x by algebraic quantities in order to transform the two PDDEs into a system of DDEs.

Because of the similarities between the two PDEs in $u(t, x)$ and $v(t, x)$ we will describe the method for the equation in $u(t, x)$. The equation in $v(t, x)$ is dealt with similarly.

Let N_x be a positive integer and discretize the interval $[0, \pi]$ by the points

$$x_0 = 0 < x_1 < x_2 < \dots < x_{N_x} = \pi,$$

where $h = x_{m+1} - x_m = \pi/N_x$; $m = 0, 1, \dots, N_x$. Let $U_m(t) \approx u(t, x_m)$.

We approximate the second order spatial derivative by

$$\frac{\partial^2 u}{\partial x^2}(t, x_m) \approx \frac{U_{m+1} - 2U_m + U_{m-1}}{\phi_m^2}, \tag{5.3.1}$$

where

$$\phi_m = \phi_m(\kappa, \lambda, h) = \frac{2}{\rho_m} \sin \frac{\rho_m h}{2}$$

and

$$\rho_m = \sqrt{\kappa/\lambda}.$$

It is obvious that $\phi_m \to h$ as $h \to 0$. The function ϕ_m^2 in equation (5.3.1) is conventionally termed as a denominator function [102]. It can be constructed by using the theory of difference equations.

Equation (5.1.5) with the initial data (5.1.3) and boundary conditions (5.1.4) then take the form

$$U_0(t) = 0 = U_{N_x}(t), \tag{5.3.2}$$

$$\frac{dU_m(t)}{dt} = \lambda \frac{U_{m+1} - 2U_m + U_{m-1}}{\phi^2(h)}$$

$$+ \kappa U_m(t) \left(1 - u_m(t - \tau) + a_{12} v_m(t - \tau)\right), \ m = 1, \ldots, N_x - 1, \tag{5.3.3}$$

with the initial data

$$u_m(\theta) = u^0(\theta, x_m), \ \theta \in [-\tau, 0]; \ m = 1, \ldots, N_x - 1, \tag{5.3.4}$$

where $u_m(t)$ is the exact value $u(t, x_m)$.

Now let N_t be a positive integer and $k = T/N_t$ where $0 < t < T$.

Discretizing the time interval $[0, T]$ through the points

$$0 = t_0 < t_1 < \ldots < t_{N_t} = T,$$

where

$$t_{n+1} - t_n = k, \ n = 0, 1, \ldots, (N_t - 1).$$

We approximate the time derivative at t_n by

$$\frac{dU_m(t_n)}{dt} \approx \frac{U_m^{n+1} - U_m^n}{\psi(k)}, \tag{5.3.5}$$

where $\psi(k) = (exp(\kappa k) - 1)/\kappa$. Again we see that $\psi(k) \to k$ as $k \to 0$.

Combining (5.3.2), (5.3.3) and (5.3.5), we obtain

$$\frac{U_m^{n+1} - U_m^n}{\psi(k)} = \lambda \frac{U_{m+1}^{n+1} - 2U_m^{n+1} + U_{m-1}^{n+1}}{\phi_m^2(h)} - \kappa U_m^n (1 - (H_u)_m^n + a_{12}(H_v)_m^n) \tag{5.3.6}$$

where

$$(H_u)_m^n \approx u(t_n - \tau, x_m)$$

and

$$(H_v)_m^n \approx v(t_n - \tau, x_m),$$

$m = 1, \ldots, N_x - 1, \ n = 0, \ldots, N_t - 1$ are the history functions corresponding to the equations in u and v.

Equation (5.3.6) can further be simplified as

$$-\frac{\lambda}{\phi_m^2}U_{m-1}^{n+1} + \left(\frac{1}{\psi} + \frac{2\lambda}{\phi_m^2}\right)U_m^{n+1} - \frac{\lambda}{\phi_m^2}U_{m+1}^{n+1} = \left(\frac{1}{\psi} + \kappa\left(1 - (H_u)_m^n + a_{12}(H_v)_m^n\right)\right)U_m^n. \tag{5.3.7}$$

Equation (5.3.7) can be written as a tridiagonal system

$$T_L U^{n+1} = \frac{1}{\psi}U_m^n + \kappa U_m^n (1 - (H_u)_m^n + a_{12}(H_v)_m^n), \tag{5.3.8}$$

where $m = 1, \ldots, N_x - 1, \ n = 0, \ldots, N_t - 1$ and

$$T_L = \mathrm{Tri}\left(-\frac{\lambda}{\phi_m^2}, \frac{1}{\psi} + \frac{2\lambda}{\phi_m^2}, -\frac{\lambda}{\phi_m^2}\right).$$

On the interval $[0, \tau]$ the delayed arguments $t_n - \tau$ belong to $[-\tau, 0]$, and therefore

the delayed variable

$$(H_u)_m^n \approx u_m(t_n - \tau)$$

is evaluated directly from the history functions $u^0(t, x)$ as

$$(H_u)_m^n = u^0(t_n - \tau, x_m), \tag{5.3.9}$$

and equation (5.3.8) takes the form

$$T_L U^{n+1} = \frac{1}{\psi} U_m^n + \kappa U_m^n (1 - u^0(t_n - \tau, x_m) + a_{12} v^0(t_n - \tau, x_m)). \tag{5.3.10}$$

Let s be the largest integer such that $t_s \leq \tau$. By using equation (5.3.10) we can compute U_m^n for $1 \leq n \leq s$. At this stage, we interpolate the data

$$(t_0, U_m^0), (t_1, U_m^1), \ldots, (t_s, U_m^s),$$

using an interpolating cubic Hermite spline $\varphi_m(t)$. Then $U_m^n = \varphi(t_n, x_m)$ for all $n = 0, 1, \ldots, s$ and $m = 1, 2, \ldots, N_x - 1$.

For $n = s + 1, s + 2, \ldots, N_t - 1$, when we move from level n to level $n + 1$ we extend the definitions of the cubic Hermite spline $\varphi_m(t)$ to the point $(t_n + k, U_m^{n+1})$. Then the history terms $(H_u)_m^n$ can be approximated by the functions $\varphi_m(t_n - \tau)$ for $n \geq s$, that is,

$$(H_u)_m^n \approx \varphi_m(t_n - \tau),$$

and equation (5.3.8) becomes of the form

$$T_L U^{n+1} = \frac{1}{\psi} U_m^n + \kappa U_m^n (1 - \varphi(t_n - \tau) + a_{12} \vartheta(t_n - \tau)), \tag{5.3.11}$$

where

$$\varphi(t_n - \tau) = [(H_u)_1^n, \ldots, (H_u)_{N_x-1}^n]^T$$

and ϑ is the set of cubic Hermite splines that interpolates the data (t_n, V_m^n).

Proceeding in a similar manner for the equation in v, we have

$$T_L V^{n+1} = \frac{1}{\psi} V_m^n + \kappa V_m^n (1 + a_{21}(H_u)_m^n - (H_v)_m^n), \qquad (5.3.12)$$

where

$$(H_v)_m^n = \begin{cases} v^0(t_n - \tau, x_m) & t_n \leq \tau \\ \\ \vartheta_m(t_n - \tau) & t_n > \tau \end{cases}$$

along with

$$V_0(t) = 0 = V_{N_x+1}. \qquad (5.3.13)$$

Our FOFDM is then consists of equations (5.3.8)-(5.3.12) along with (5.3.2) and (5.3.13).

This method is analyzed for convergence in next section whereas the corresponding numerical results are presented in Section 5.5.

5.4 Analysis of convergence

As usual with most of the classical convergence finite difference methods, the convergence for the proposed FOFDM is proved via consistency and stability.

Consistency of the numerical method

We assume that the function $u(t, x)$ and its partial derivatives with respect to both t and x are smooth and satisfy

$$\left| \frac{\partial^{i+j} u(t,x)}{\partial t^i x^j} \right| \leq C; \ \forall i, j \geq 0, \qquad (5.4.1)$$

where C is a constant that is independent of the time and space step-sizes.

The local truncation error (LTE) for the discrete equations in u in the FOFDM

(5.3.10) and (5.3.11) is given by

$$(\text{LTE})_u = \left(u_t(t_n, x_m) - \frac{u_m^{n+1} - u_m^n}{\psi} \right) - \lambda \left(u_{xx} - \frac{u_{m-1}^{n+1} - 2u_m^{n+1} + u_{m+1}^{n+1}}{\phi_m^2} \right). \quad (5.4.2)$$

The first term on the right hand side of equation (5.4.2) satisfies

$$
\begin{aligned}
&\left| u_t(t_n, x_m) - \frac{u_m^{n+1} - u_m^n}{\psi} \right| \\
&= \left| u_t(t_n, x_m) - \frac{u_m^{n+1} - u_m^n}{k} + \frac{u_m^{n+1} - u_m^n}{k} - \frac{u_m^{n+1} - u_m^n}{\psi} \right| \\
&\leq \left| u_t(t_n, x_m) - \frac{u_m^{n+1} - u_m^n}{k} \right| + \left| \frac{u_m^{n+1} - u_m^n}{k} - \frac{u_m^{n+1} - u_m^n}{\psi} \right| \\
&\leq \frac{k}{2} \left| u_{tt}(\xi, x_m) \right| + \frac{\kappa k(\frac{1}{2} + \frac{\kappa k}{6} + \dots)}{1 + \frac{\kappa k}{2} + \dots}(u_m^{n+1} - u_m^n), \ \xi \in [t_n, t_{n+1}] \\
&\leq \frac{k}{2}C + \frac{\kappa k(\frac{1}{2} + \frac{\kappa k}{6} + \dots)}{1 + \frac{\kappa k}{2} + \dots}(u_m^{n+1} - u_m^n) \ (\text{using (5.4.1)}) \\
&\to 0 \text{ as } k \to 0. \quad\quad\quad\quad\quad\quad\quad\quad\quad\quad\quad\quad\quad\quad (5.4.3)
\end{aligned}
$$

The second term on the right-hand side of equation (5.4.2) satisfies

$$
\begin{aligned}
&\left| u_{xx}(t_n, x_m) - \left(u_{xx} - \frac{u_{m-1}^{n+1} - 2u_m^{n+1} + u_{m+1}^{n+1}}{\phi^2} \right) \right| \\
&\leq \left| u_{xx}(t_n, x_m) - \left(\frac{u_{m-1}^n - 2u_m^n + u_{m+1}^n}{h^2} \right) \right| \\
&\quad + \left| \left(\frac{u_{m-1}^n - 2u_m^n + u_{m+1}^n}{h^2} - \frac{u_{m-1}^{n+1} - 2u_m^{n+1} + u_{m+1}^{n+1}}{\phi^2} \right) \right| \\
&\leq \frac{h^2}{12} \left| u_{xxxx}(t_n, \zeta) \right| + \left| \frac{(\rho h/2)^2/3 - (\rho h/2)^4/60 + \dots}{1 - (\rho h/2)^2/6 + \dots} \right| + k \left| u_{xxt}(\xi, x_m) \right|, \\
&\leq \frac{h^2}{12}C + h^2 \left(\left| \frac{(\rho/2)^2/3 - h^2(\rho/2)^4/60 + \dots}{1 - (\rho h/2)^2/6 + \dots} \right| \right) + kC \ (\text{using (5.4.1)}), \\
&\to 0 \text{ as } h \to 0 \text{ and } k \to 0, \quad\quad\quad\quad\quad\quad\quad\quad\quad (5.4.4)
\end{aligned}
$$

where $x_{m-1} < \zeta < x_{m+1}$ in the third last inequality above.

The results that we obtained in equations (5.4.3) and (5.4.4) prove that LTE $\to 0$ as $k \to 0$ and $h \to 0$. Similarly, we can see that the LTE for the equation in v tends

to 0, as $h \to 0$ and $k \to 0$. This proves the consistency of our FOFDM.

Stability of the numerical method

In this section we apply the von Neumann analysis to prove the stability of our method.

Plugging the solution

$$U_m^n = w_n e^{imh},$$

where $i = \sqrt{-1}$ in equation (5.3.8), we obtain

$$\left(\left(\frac{1}{\psi} + \frac{2\lambda}{\phi^2} \right) - \frac{1}{\psi} \left(e^{imh} + e^{-imh} \right) \right) w_{n+1} = \left(\frac{1}{\psi} + \kappa \left(1 - U_{\tau,m}^n + a_{21} V_{\tau,m}^n \right) \right) w_n \quad (5.4.5)$$

From equation (5.4.5), the amplification factor ς is given by

$$\varsigma = \frac{\frac{1}{\psi} + \kappa(1 - (H_u)_m^n + a_{21}(H_v)_m^n}{\frac{1}{\psi} + \frac{4\lambda}{\phi_m^2} \sin^2 \frac{mh}{2}}. \quad (5.4.6)$$

We notice that both the quantities in the numerator and denominator in the right-hand side of equation (5.4.6) are positive, hence the amplification factor ς satisfies

$$|\varsigma| \le 1,$$

if

$$\frac{1}{\psi} + \kappa \left(1 - (H_u)_m^n + a_{21}(H_v)_m^n \right) \le \frac{1}{\psi} + \frac{4\lambda}{\phi_m^2} \sin^2 \frac{mh}{2}. \quad (5.4.7)$$

Simplifying the inequality (5.4.7) we obtain

$$\frac{\kappa}{\lambda} \left(1 - (H_u)_m^n + a_{12}(H_v)_m^n \right) \le \frac{4}{\phi_m^2} \sin^2 \frac{mh}{2} \le \frac{4}{\phi_m^2}. \quad (5.4.8)$$

From the discussion in Section 2, we see that the ratio $\tilde{\kappa} = \frac{\kappa}{\lambda}$ can not exceed κ^* which is always less than 2. This implies that the left hand side of inequality (5.4.8) is always less than 2. On the other hand, we see that the right hand side of inequality (5.4.8) is $\frac{4}{\phi_m^2}$ which is much greater than 2. Hence, the amplification factor ς is always less than

1 and therefore, the proposed FOFDM is unconditionally stable.

Using the Lax-Richtmyer theory [108, 125], we have the following theorem

Theorem 5.4.1 *The FOFDM given by (5.3.11)-(5.3.12) along with (5.3.2) and (5.3.13)
is convergent of order $\mathcal{O}(k + h^2)$ in the sense that*

$$\max \left\{ \max_{1 \leq m,n \leq N-1} \{|u(t_n, x_m) - U_m^n|\} \, , \, \max_{1 \leq m,n \leq N-1} \{|v(t_n, x_m) - V_m^n|\} \right\} \leq C(k + h^2),$$

*where U and V are the numerical solutions obtained by this FOFDM and N is the total
number of subintervals taken in either directions.*

5.5   Numerical results

To see the performance of the proposed FOFDM, we consider the following example.

Example 5.5.1 [86] Consider problem (5.1.5)-(5.1.6) with $a_{12} = 0.5$, $a_{21} = 0.8$, λ
takes values in $[0.0085, 0.0105] \cup [0.999, 1.0105]$, $\kappa \in \{0.01, 1.01\}$, $\tau \in \{1, 20, 100, 170\}$
and $T \in \{100, 800, 2500, 4500\}$. The initial data is taken as

$$u(\theta, x) = v(\theta, x) = 0.1 \left(1 + \frac{\theta}{\tau}\right) \sin x, \theta \in [-\tau, 0], 0 \leq x \leq \pi, \ t \geq 0$$
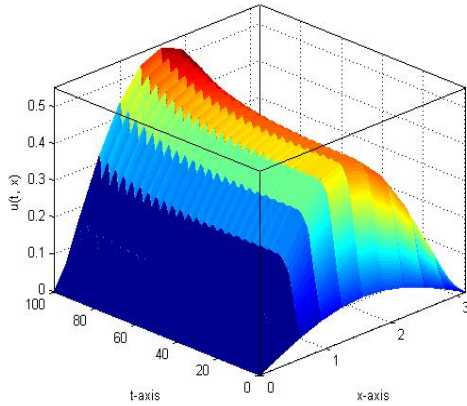
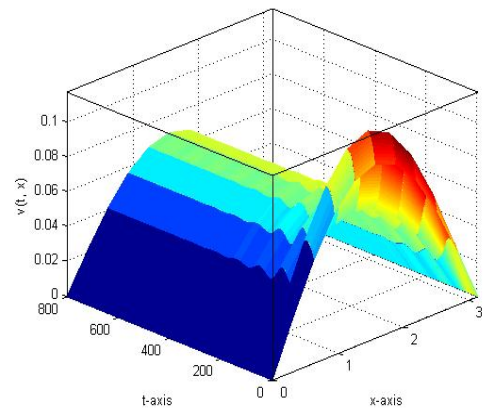Figure 5.5.1: Profile of $u(t,x)$ for $\lambda = 0.0085, \kappa = 0.01, \tau = 1$ and $T = 100$
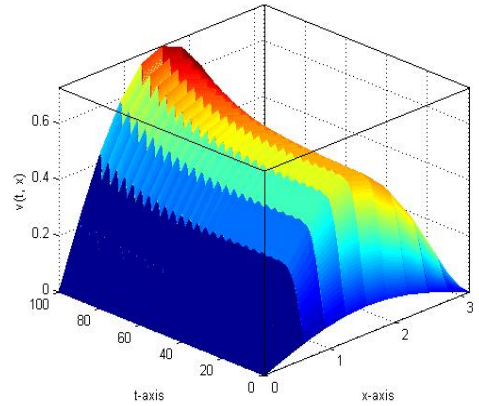
Figure 5.5.2: Profile of $v(t,x)$ for $\lambda = 0.0085, \kappa = 0.01, \tau = 1$ and $T = 100$
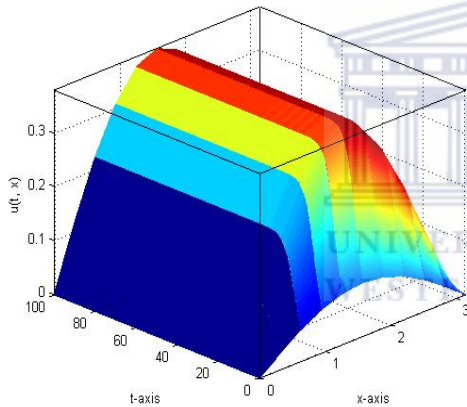
Figure 5.5.3: Profile of $u(t,x)$ for $\lambda = 0.0087, \kappa = 0.01, \tau = 1$ and $T = 100$
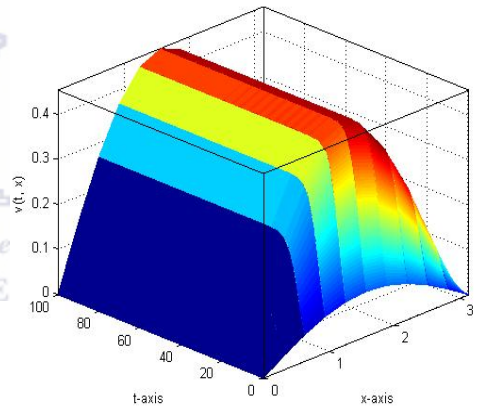
Figure 5.5.4: Profile of $v(t,x)$ for $\lambda = 0.0087, \kappa = 0.01, \tau = 1$ and $T = 100$
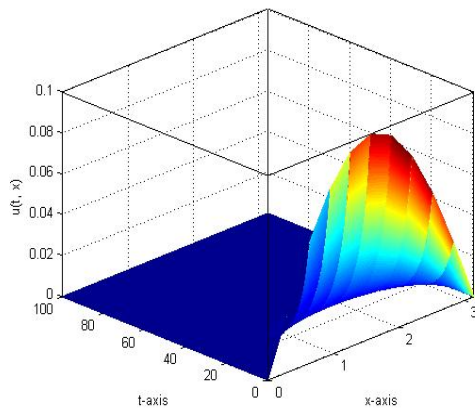
Figure 5.5.5: Profile of $u(t,x)$ for $\lambda = 0.0105, \kappa = 0.01, \tau = 1$ and $T = 100$
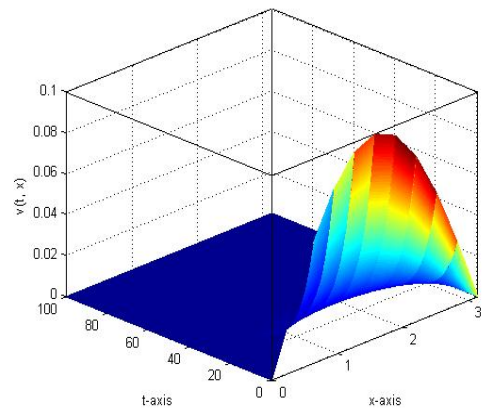
Figure 5.5.6: Profile of $v(t,x)$ for $\lambda = 0.0105, \kappa = 0.01, \tau = 1$ and $T = 100$
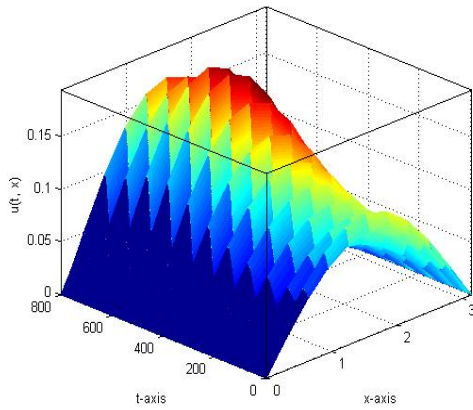
Figure 5.5.7: Profile of $u(t,x)$ for $\lambda = 0.0097, \kappa = 0.01, \tau = 20$ and $T = 800$
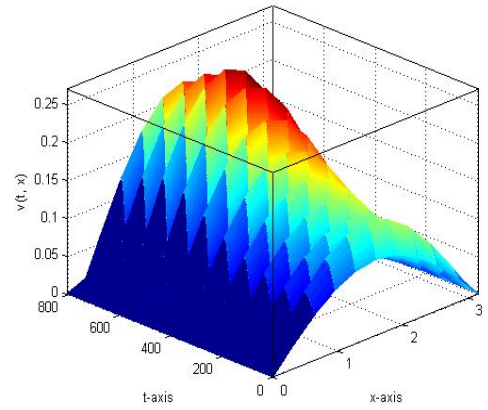
Figure 5.5.8: Profile of $v(t,x)$ for $\lambda = 0.0097, \kappa = 0.01, \tau = 20$ and $T = 800$
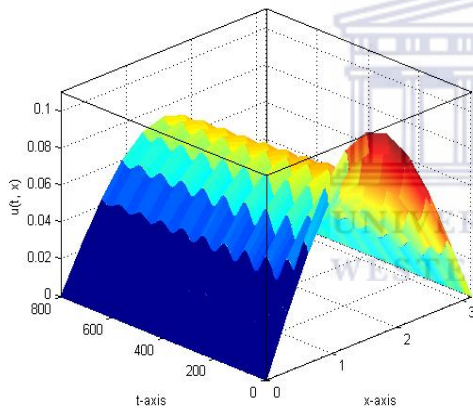
Figure 5.5.9: Profile of $u(t,x)$ for $\lambda = 0.0098, \kappa = 0.01, \tau = 20$ and $T = 800$
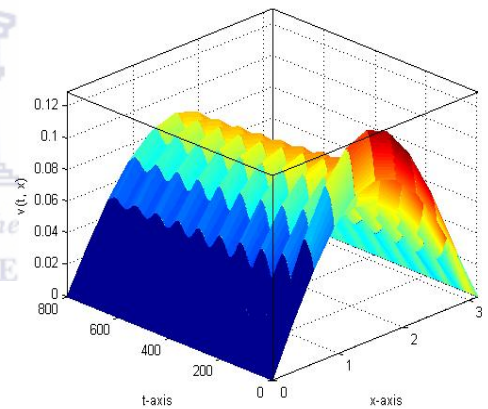
Figure 5.5.10: . Profile of $v(t,x)$ for $\lambda = 0.0098, \kappa = 0.01, \tau = 20$ and $T = 800$
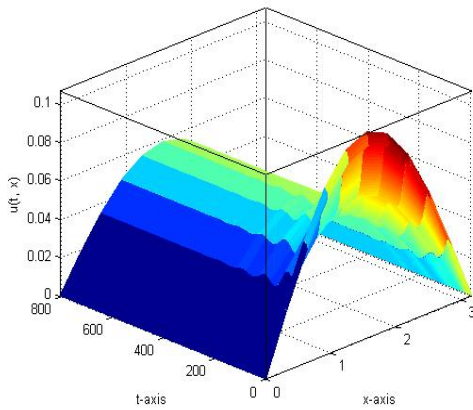
Figure 5.5.11: . Profile of $u(t,x)$ for $\lambda = 0.0099, \kappa = 0.01, \tau = 20$ and $T = 800$

Figure 5.5.12: . Profile of $v(t,x)$ for $\lambda = 0.0099, \kappa = 0.01, \tau = 20$ and $T = 800$
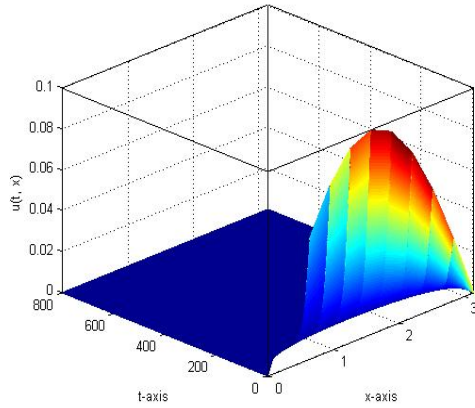
Figure 5.5.13: . Profile of $u(t,x)$ for $\lambda = 0.0105, \kappa = 0.01, \tau = 20$ and $T = 800$
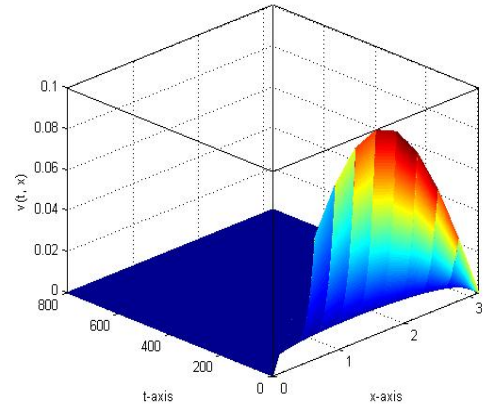
Figure 5.5.14: . Profile of $v(t,x)$ for $\lambda = 0.0105, \kappa = 0.01, \tau = 20$ and $T = 800$
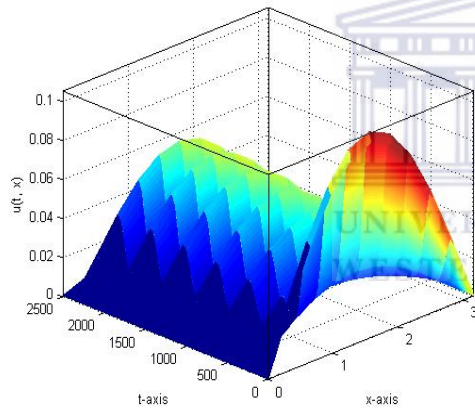
Figure 5.5.15: . Profile of $u(t,x)$ for $\lambda = 0.999, \kappa = 1.01, \tau = 100$ and $T = 2500$
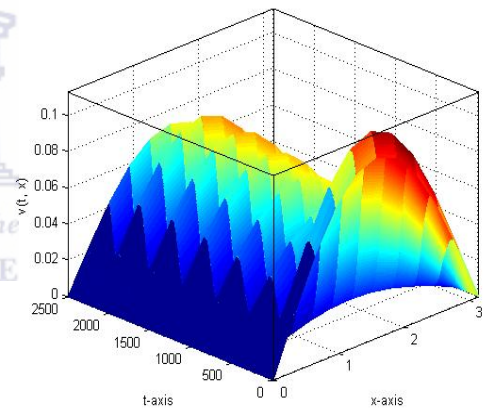
Figure 5.5.16: . Profile of $v(t,x)$ for $\lambda = 0.999, \kappa = 1.01, \tau = 100$ and $T = 2500$
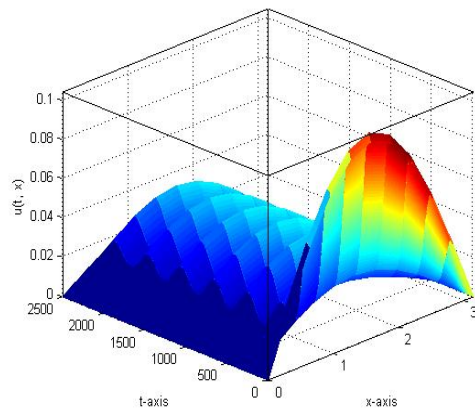
Figure 5.5.17: . Profile of $u(t,x)$ for $\lambda = 1.000, \kappa = 1.01, \tau = 100$ and $T = 2500$
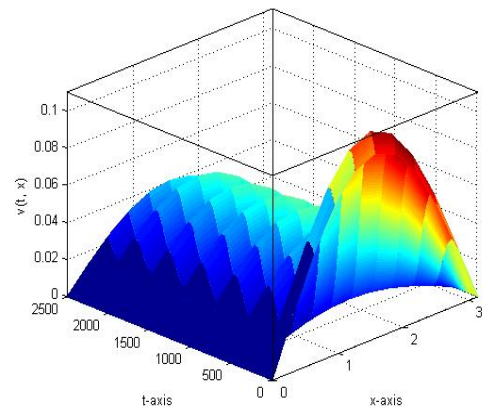
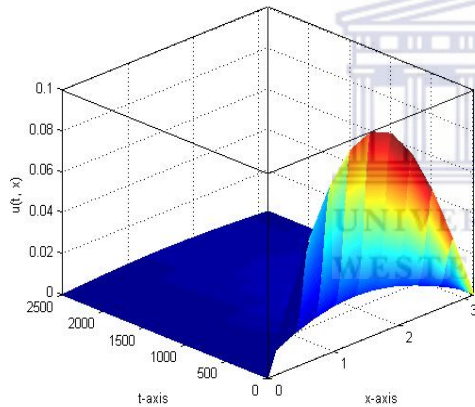Figure 5.5.18: . Profile of $v(t,x)$ for $\lambda = 1.000, \kappa = 1.01, \tau = 100$ and $T = 2500$
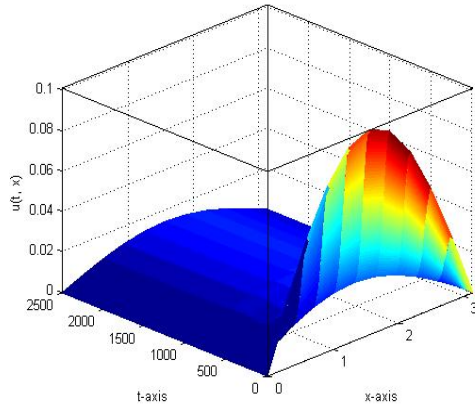
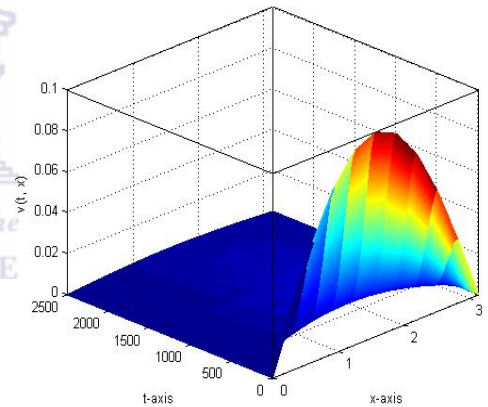Figure 5.5.19: . Profile of $u(t,x)$ for $\lambda = 1.005, \kappa = 1.01, \tau = 100$ and $T = 2500$
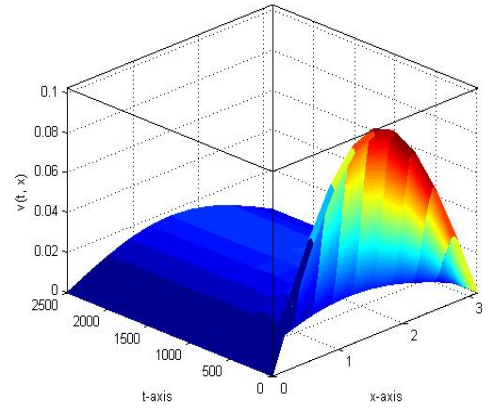
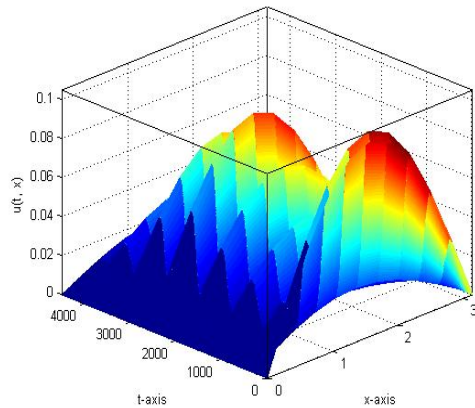Figure 5.5.20: . Profile of $v(t,x)$ for $\lambda = 1.005, \kappa = 1.01, \tau = 100$ and $T = 2500$

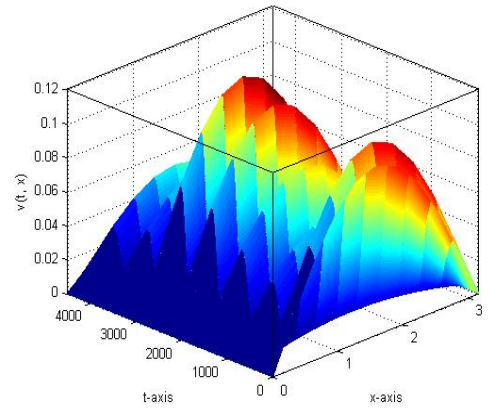Figure 5.5.21: . Profile of $u(t,x)$ for $\lambda = 1.0105, \kappa = 1.01, \tau = 100$ and $T = 2500$

Figure 5.5.22: . Profile of $v(t,x)$ for $\lambda = 1.0105, \kappa = 1.01, \tau = 100$ and $T = 2500$

Figure 5.5.23: . Profile of $u(t,x)$ for $\lambda = 1.003, \kappa = 1.01, \tau = 170$ and $T = 4500$

Figure 5.5.24: . Profile of $v(t,x)$ for $\lambda = 1.003, \kappa = 1.01, \tau = 170$ and $T = 4500$
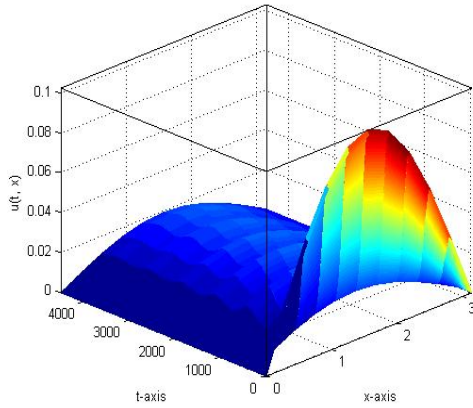
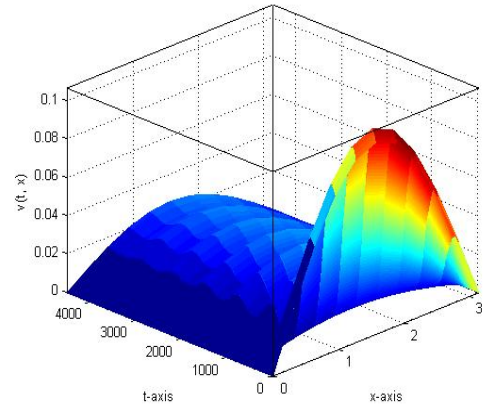Figure 5.5.25: . Profile of $u(t,x)$ for $\lambda = 1.005, \kappa = 1.01, \tau = 170$ and $T = 4500$

Figure 5.5.26: . Profile of $v(t,x)$ for $\lambda = 1.005, \kappa = 1.01, \tau = 170$ and $T = 4500$

Figure 5.5.27: . Profile of $u(t,x)$ for $\lambda = 1.007, \kappa = 1.01, \tau = 170$ and $T = 4500$

Figure 5.5.28: . Profile of $v(t,x)$ for $\lambda = 1.007, \kappa = 1.01, \tau = 170$ and $T = 4500$

Figure 5.5.29: . Profile of $u(t,x)$ for $\lambda = 1.0105, \kappa = 1.01, \tau = 170$ and $T = 4500$

Figure 5.5.30: . Profile of $v(t,x)$ for $\lambda = 1.0105, \kappa = 1.01, \tau = 170$ and $T = 4500$
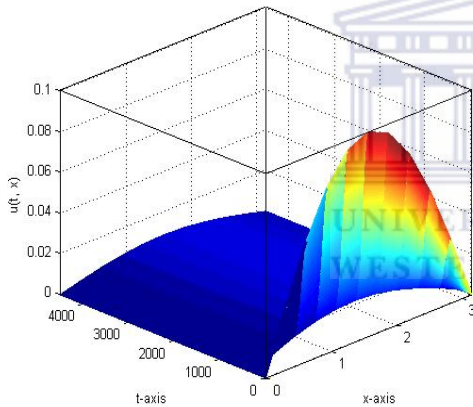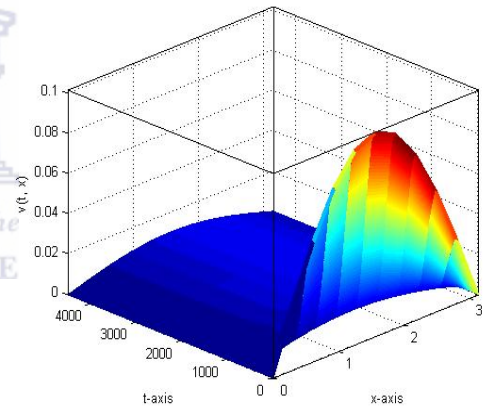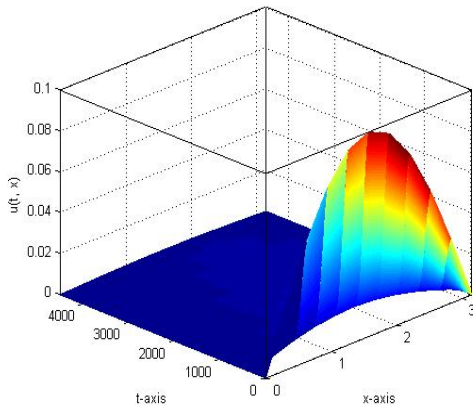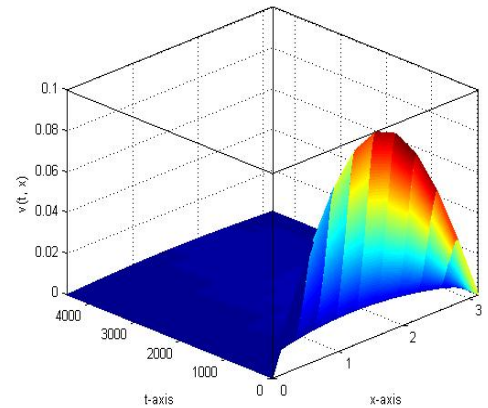
5.6   Discussion

In this chapter we have designed and analyzed a fitted operator finite difference method (FOFDM) for a coupled system of two partial delay differential equations. Using the method of lines, this problem is transformed into a system of ordinary delay differential equations which are then solved with the proposed FOFDM. This FOFDM is analyzed for convergence and we found that this method is of order 1 with respect to time- and is of order 2 with respect to space-discretizations.

In our test example, we considered many scenarios for the selection of the parameters κ and λ such that the ratio κ/λ remains close to one. The results are presented in figures 5.5.1-5.5.30. We have noticed that when $\kappa/\lambda < 1$, the solutions do always tend to the unique stable trivial attractor $(0,0)$ (See figures 5.5.5, 5.5.6, 5.5.13, 5.5.14, 5.5.21, 5.5.22, 5.5.29 and 5.5.30). When the ratio κ/λ passes unity, a stable or a stable periodic solution bifurcates from $\kappa/\lambda = 1$ (See figures 5.5.3, 5.5.4, 5.5.11, 5.5.12, 5.5.19, 5.5.20, 5.5.25, 5.5.26, 5.5.27 and 5.5.28). When we continue increasing the ratio κ/λ unstable periodic solutions bifurcate from $\kappa/\lambda = 1$ as seen in figures 5.5.9, 5.5.10, 5.5.17 and 5.5.18. Finally, by increasing the ratio κ/λ, unstable aperiodic solutions appear as seen in figures 5.5.1,5.5.2 5.5.7, 5.5.8, 5.5.15, 5.5.16, 5.5.23 and 5.5.24. This confirms the theoretical results.

The results which we have obtained by fixing the value of the time delay $\tau = 100$ show that the model is very sensitive to change in values of the parameters. Changes in the ratio κ/λ from 0.99951 passing by 1.01 and 1.005 to 1.01101 have shown four different scenarios about the behaviour of the positive equilibrium. A similar situation is seen for $\tau = 170$, where changes in the ratio κ/λ from 0.99951 to 1.007 have shown four different stability scenarios for the positive equailibrium. These scenarios are the trivial equilibrium $(0,0)$, a stable positive equilibrium, a periodic positive equilibrium and aperiodic positive equilibrium. This again confirms the theoretical results.

In summary, from the results that we have obtained by our simulations, we conclude that for a fixed $\tau > \tau_{\kappa_0} > 0$ if

- the ratio κ/λ is less than or equal to 1 then the solution tends to the trivial attractor $(0,0)$ and the solution is stable and no positive equilibrium exists.

- the ratio κ/λ is greater than 1 then there is a positive equilibrium and a positive real number $\kappa_1 \in (1, \kappa^\star)$ such that if $1 < \kappa/\lambda \leq \kappa_1$ then the positive equilibrium solution is stable, and if $\kappa/\lambda \in (\kappa_1, \kappa^\star]$ then it is unstable, periodic or aperiodic.

Hence, these results that we have obtained by our FOFDM confirm the theory for the existence and stability of the positive equilibrium when $\tau > 0$ and $\kappa/\lambda > 1$. Moreover, our results are comparable to those obtained in [86] in which the authors solved problem (5.1.5)-(5.1.6) using the method of steps (where one transforms the DPDE into a system of ordinary PDEs) and the MATLAB PDE toolbox for $\tau = 20, 100$ and 170 and $T = 200, 2500$ and 4500. Their simulations show that the solution is stable for $\kappa/\lambda = 0.98$ and tends to the trivial attractor $(0,0)$, when they took κ/λ as 1.01 and $\tau = 100$, a bifurcating periodic stable solution is noticed and finally when they took $\tau = 170$ and $\kappa/\lambda = 1.01$ they obtained an unstable Hopf bifurcating solution.

Another remarkable fact is that we have tested the MATLAB dde23 solver for solving the transformed system of DDEs and the dde23 could solve the problem for the delay $\tau = 20$ and $T = 800$ but it failed to solve the system for $\tau = 100$ and $\tau = 170$ on the domains $[0, T]$ with $T = 2500$ and $T = 4500$. The dde23 solved the problem using 12371 grid points and took 70.02 seconds to compute the solution. On the other-hand, our FOFDM solved the same problem using 3000 grid points and took 2.95 seconds to compute the solution. It is worth mentioning here that basically our method is able to produce a reliable solution to the problem with fewer grid points and in fairly less CPU time compared to other in-built solvers.

Chapter 6

A Fitted Numerical Method for a Delayed Model of Two Competitive Species
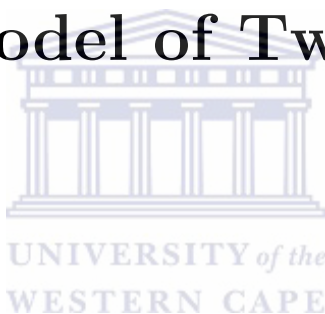
In the previous chapter, we considered a delayed model of two co-operative species. In this chapter, we consider such a model for two competitive species. It is given by a system of two coupled partial delay differential equations (PDDEs). We construct a fitted operator finite difference method (FOFDM) to solve this system. This FOFDM is analyzed for convergence and it is seen that this method is unconditionally stable and has the accuracy of $\mathcal{O}(k+h^2)$, where k and h denote time and space step-sizes, respectively. Some numerical results confirming theoretical observations are also presented. These results are comparable with those obtained in the literature.

6.1   Introduction

Competition between two or more species is a natural phenomenon which appears widely in biological and ecological systems. As per Vries et al. [143], populations are influenced by changes in the weather, a limited food supply, competition for resources such as nutrients and space, territoriality, predation, diseases, etc. Some examples

include: the competition between the immune system and tumor cells, in which the
immune system responds to the tumor cells through the macrophages which absorb
and destroy the tumor cells and send signals to activate the helper T cells, whereas
those helper T cells mark the tumor cells and send signals to the killer T cells [11];
the competition between two species on a common pool of resources, in which each
one of the two species produces a toxic substance against the existing other species
[23]; the competition between the grey and red squirrels in Britain where it had been
noticed that the release of the American grey squirrels from various sites in Britain
led to the disappearance of the red squirrels after a few years [111]; the competition
between two predators on one prey [74], etc. Such phenomena are modelled by partial
delay differential equations (PDDEs), in which the delay might be the time until some
action is taken by one species against the other or the non-immediate effect of that
action on the other species.

Many mathematical models were established to describe the competition between
two or more species, (see for example [15, 24, 78, 111, 146], [151]). Some of these
models consider the spatial spread of the species whereas others do not.

In this chapter, we consider a system of two coupled PDDEs describing the dynamics
of two competitive species [151] having densities $u(t,x)$ and $v(t,x)$ given by

$$\frac{\partial u}{\partial t}(t,x) = \frac{\partial^2 u}{\partial x^2}(t,x) + \kappa u(t,x)\left(1 - a_1 u(t-\tau,x) - b_1 v(t-\tau,x)\right), \quad (6.1.1)$$

$$\frac{\partial v}{\partial t}(t,x) = \frac{\partial^2 v}{\partial x^2}(t,x) + \kappa v(t,x)\left(1 - a_2 u(t-\tau,x) - b_2 v(t-\tau,x)\right), \quad (6.1.2)$$

where $0 < x < \pi$ and $t > 0$, subject to the initial data

$$u(t,x) = u^0(t,x), \quad v(t,x) = v^0(t,x), \quad t \in [-\tau, 0], \tag{6.1.3}$$

and Dirichlet boundary conditions

$$u(t,0) = u(t,\pi) = v(t,0) = v(t,\pi) = 0, \; t \geq 0. \tag{6.1.4}$$

The coefficients a_1, b_1, a_2, b_2 and κ are positive constants. Finally, the positive parameter τ represents delay in the maturation time.

In this chapter, we design a fitted operator finite difference method (FOFDM) to solve the above system of PDDEs.

The rest of this chapter is organized as follows. In Section 6.2, we discuss the existence and stability of equilibria for the model under consideration. Section 6.3 deals with the construction of the fitted operator finite difference method which is analyzed for convergence in Section 6.4. Illustrative numerical results are presented in Section 6.5. Finally, we discuss these results and draw some conclusions in Section 6.6.

6.2   Existence and stability of equilibria

In this section we retrieve some of the results about the existence and Hopf bifurcation of a positive equilibrium, following the work in [151].

The trivial solution $(0,0)$ satisfies (6.1.1)-(6.1.2). For $\kappa < 1$ this trivial solution is asymptotically stable and it is the only global attractor for all non-negative solutions. The question arises about the qualitative behaviour of the model for $\kappa > 1$. Hence, the main consideration of Zhou et al. in [151] was to study the existence and stability of non-trivial steady state spatial solutions $(U_\kappa(x), V_\kappa(x)) \neq (0,0)$ and to determine whether increases in the time delay τ can destabilize the steady state and lead to the occurrence of periodic solutions. To discuss this further, we note that an equilibrium solution for problem (6.1.1)-(6.1.2) should solve the system

$$
\begin{aligned}
\frac{d^2u}{dx^2} + \kappa u(x)(1 - a_1 u(x) - b_1 v(x)) &= 0, \\
\\
\frac{d^2v}{dx^2} + \kappa v(x)(1 - a_2 u(x) - b_2 v(x)) &= 0,
\end{aligned}
\tag{6.2.1}
$$

with

$$
u(0) = u(\pi) = v(0) = v(\pi) = 0,
\tag{6.2.2}
$$

where κ is restricted to some neighbourhood of 1.

Existence of equilibria

Let D^2 denote the differential operator $\frac{d^2}{dx^2}$, and $\mathcal{N}(D^2+1)$ and $\mathcal{R}(D^2+1)$ denote the null and range spaces of the differential operator D^2+1 respectively, then

$$L^2[0,\pi] = \mathcal{N}(D^2+1) \oplus \mathcal{R}(D^2+1),$$

where

$$\mathcal{N}(D^2+1) = \mathrm{span}\{\sin x\}$$

and

$$\mathcal{R}(D^2+1) = \{y(x) \in L^2[0,\pi] : <\sin x, y(x)> = \int_0^\pi (\sin x)y(x)dx = 0\}.$$

The domain of the operator D^2+1 denoted by $\mathcal{D}(D^2+1)$ is given by

$$\mathcal{D}(D^2+1) = \{y \in L^2(0,\pi) : y(0) = y(\pi) = 0\}.$$

Assume that the pair of functions $(U_\kappa(x), V_\kappa(x))$ is an equilibrium solution of the system (6.1.1)-(6.1.3) with

$$U_\kappa(x) \;\; = \;\; \alpha(\kappa-1)(\sin x + (\kappa-1)\xi) \tag{6.2.3}$$

and

$$V_\kappa(x) \;\; = \;\; \beta(\kappa-1)(\sin x + (\kappa-1)\eta), \tag{6.2.4}$$

where $\xi, \eta \in \mathcal{R}(D^2+1)$ and α and β are real numbers.

Using (6.2.1) along with equations (6.2.3)-(6.2.4), one obtains

$$(D^2 + 1)\xi + \sin x + (\kappa - 1)\xi - \kappa \left(a_1(\alpha \sin x + (\kappa - 1)\xi)^2 \right.$$
$$\left. + b_2\beta(\sin x + (\kappa - 1)\xi)(\sin x + (\kappa - 1)\eta) \right) = 0 \tag{6.2.5}$$

and

$$(D^2 + 1)\eta + \sin x + (\kappa - 1)\eta - \kappa \left(a_2\alpha(\sin x + (\kappa - 1)\xi) \right.$$
$$\left. (\sin x + (\kappa - 1)\eta) + b_2\beta(\sin x + (\kappa - 1)\eta)^2 \right) = 0. \tag{6.2.6}$$

For $\kappa = 1$, we get

$$\alpha_1 = \alpha^\star \frac{b_2 - b_1}{a_1 b_2 - a_2 b_1} \text{ and } \beta_1 = \alpha^\star \frac{a_1 - a_2}{a_1 b_2 - a_2 b_1},$$

provided that $a_1 b_2 - a_2 b_1 \neq 0$ where

$$\alpha^\star = \frac{\int_0^\pi \sin^2 x \, dx}{\int_0^\pi \sin^3 x \, dx} = \frac{3}{8}$$

and hence, $\xi_1 = \eta_1$ are the solutions to the boundary value problem

$$(D^2 + 1)y + \sin x - \alpha^* \sin^2 x = 0, \ 0 < x < \pi, \ y(0) = y(\pi) = 0, \tag{6.2.7}$$

with $< y, \sin x > = 0$.

For the general case $\kappa \geq 1$ (which also includes the above case $\kappa = 1$ also), it has been proven in [151] that there is a constant $\kappa^\star$ and a continuously differentiable mapping $\kappa \to (\xi_\kappa, \beta_\kappa, \alpha_\kappa, \beta_\kappa)$ from $[1, \kappa^\star] \to H^2 \times H^2 \times \mathbb{R} \times \mathbb{R}$ such that equations (6.2.5) and (6.2.6) hold and

$$< \sin x, \xi_\kappa > = < \sin x, \eta_\kappa > = 0.$$

The existence of the positive equilibrium (U_κ, V_κ) then follows from the existence and uniqueness of the couple $(\xi_\kappa, \eta_\kappa)$ in the interval $(1, \kappa^\star]$.

Stability of the equilibria

To study the stability of the positive equilibrium (U_κ, V_κ), let $1 < \kappa \leq \kappa^\star$ and consider
the linearized version of the system (6.1.1)-(6.1.2) around this equilibrium, i.e.,

$$\frac{\partial}{\partial t} \begin{pmatrix} u(t,x) \\ v(t,x) \end{pmatrix} = \left(\frac{\partial^2}{\partial x^2} + \kappa \right) I_2 \begin{pmatrix} u(t,x) \\ v(t,x) \end{pmatrix}$$

$$+\kappa \begin{pmatrix} -a_1 U_\kappa & -b_1 U_\kappa \\ -a_2 V_\kappa & -b_2 V_\kappa \end{pmatrix} \begin{pmatrix} u(t-\tau,x) \\ v(t-\tau,x) \end{pmatrix}, \tag{6.2.8}$$

$$\begin{pmatrix} u(\theta,x) \\ v(\theta,x) \end{pmatrix} = \begin{pmatrix} u^0(\theta,x) \\ v^0(\theta,x) \end{pmatrix}, \ \theta \in [-\tau, 0] \tag{6.2.9}$$

$$\begin{pmatrix} u(t,0) \\ v(t,0) \end{pmatrix} = \begin{pmatrix} u(t,\pi) \\ v(t,\pi) \end{pmatrix} = 0 \tag{6.2.10}$$

where I_2 is the 2×2 identity matrix.

By writing $u(t) = u(t,\cdot)$, $v(t) = v(t,\cdot)$ and letting

$$Y(t) = [u(t), v(t)]^T, \ Y_0(t) = [u^0(t,\cdot), v^0(t,\cdot)]^T,$$

$$A(\kappa) = (D^2 + \kappa)I_2$$

and

$$B(\kappa) = \begin{pmatrix} -U_\kappa & a_{12}U_\kappa \\ a_{21}V_\kappa & -V_\kappa \end{pmatrix},$$

the stability of (U_κ, V_κ) is determined through solving the eigenvalue problem

$$\left[A(\kappa) + \kappa B(\kappa)e^{-\lambda\tau} - \lambda I_2 \right] Y = \mathbf{0}. \tag{6.2.11}$$

An infinitesimal generator $A_\tau(\kappa)$ of a compact semi-group ([136]) and the stability
of the equilibrium (U_κ, V_κ) is determined by the eigenvalues of $A_\tau(\kappa)$ which depend
continuously on τ. For $\tau = 0$ all the eigenvalues of A_τ have negative real parts. By

increasing the time delay τ the eigenvalues of $A_\tau(\kappa)$ may move towards the positive real part of the complex plane and the problem is then to determine whether there exists a delay $\tau^\star$ for which $A_{\tau^\star}(\kappa)$ has a pure imaginary eigenvalue $\lambda = i\nu$. However, $\lambda = i\nu$ is a pure imaginary eigenvalue of $A_\tau(\kappa)$ if and only if the equation

$$\left[A(\kappa) + \kappa B(\kappa)e^{-i\theta} - i\nu I_2\right] Y = \mathbf{0}, \tag{6.2.12}$$

is solvable for the pair $\nu > 0$ and $\theta \in [0, 2\pi]$. Then, (6.2.12) is satisfied for all

$$\tau_n = \frac{\theta + 2n\pi}{\nu}, \quad n = 0, 1, \ldots.$$

It has been proved in [151] that if the triplet (ν, θ, Y) solves the eigenvalue problem (6.2.11) with $Y \neq 0$ and $\kappa \in (1, \kappa^\star]$, then $\varrho = \nu/(\kappa - 1)$ is uniformly bounded and

$$Y = [\sin x + (\kappa - 1)\gamma(x), (a + ib)\sin x + (\kappa - 1)\delta(x)]^T,$$

where $\gamma(x)$ and $\delta(x)$ are two smooth functions such that

$$<\sin x, \gamma(x)> = 0$$

and

$$<\sin x, \delta(x)> = 0.$$

Zhou et al. [151] proved that solving the eigenvalue problem (6.2.11) is equivalent

to solve the following system of equations:

$$
\begin{aligned}
g_1(\gamma, \delta, \varrho, \theta, a, b) &= (D^2 + 1)\gamma + (1 - i\varrho)[\sin x + (\kappa - 1)\gamma] + \kappa(-a_1\alpha_\kappa(\sin x + (\kappa - 1)\xi_\kappa) \\
&\quad + b_1\beta_\kappa(\sin x + (\kappa - 1)\eta_\kappa))(\sin x + (\kappa - 1)\gamma) \\
&\quad + \kappa e^{-i\theta}\alpha_\kappa[\sin x + (\kappa - 1)\xi_\kappa](a_1(\sin x + (\kappa - 1)\gamma) \\
&\quad + b_1((a + ib)\sin x + (\kappa - 1)\delta)), \\
g_2(\gamma, \delta, \varrho, \theta, a, b) &= (D^2 + 1)\delta + (1 - i\varrho)[(a + ib)\sin x + (\kappa - 1)\delta] \\
&\quad - \kappa(a_2\alpha_\kappa(\sin x + (\kappa - 1)\xi_\kappa) + b_2\beta_\kappa(\sin x + (\kappa - 1)\eta_\kappa)) \\
&\quad ((a + ib)\sin x + (\kappa - 1)\delta) - \kappa e^{-i\theta}\beta_\kappa[\sin x + (\kappa - 1)\eta_\kappa] \\
&\quad (a_2(\sin x + (\kappa - 1)\gamma) + b_2((a + ib)\sin x + (\kappa - 1)\delta)), \qquad (6.2.13) \\
g_3(\gamma, \delta, \varrho, \theta, a, b) &= Re < \sin x, \gamma >= 0, \\
g_4(\gamma, \delta, \varrho, \theta, a, b) &= Im < \sin x, \gamma >= 0, \\
g_5(\gamma, \delta, \varrho, \theta, a, b) &= Re < \sin x, \delta >= 0, \\
g_6(\gamma, \delta, \varrho, \theta, a, b) &= Im < \sin x, \delta >= 0.
\end{aligned}
$$

Finally, the authors in [151] proved that for each $\kappa \in (1, \kappa^\star]$, Hopf bifurcation occurs as the delay increasingly passes through τ_{k_0} and there exists a $\delta_0 > 0$ such that for each $\tau \in (\tau_{k_0}, \tau_{k_0} + \delta_0]$ system (6.1.1)-(6.1.2) has a periodic solution $(U_\kappa^\tau(x), V_\kappa^\tau(x))$ near $(U_\kappa(x), V_\kappa(x))$ with a period $2\pi/\nu_\kappa$.

In summary,

- If $\kappa \leq 1$, then the zero solution is stable and is the only global attractor of all non-negative solutions.

- If $\kappa > 1$, a unique positive equilibrium (U_κ, V_κ) bifurcates from $\kappa = 1$ and $(u, v) = (0, 0)$ while the zero solution is unstable.

- For each fixed $0 < \kappa - 1 \ll 1$ there exists a sequence $\{\tau_{\kappa_n}\}_{n=0}^{\infty}$ such that the positive equilibrium (U_κ, V_κ) is asymptotically stable if $0 \leq \tau < \tau_{\kappa_0}$ and periodic if $\tau > \tau_{\kappa_0}$.

- A Hopf bifurcation will occur as the delay τ increasingly passes through each point τ_{κ_n}, $n = 1, 2, \ldots$.

The above information will be useful in designing a dynamically consistent numerical method in the next section.

6.3   Construction of the numerical method

In this section, we describe the construction of the fitted numerical method for solving the system (6.1.1)-(6.1.2) with the initial data (6.1.3) and boundary conditions (6.1.4).

Following the method of lines, we determine an approximation to the derivatives of the functions $u(t, x)$ and $v(t, x)$ with respect to the spatial variable x. By doing so, we transform the two PDDEs into a system of DDEs.

Because of the similarities between the two PDEs in $u(t, x)$ and $v(t, x)$ we will describe the method for the equation in $u(t, x)$. The equation in $v(t, x)$ is dealt with similarity.

Let N_x be a positive integer. Discretize the interval $[0, \pi]$ through the points

$$x_0 = 0 < x_1 < x_2 < \ldots < x_{N_x} = \pi,$$

where $h = x_{m+1} - x_m = \pi/N_x$; $m = 0, 1, \ldots, N_x$.

Let $U_m(t)$ be used to denote $u(t, x_m)$.

We approximate the second order spatial derivative by

$$\frac{\partial^2 u}{\partial x^2}(t, x_m) \approx \frac{U_{m+1} - 2U_m + U_{m-1}}{\phi_m^2}, \tag{6.3.1}$$

where

$$\phi_m = \phi_m(\kappa, \lambda, h) = \frac{2}{\rho_m} \sin \frac{\rho_m h}{2}$$

and

$$\rho_m = \sqrt{\kappa}.$$

It is obvious that $\phi_m \to h$ as $h \to 0$. The function ϕ_m^2 in equation (6.3.1) is conventionally termed as a denominator function ([102]). It can be constructed by using the theory of difference equations (See, e.g., [88, 102, 114]).

Let N_t be a positive integer and $k = T/N_t$ where $0 < t < T$. Discretizing the time interval $[0, T]$ through the points

$$0 = t_0 < t_1 < \ldots < t_{N_t} = T$$

where

$$t_{n+1} - t_n = k, \; n = 0, 1, \ldots, (N_t - 1).$$

We approximate the time derivative at t_n by

$$\frac{dU_m(t_n)}{dt} \approx \frac{U_m^{n+1} - U_m^n}{\psi}, \tag{6.3.2}$$

where

$$\psi = \psi(k) = (exp(\kappa k) - 1)/\kappa.$$

Again we see that $\psi(k) \to k$ as $k \to 0$.

Combining the formulae for the spatial and time derivatives, we obtain

$$\frac{U_m^{n+1} - U_m^n}{\psi(k)} = \lambda \frac{U_{m+1}^{n+1} - 2U_m^{n+1} + U_{m-1}^{n+1}}{\phi_m^2(h)}$$
$$- \kappa U_m^n (1 - a_1(H_u)_m^n - b_1(H_v)_m^n) \tag{6.3.3}$$
$$U_0^n = 0 = U_{N_x}^n \tag{6.3.4}$$

where

$$(H_u)_m^n \approx u(t_n - \tau, x_m)$$

and

$$(H_v)_m^n \approx v(t_n - \tau, x_m),$$

$m = 1, \ldots, N_x - 1, \; n = 0, \ldots, N_t - 1$ are the history functions corresponding to the

equations in u and v.

Equation (6.3.3) can further be simplified as

$$-\frac{\lambda}{\phi_m^2}U_{m-1}^{n+1} + \left(\frac{1}{\psi} + \frac{2\lambda}{\phi_m^2}\right)U_m^{n+1} - \frac{\lambda}{\phi_m^2}U_{m+1}^{n+1} = \left(\frac{1}{\psi} + \kappa\left(1 - a1(H_u)_m^n - b_1(H_v)_m^n\right)\right)U_m^n.$$
(6.3.5)

Equation (6.3.5) can be written as a tridiagonal system given by

$$T_L U^{n+1} = \frac{1}{\psi}U_m^n + \kappa U_m^n(1 - a_1(H_u)_m^n - b_1(H_v)_m^n),$$
(6.3.6)

where $m = 1, \ldots, N_x-1$, $n = 0, \ldots, N_t - 1$ and

$$T_L = \text{Tri}\left(-\frac{\lambda}{\phi_m^2}, \frac{1}{\psi} + \frac{2\lambda}{\phi_m^2}, -\frac{\lambda}{\phi_m^2}\right).$$

On the interval $[0, \tau]$ the delayed arguments $t_n - \tau$ belong to $[-\tau, 0]$, and therefore the delayed variable

$$(H_u)_m^n \approx u_m(t_n - \tau)$$

is evaluated directly from the history functions $u^0(t, x)$ as

$$(H_u)_m^n = u^0(t_n - \tau, x_m),$$
(6.3.7)

and equation (6.3.6) becomes

$$T_L U^{n+1} = \frac{1}{\psi}U^n + \kappa U^n(1 - a_1 u^0(t_n - \tau, x_m) - b_1 v^0(t_n - \tau, x_m)).$$
(6.3.8)

Let s be the largest integer such that $t_s \le \tau$. By using equation (6.3.8) we can compute U_m^n for $1 \le n \le s$. Up to this stage, we interpolate the data

$$(t_0, U_m^0), (t_1, U_m^1), \ldots, (t_s, U_m^s)$$

using an interpolating cubic Hermite spline $\varphi_m(t)$. Then $U_m^n = \varphi(t_n, x_m)$ for all $n =$

$0, 1, \ldots, s$ and $m = 1, 2, \ldots, N_x - 1$.

For $n = s+1, s+2, \ldots, N_t-1$, when we move from level n to level $n+1$ we extend the definitions of the cubic Hermite spline $\varphi_m(t)$ to the point $(t_n + k, U_m^{n+1})$. Then the history terms $(H_u)_m^n$ can be approximated by the functions $\varphi_m(t_n - \tau)$ for $n \geq s$. That is,

$$(H_u)_m^n \approx \varphi_m(t_n - \tau),$$

and equation (6.3.6) becomes

$$T_L U^{n+1} = \frac{1}{\psi} U^n + \kappa U^n (1 - a_1 \varphi(t_n - \tau) - b_1 \vartheta(t_n - \tau)), \tag{6.3.9}$$

where

$$\varphi(t_n - \tau) = [(H_u)_1^n, \ldots, (H_u)_{N_x-1}^n]^T$$

and ϑ is the set of cubic Hermite splines that interpolate the data (t_n, V_m^n).

Proceeding in the similar manner for the equation in v, we have

$$T_L V^{n+1} = \frac{1}{\psi} V^n + \kappa V^n (1 - a_2 (H_u)^n - b_2 (H_v)^n), \tag{6.3.10}$$

where

$$(H_v)^n = \begin{cases} v^0(t_n - \tau) & t_n \leq \tau \\ \\ \vartheta(t_n - \tau) & t_n > \tau \end{cases}$$

along with

$$V_0(t) = 0 = V_{N_x}. \tag{6.3.11}$$

Our FOFDM is then consists of equations (6.3.6)-(6.3.10) along with (6.3.4) and (6.3.11).

This method is analyzed for convergence in next section and the corresponding numerical results are presented in Section 6.5.

6.4 Analysis of convergence

The convergence for the proposed FOFDM is proved via consistency and stability.

Consistency of the numerical method

We assume that the function $u(t, x)$ and its partial derivatives with respect to both t and x are smooth and satisfy

$$\left| \frac{\partial^{i+j} u(t, x)}{\partial t^i x^j} \right| \leq C; \ \forall \, i, j \geq 0, \tag{6.4.1}$$

where C is a constant that is independent of the time and space step-sizes.

The local truncation error (LTE) for the discrete equations in u in the FOFDM (6.3.8) and (6.3.9) is given by

$$(\text{LTE})_u = \left(u_t(t_n, x_m) - \frac{u_m^{n+1} - u_m^n}{\psi} \right) - \left(u_{xx} - \frac{u_{m-1}^{n+1} - 2u_m^{n+1} + u_{m+1}^{n+1}}{\phi_m^2} \right). \tag{6.4.2}$$

The first term on the right hand side of equation (6.4.2) satisfies

$$
\begin{aligned}
&\left| u_t(t_n, x_m) - \frac{u_m^{n+1} - u_m^n}{\psi} \right| \\
&= \left| u_t(t_n, x_m) - \frac{u_m^{n+1} - u_m^n}{k} + \frac{u_m^{n+1} - u_m^n}{k} - \frac{u_m^{n+1} - u_m^n}{\psi} \right| \\
&\leq \left| u_t(t_n, x_m) - \frac{u_m^{n+1} - u_m^n}{k} \right| + \left| \frac{u_m^{n+1} - u_m^n}{k} - \frac{u_m^{n+1} - u_m^n}{\psi} \right| \\
&\leq \frac{k}{2} \left| u_{tt}(\xi, x_m) \right| + \frac{\kappa k (\frac{1}{2} + \frac{\kappa k}{6} + \ldots)}{1 + \frac{\kappa k}{2} + \ldots} (u_m^{n+1} - u_m^n), \ \xi \in [t_n, t_{n+1}] \\
&\leq \frac{k}{2} C + \frac{\kappa k (\frac{1}{2} + \frac{\kappa k}{6} + \ldots)}{1 + \frac{\kappa k}{2} + \ldots} (u_m^{n+1} - u_m^n) \ (\text{using } (6.4.1)) \\
&\to 0 \text{ as } k \to 0.
\end{aligned}
\tag{6.4.3}
$$

The second term on the right-hand side of equation (6.4.2) satisfies

$$\left| u_{xx}(t_n, x_m) - \left(u_{xx} - \frac{u_{m-1}^{n+1} - 2u_m^{n+1} + u_{m+1}^{n+1}}{\phi^2} \right) \right|$$

$$\leq \left| u_{xx}(t_n, x_m) - \left(\frac{u_{m-1}^n - 2u_m^n + u_{m+1}^n}{h^2} \right) \right|$$

$$+ \left| \left(\frac{u_{m-1}^n - 2u_m^n + u_{m+1}^n}{h^2} - \frac{u_{m-1}^{n+1} - 2u_m^{n+1} + u_{m+1}^{n+1}}{\phi^2} \right) \right|$$

$$\leq \frac{h^2}{12} |u_{xxxx}(t_n, \zeta)| + \left| \frac{(\rho h/2)^2/3 - (\rho h/2)^4/60 + \dots}{1 - (\rho h/2)^2/6 + \dots} \right| + k |u_{xxt}(\xi, x_m)| ,$$

$$\leq \frac{h^2}{12} C + h^2 \left(\left| \frac{(\rho/2)^2/3 - h^2(\rho/2)^4/60 + \dots}{1 - (\rho h/2)^2/6 + \dots} \right| \right) + kC \text{ (using (6.4.1))},$$

$$\to 0 \text{ as } h \to 0 \text{ and } k \to 0, \tag{6.4.4}$$

where $x_{m-1} < \zeta < x_{m+1}$ in the third last inequality above.

The results that we obtained in equations (6.4.3) and (6.4.4) prove that LTE $\to 0$ as $k \to 0$ and $h \to 0$. Similarly, the LTE for the equation in v tends to 0, as $h \to 0$ and $k \to 0$. This proves the consistency of our FOFDM.

Stability of the numerical method

In this section we apply the von Neumann stability analysis to prove the stability of our method.

Plugging

$$U_m^n = w_n e^{imh},$$

in equation (6.3.6) where $i = \sqrt{-1}$, we obtain

$$\left(\left(\left(\frac{1}{\psi} + \frac{2\lambda}{\phi^2} \right) - \frac{1}{\psi} \left(e^{imh} + e^{-imh} \right) \right) w_{n+1} = \left(\frac{1}{\psi} + \kappa \left(1 - a_1 U_{\tau,m}^n - b_1 V_{\tau,m}^n \right) \right) w_n \tag{6.4.5}$$

From equation (6.4.5), the amplification factor ς is given by

$$\varsigma = \frac{\frac{1}{\psi} + \kappa(1 - a_1 (H_u)_m^n b_1 (H_v)_m^n)}{\frac{1}{\psi} + \frac{4\lambda}{\phi_m^2} \sin^2 \frac{mh}{2}}. \tag{6.4.6}$$

We notice that both the quantities in the numerator and denominator in the right-hand side of equation (6.4.6) are positive. Hence the amplification factor ς satisfies

$$|\varsigma| \leq 1$$

if

$$\frac{1}{\psi} + \kappa \left(1 - a_1(H_u)_m^n - b_1(H_v)_m^n\right) \leq \frac{1}{\psi} + \frac{4}{\phi_m^2} \sin^2 \frac{mh}{2}. \qquad (6.4.7)$$

Simplifying the inequality (6.4.7) we obtain

$$\kappa \left(1 - a_1(H_u)_m^n - b_1(H_v)_m^n\right) \leq \frac{4}{\phi_m^2} \sin^2 \frac{mh}{2} \leq \frac{4}{\phi_m^2}. \qquad (6.4.8)$$

From the discussion in Section 6.2, we see that κ can not exceed κ^* which is always less than 2. This implies that the left hand side of the inequality (6.4.8) is always less than 2. On the other hand, we see that the right hand side of the inequality (6.4.8) is $4/\phi_m^2$ which is much greater than 2. Hence, the amplification factor ς is always less than 1 and therefore, the proposed FOFDM is unconditionally stable.

Hence, using the Lax-Richtmyer theory [108, 125], we have the following theorem.

Theorem 6.4.1 *The FOFDM given by (6.3.9)-(6.3.10) along with (6.3.4) and (6.3.11) is convergent of order $\mathcal{O}(k + h^2)$ in the sense that*

$$\max \left\{ \max_{1 \leq m,n \leq N-1} \left\{ |u(t_n, x_m) - U_m^n| \right\}, \max_{1 \leq m,n \leq N-1} \left\{ |v(t_n, x_m) - V_m^n| \right\} \right\} \leq C(k + h^2),$$

where U and V are the numerical solutions obtained by this FOFDM and N is the total number of subintervals taken in either directions.

6.5 Numerical results

To see the performance of the proposed FOFDM, we consider the following example.

Example 6.5.1 Consider problem (6.1.1)-(6.1.2) with $a_1 = 1$, $b_1 = 0.5$, $a_2 = 0.8$, $b_2 = 1$, $\kappa \in [0.95, 1.9]$, $\tau \in \{10, 20, 50\}$ and $T = 500$. The initial data is taken as

$$u(\theta, x) = v(\theta, x) = 0.1 \left(1 + \frac{\theta}{\tau}\right) \sin x, \theta \in [-\tau, 0], 0 \leq x \leq \pi, \ t \geq 0.$$
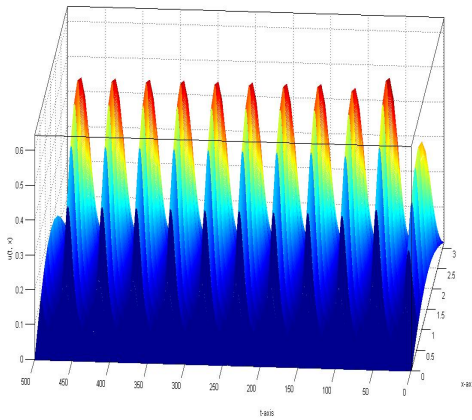
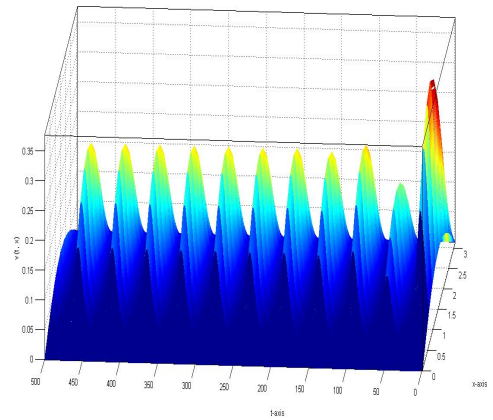Figure 6.5.1:   Profile of $u(t,x)$ for $\kappa =$ 1.25 and $\tau = 10$
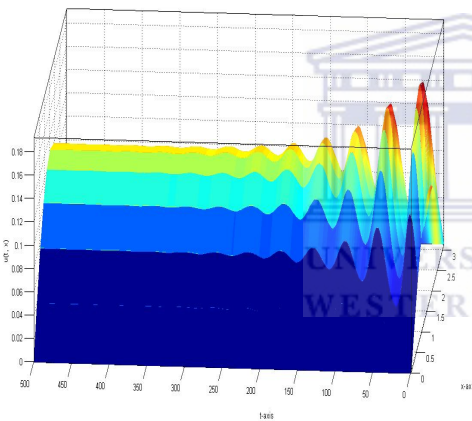

Figure 6.5.2:   Profile of $v(t,x)$ for $\kappa =$ 1.25 and $\tau = 10$

Figure 6.5.3:   Profile of $u(t,x)$ for $\kappa =$ 1.15 and $\tau = 10$
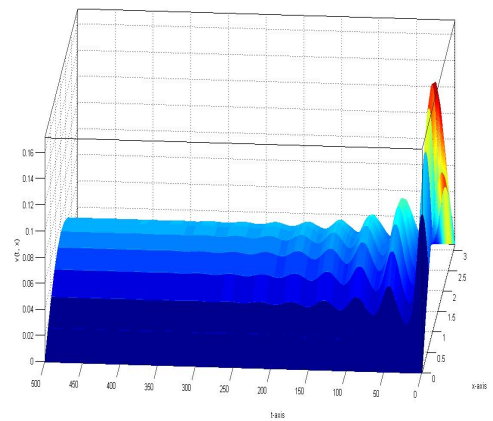
Figure 6.5.4:   Profile of $v(t,x)$ for $\kappa =$ 1.15 and $\tau = 10$
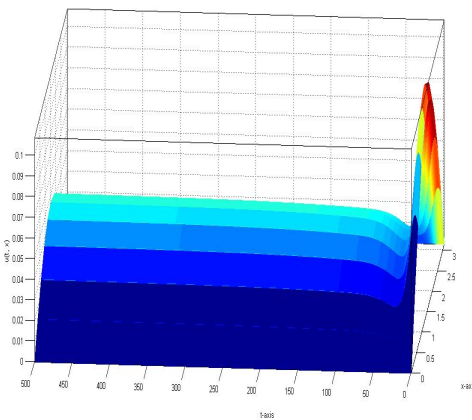
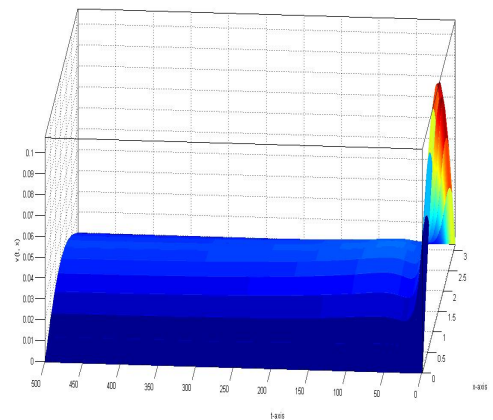Figure 6.5.5:   Profile of $u(t,x)$ for $\kappa =$ 1.05 and $\tau = 10$

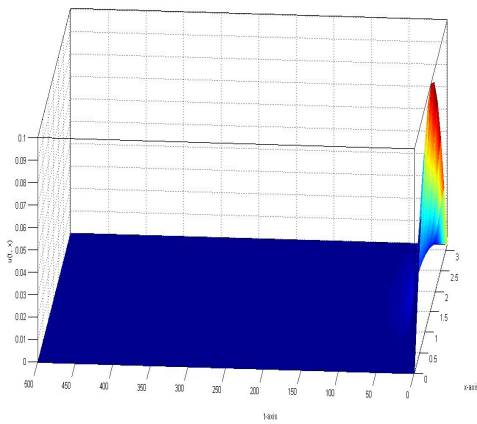Figure 6.5.6:   Profile of $v(t,x)$ for $\kappa =$ 1.05 and $\tau = 10$

Figure 6.5.7:   Profile of $u(t,x)$ for $\kappa = 0.95$ and $\tau = 10$
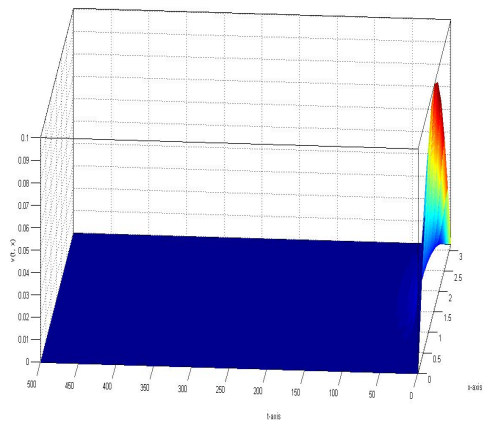

Figure 6.5.8:   Profile of $v(t,x)$ for $\kappa = 0.95$ and $\tau = 10$
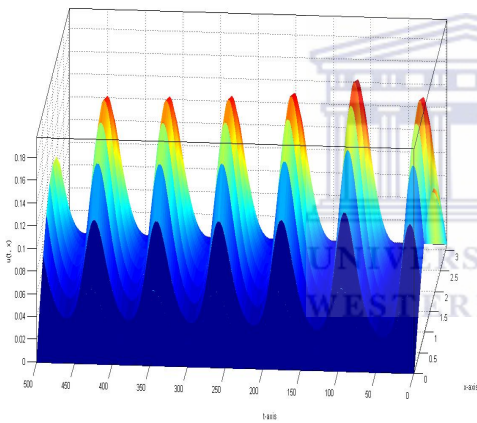

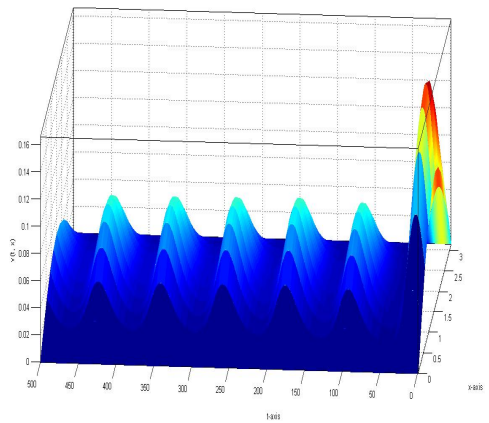Figure 6.5.9:   Profile of $u(t,x)$ for $\kappa = 1.1$ and $\tau = 20$

Figure 6.5.10: . Profile of $v(t,x)$ for $\kappa = 1.1$ and $\tau = 20$
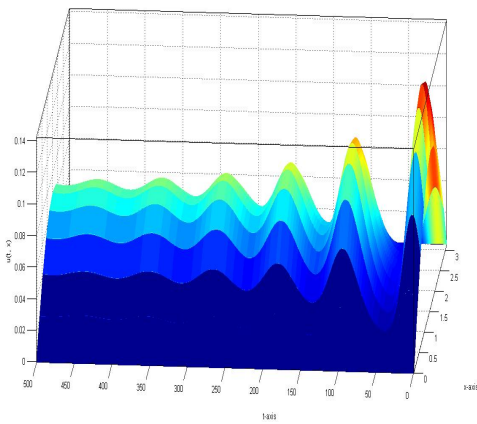

Figure 6.5.11: . Profile of $u(t,x)$ for $\kappa = 1.075$ and $\tau = 20$

Figure 6.5.12: . Profile of $v(t,x)$ for $\kappa = 1.075$ and $\tau = 20$

Figure 6.5.13: . Profile of $u(t, x)$ for $\kappa = 1.05$ and $\tau = 20$

Figure 6.5.14: . Profile of $v(t, x)$ for $\kappa = 1.05$ and $\tau = 20$

Figure 6.5.15: . Profile of $u(t, x)$ for $\kappa = 1.0$ and $\tau = 20$

Figure 6.5.16: . Profile of $v(t, x)$ for $\kappa = 1.0$ and $\tau = 20$

Figure 6.5.17: . Profile of $u(t, x)$ for $\kappa = 1.06$ and $\tau = 50$
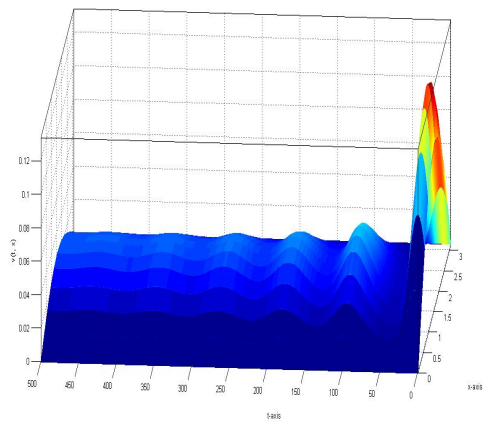

Figure 6.5.18: . Profile of $v(t, x)$ for $\kappa = 1.06$ and $\tau = 50$

Figure 6.5.19: . Profile of $u(t,x)$ for $\kappa = 1.04$ and $\tau = 50$

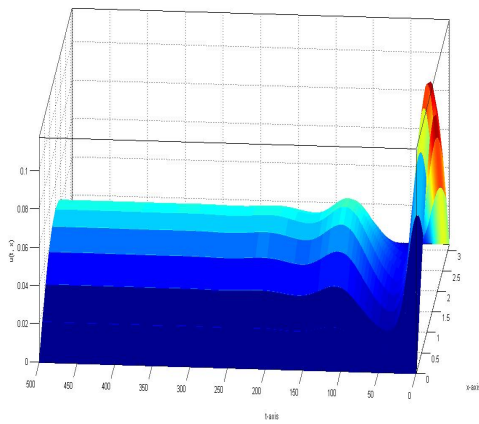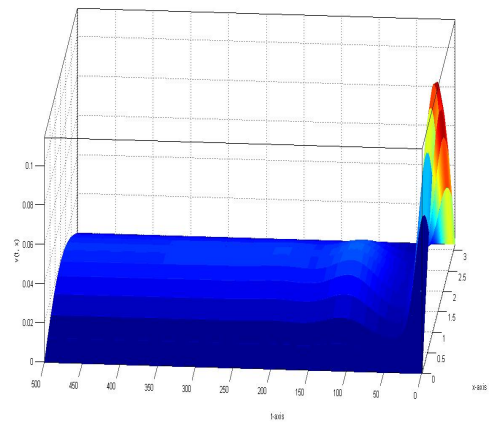Figure 6.5.20: . Profile of $v(t,x)$ for $\kappa = 1.04$ and $\tau = 50$

Figure 6.5.21: . Profile of $u(t,x)$ for $\kappa = 1.02$ and $\tau = 50$

Figure 6.5.22: . Profile of $v(t,x)$ for $\kappa = 1.02$ and $\tau = 50$

Figure 6.5.23: . Profile of $u(t,x)$ for $\kappa = 1.0$ and $\tau = 50$

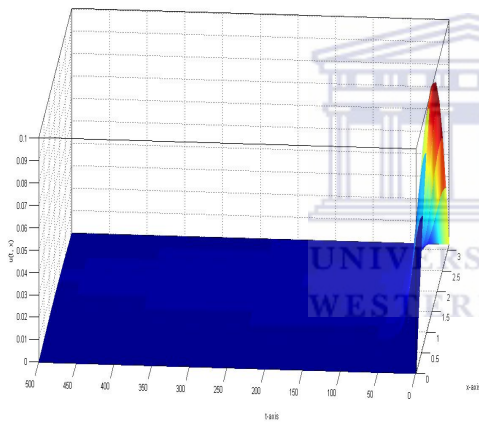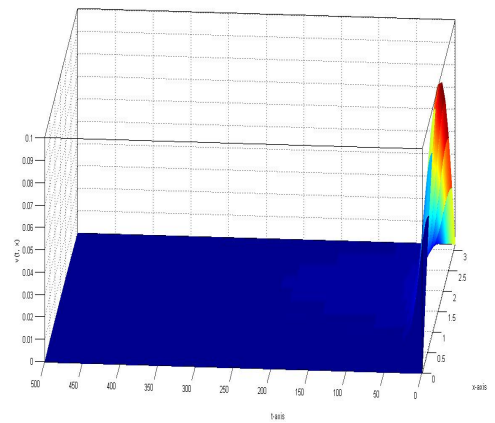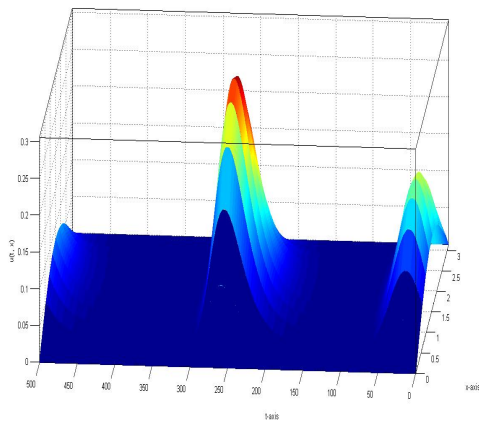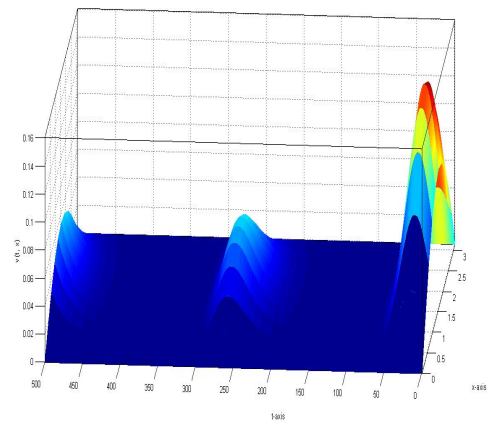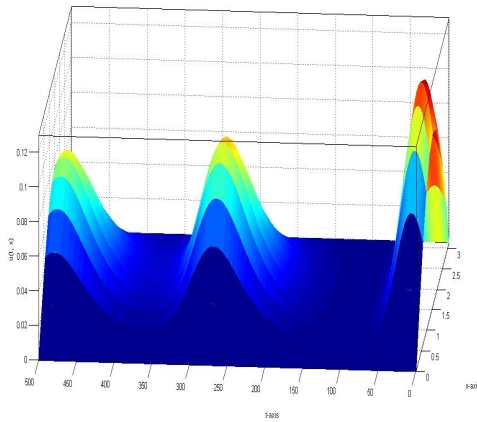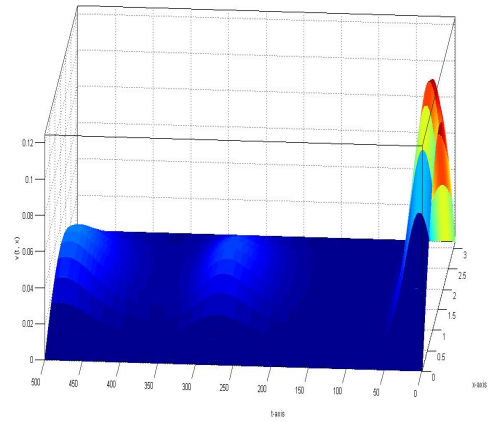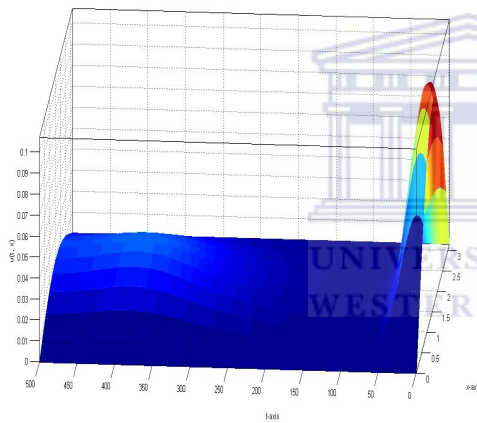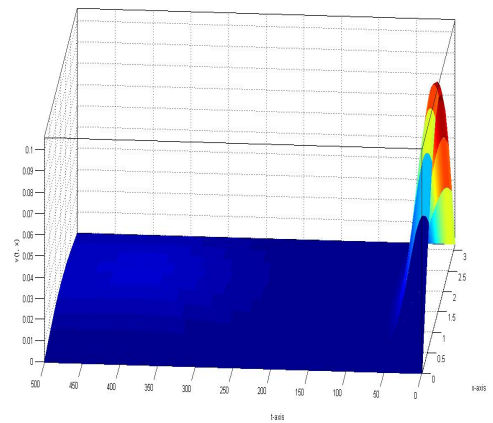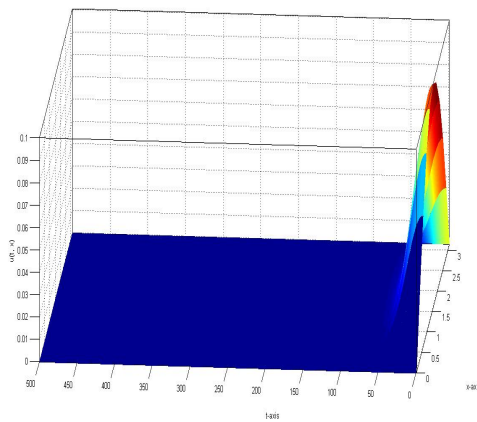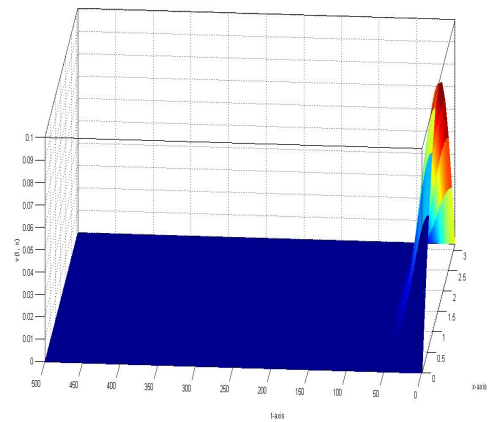Figure 6.5.24: . Profile of $v(t,x)$ for $\kappa = 1.0$ and $\tau = 50$

6.6 Discussion

In this chapter, we have designed a fitted operator finite difference method (FOFDM)
for a competition model that is described by a system of two coupled partial delay
differential equations. This FOFDM is analyzed for convergence and we found that
this method is of order $\mathcal{O}(k + h^2)$ where k and h are the step-sizes in the time and
space directions, respectively.

In our test example, we considered many scenarios for the selection of the parameter
κ such that it remains close to unity. The results are presented in figures 6.5.1-6.5.24.

By taking $\kappa = 0.95$ and 1.0, only the trivial solution is obtained as t increases (both
the two species will extinct). This can be viewed in figures 6.5.7, 6.5.8, 6.5.15, 6.5.16,
6.5.23 and 6.5.24. By increasing κ slightly to values above 1.0 ($\kappa = 1.02$ and 1.05),
we have noticed the appearance of stable positive equilibrium (both the two species
will exist). This can be seen in figures 6.5.5, 6.5.6, 6.5.3, 6.5.4, 6.5.13, 6.5.14, 6.5.11,
6.5.12, 6.5.21 and 6.5.22. By increasing the value of κ ($\kappa = 1.25, 1.1, 1.04$ and 1.06), we
obtained periodic solutions as can be seen in figures 6.5.1, 6.5.2, 6.5.9, 6.5.10, 6.5.19,
6.5.20, 6.5.17 and 6.5.18.

We found that our results do agree with the theory about the existence of a positive
equilibrium for $\tau > 0$ and $\kappa > 1$, where different behaviour of the system, ranging
from the trivial zero attractor, passing a stable positive equilibrium and ending with a
periodic equilibrium are obtained.

From the results that we have obtained with our simulations, we conclude that for
a fixed $\tau > \tau_{\kappa_0} > 0$, if

- κ is less than or equal to 1 then the solution tends to the trivial attractor $(0,0)$
  and the solution is stable and no positive equilibrium exists.

- κ is greater than 1 then there is a positive equilibrium and a positive real number
  $\kappa_1 \in (1, \kappa^\star)$ such that if $1 < \kappa \leq \kappa_1$ then the positive equilibrium solution is
  stable, and if $\kappa \in (\kappa_1, \kappa^\star]$ then the positive equilibrium is periodic.

Hence, the results that we have obtained confirm the theory about the existence and
stability of the positive equilibrium.

The clear difference between the qualitative behaviour of the solutions of the com-
petition model under consideration and the co-operative model by Li et al. [86] is that
in the co-operative model, chaotic behaviour of the solution can be obtained for some
values of the parameter κ, whereas no aperiodic behaviour can be obtained for the
competition model. The theories about the qualitative behaviour for the two models
confirm these results. By looking at the simulations in [86] and our simulations here,
one can notice the agreement between our numerical simulations and the theoretical
results for the two different models.

Chapter 7

Concluding Remarks and Future Directions

In this thesis, we considered different classes of delay differential equation (DDE) models having biological applications. These biological models include a single delay differential equation model, a system of delay differential equations, a boundary value problem of a singularly perturbed second-order delay differential equation, a singularly perturbed delay parabolic partial differential equation and a system of delay parabolic partial differential equations. For each class of these DDEs, we have designed and analyzed fitted numerical methods. To the best of our knowledge we have not seen any numerical methods in the literature for some of the models considered in this thesis, and therefore, our quantitative work is a new contribution to the numerical world for these problems. Moreover, these numerical methods are very robust.

In Chapter 2, we considered two systems of delay differential equations modelling the dynamics of a mature population and the periodic chronic myelogenous leukemia. The fitted numerical methods (PPMs) that we have designed are of relatively low order, but that is the best that one could do at this stage. Currently, we are busy investigating how we can improve the order of convergence of these PPMs. Our future plans for these problems include the construction of direct higher order numerical methods.

In Chapter 3, we developed a fitted numerical method for solving a singularly perturbed second-order delay differential equation. The numerical method developed in that chapter discretizes the original problem without using Taylor expansions as is done in the literature in the past. In this way, we could say that this was the direct method to solve original problems. The proposed approach is very simplistic in nature and hence we can easily extend it to solve higher order problems in this class.

Chapter 4 dealt with singularly perturbed delay parabolic partial differential equations. While the theoretical estimates that we have designed add the mathematical theory about these problems, the numerical methods designed there were extremely robust and easily adaptable to more complex problems. To the best of our knowledge, the order of convergence which we achieved by applying the fitted mesh and fitted operator finite difference methods for the singularly perturbed delay parabolic partial differential equations in that chapter has not been achieved by anyone in the literature to date. A further improvement on our own results obtained by the fitted mesh method can be made if we use the proposed method on a mesh of Bakhvalov type rather than a mesh of Shishkin type. We are currently investigating this aspect.

The problems considered in chapters 5 and 6 describe the dynamics of two co-operative and competitive species have oscillatory solutions. The theories about the qualitative behaviour of the solutions of the two models are different. In the co-operative model stable, periodic and chaotic behaviour can be seen for the solution, while only stable and periodic solutions can be obtained for the competitive model. (It is to be noted that in Chapter 5, we have considered the case when both diffusion coefficients λ_1 and λ_2 are the same. However, our approach can be extended for the general cases (for instance problem (5.1.1)-(5.1.2)) where $\lambda_1 \neq \lambda_2$ with necessary modifications.) Due to the oscillatory nature of the solutions, the fitted mesh methods cannot be designed for such problems and hence we have developed only the fitted operator numerical methods there. These numerical methods are already very competitive but we are still planning to improve them further in near future.

Finally, it should be noted that almost all the numerical methods that we have developed for different problems in this thesis are comparable with (and in some cases better than) the well-known DDE solvers, like MATLAB *dde23*. Moreover, some of these methods developed in this thesis can be extended to solve other classes of problems, for instance, delay problems in higher dimensions, multiple state-dependent delay problems, etc.

Bibliography

[1] A.R. Ansari, S.A. Bakr and G.I. Shishkin, A parameter-rubust finite difference method for singularly perturbed dela parabolic partial differential equations, *Journal of Computational and Applied Mathematics* **205**(2007), 552-566.

[2] O. Arino, M.L. Hbid, E. Ait Dads, *Delay Differential Equations and Applications*, Proceedings of the NATO Advanced Study Institute on Delay Differential Equations and Applications, Springer, 2002.

[3] F.M. Asl and A.G. Ulsoy, Analytical solution of a system of homogeneous delay differential equations via the Lambert function, *Proceedings of the American ControlConference*, Chicago, Illinois, 2496-2500, 2000.

[4] F.M. Asl and A.G. Ulsoy, Analysis of a system of delay differential equations, *Journal of Dynamics System Measure and Control* **125**(2003), 215-223.

[5] A. Bahra and K. Cikurel, *Neurology*, Elsevier Health Sciences, 1999.

[6] C.T.H. Baker, C.A.H. Paul and D.R. Wille, Issues in the Numerical Solutions of Evolutionary Delay Differntial Equations, *Numerical Analysis Report No. 248* (1994).

[7] C.T.H. Baker and C.A.H. Paul, A global convergence theorem for a class of parallel continuous explicit Runge-Kutta methods and vanishing lag delay differential equations, *SIAM Journal in Numerical Analysis* **33**(1996), 1559-1576.

[8] J. Belair and S.A. Campbell, Stability and bifurcations of equilibria in a Multiple-Delayed differential equation, *SIAM Journal on Applied Mathematics* **54 (5)** (1994), 1402-1424.

[9] A. Bellen and M. Zennaro, *Numerical Methods for Delay Differential Equations*, Oxford University Press, 2003.

[10] R.E. Bellman and R.S. Roth, *The Laplace transform*, World Scientific, 1984.

[11] A. Bellouquid and M. Delitala, *Mathematical Modeling of Complex Biological Systems, A Kinetic Theory Approach*, Birkhäuser, Boston, 2006.

[12] L. Berezansky and E. Braverman, On oscillation of a food-limited population model with time delay, *Abstract and Applied Analysis1* **1** (2003), 55-66.

[13] A.E. Berger, J.M. Solomon and M. Ciment, An analysis of a uniformly accurate difference method for a singular perturbation problem, *Mathematics of Computation* **37** (1981), 79-94.

[14] E. Beretta and Y. Kuang, Modeling and analysis of a marine bacteriophage infection with latency period, *Nonlinear Analysis: Real World Applications* **2** (2001), 35-74.

[15] R. Bernstein, *Population Ecology, An Introduction to Computer Simulations*, John Wiley & Sons Ltd, 2003.

[16] E. Berreta and Y. Kuang, Geometric stability switch criteria in delay differential systems with delay dependent parameters, *SIAM Journal of Mathematical Analysis* **33(5)** (2002), 1144-1165.

[17] G.A. Bocharov and A.A. Romanyukha, Numerical treatment of the parameter identification problem for delay-differential systems arising in immune response modelling, *Applied Numerical Mathematics* **15** (1994), 307-326.

[18] J.B. Buriea, A. Calonnec and A. Ducrot, Singular perturbation analysis of travelling waves for a model in Phytopathology, *Mathematical Modelling of Natural Phenomena* **1(1)**(2006), 49-62.

[19] S. Busenberg and W. Huang, Stability and Hopf bifurcation for a population model with diffusion effects, *Journal of Differential Equations* **124** (1996), 80-107.

[20] J.C. Butcher, Implicit Runge-Kutta processes, *Mathematics of Computation* **18(85)** (1964), 50-64.

[21] J.C. Butcher, Numerical Methods for Ordinary Differential Equations, *John Wiley & Sons, Ltd*, Second edition, 2008.

[22] S. Chatterjee, K. Das and J. Chattopadhyay, Time delay factor can be used as a key factor for preventing the outbreak of a disease Results drawn from a mathematical study of a one season eco-epidemiological model, *Nonlinear Analysis: Real World Applications* **8(5)** (2007), 1472-1493.

[23] J. Chattopadhyay, Effect of toxic substance on a two-species competitive system, *Ecological Modelling* **84** (1996) 287-289.

[24] F. Chen, Z. Li, X. Chen, J. Laitochova', Dynamic behaviors of a delay differential equation model of plankton allelopathy, *Journal of Computational and Applied Mathematics* **206** (2007), 733-754.

[25] O. Cheng and M. Jia-qi, The nonlinear singularly perturbed problems for predator-prey reaction diffusion equations, *Journal of Biomathematics* **20(2)** (2005), 135-141.

[26] C. Colijn and M.C. Mackey, A mathematical model of hematopoiesis: Periodic chronic myelogenous leukemia, part I, *Journal of Theoretical Biology* **237** (2005), 117-132.

[27] S.P. Corwin, D. Safaryan and S. Thompson, DKLAG6: a code based on continuously imbedded sixth-order Runge-Kutta methods for the solution of state-dependant functional differential equations, *Applied Numerical Mathematics* **24** (1997), 319-330.

[28] K.L. Cooke, Book review of retarded dynamical systems by G. Stepan, *Bulletin of the American Mathematical Society* **26(1)** (1992), 175-179.

[29] K. Cooke, P. van den Driessche and X. Zou, Interaction of maturation delay and nonlinear birth in population and epidemic models, *Journal of Mathematical Biology* **39** (1999), 332-352.

[30] R.M. Corless, G.H. Gonnet, D.E.G. Hare, D.J. Jefrey and D.E. Knuth, On the Lambert W function, *Advances in Computational Mathematics* **5** (1996), 329-359.

[31] J. Cortes and M. Deininger, *Chronic Myelogenous Leukemia*, Informa Healthcare USA, Inc., 2007.

[32] R.V. Culshaw and S. Ruan, A delay-differential equation model of HIV infection of CD4$^+$T-cells, *Mathematical Biosciences* **165** (2000), 27-39.

[33] X. Ding and W. Li, Stability and bifurcation of numerical discretization Nicholson blowflies equation with delay, *Discrete Dynamics in Nature and Society* **2006**(2006), 12 pages.

[34] A. Deutsch, R.B. de la Parra, R.J. de Boer, O. Diekmann, P. Jagers, E. Kisdi, M. Kretzschmar, P. Lansky, H. Metz, *Mathematical Modeling of Biological Systems, Volume II*, Birkhüser, Boston, 2008.

[35] E.P. Doolan, J.J.H. Miller and W.H.A. Schilders, *Uniform Numerical Methods for Problems with Initial and Boundary Layers*, Boole Press, Dublin, 1980.

[36] P.P.G. Dyke, *An Introduction to Laplace Transforms and Fourier Series*, Springer, 1999.

[37] K. Engelborghs, V. Lemaire, J. Belair and D. Roose, Numerical bifurcation analysis of delay differential equations arising from physiological modeling, *Journal of Mathematical Biology* **42** (2001), 361-385.

[38] K. Engelborghs, T. Luzyanina and D. Roose, Numerical bifurcation analysis of delay differential equations using DDE-BIFTOOL, *ACM Transactions on Mathematical Software* **28(1)** (2002), 1-21.

[39] W.H. Enright and H. Hayashi, A delay differential equation solver based on a continuous Runge-Kutta method with defect control, *Numerical Algorithms*, **16**(1997), (349-364).

[40] W.H. Enright and H. Hayashi, Convergence analysis of the solution of retarded and neu-tral differential equations by continuous methods, *SIAM Journal in Numerical Analysis* **35** (1998), 572-585.

[41] R.J. Epstein, *Human molecular biology: An Introduction to the Molecular Basis of Health and Disease*, Cambridge University Press, 2002.

[42] M. Fan and K. Wang, Periodicity in a Food-limited population model with toxicants and time delays, *Acta Mathematicae Applicatae Sinica* **18 (2)** (2002), 309-314.

[43] J. Forde and P. Nelson, Applications of Sturm sequences to bifurcation analysis of delay differential equation models, *Journal of Mathematical Analysis and Applications* **300** (2004), 273-284.

[44] J.E. Forde, Delay differential equation models in mathematical biology, *PhD thesis*, University of Michigan, 2005.

[45] B. Fornberg, *A Practical Guide to Pseudospectral Methods*, Cambridge University Press, 1998.

[46] S. Gan, G. Sun and W. Zheng, Errors of linear multistep methods and Runge-Kutta methods for singular perturbation problems with delays, *Computers and Mathematics with Applications* **44 (8-9)**, 1157-1173, 2002.

[47] N.H. Gazi and M. Bandyopadhyay, Effect of time delay on a harvested predator-prey model, *Journal of Applied Mathematics and Computing* **26(1-2)** (2008), 263-280.

[48] K. Gopalsamy, M.R.S. Kulenovi'c and G. Ladas, Time lags in a food-limited population model, *Applied Analysis* **31 (3)** (1988), 225-237.

[49] S.A. Gourley, J.W.-H. So and J.H. Wu, Non Locality of Reaction-Diffusion Equations Induced by Delay: Biological Modeling and Nonlinear Dynamics, *Journal of Mathematical Sciences* **124(4)** (2004), 5119-5153.

[50] S. Gourley and Y. Kuang, A delay reaction diffusion model of the spread of bacterio-phage infection, *SIAM Journal in Applied Mathematics* **65(2)** (2005), 550-566.

[51] N. Guglielmi, L'Aquila and E. Hairer, Geneva, Implementing Radau IIA Methods for stiff delay differential equations, *Computing* **67** (2001), 1-12.

[52] A.B. Gumel, K.C. Patidar and R.J. Spiteri, Asymptotically consistent nonstandard finite difference methods for solving mathematical models arising in population biology. In R.E. Mickens (ed.): Applications of Nonstandard Finite Difference Schemes, *World Scientific* (2005), pp. 385-421.

[53] M.S. Gurney, S.P. Blythe and R.M. Nisbee, Nicholson's blowflies revisited, *Nature* **287** (1980), 17-21.

[54] H. Hayashi, *Numerical Solution of Retarded and Neutral Delay Differential Equations using Continuous Runge-Kutta Methods*, PhD thesis, University of Toronto, 1996.

[55] E. Hairer, S.P. Norsett and G. Wanner, *Solving Ordinary Differential Equations: Stiff and differential-algebraic problems*, springer, 1993.

[56] J.M. Heffernan and R.M. Corless, Solving some delay differential equations with computer algebra, *Mathematical Scientist* **31(1)** (2006), 21-34.

[57] A.V.M. Herz, S. Bonhoeffer, R.M. Anderson, R.M. May, and M.A. Nowak, Viral dynamics in vivo: Limitations on estimates of intracellular delay and virus decay, *Proc. Natl. Acad. Sci.* **93** (1996), 7247-7251.

[58] M.H. Holmes, *Introduction to Numerical Methods for Differential Equations*, Springer, New York, 2007.

[59] P. Hu, C. Huang and S. Wu, Asymptotic stability of linear multistep methods for nonlinear neutral delay differential equations, *Applied Mathematics and Computation* **211(1)** (2009), 95-101.

[60] C. Huang, Asymptotic stability of multistep methods for nonlinear delay differential equations, *Applied Mathematics and Computation* **203** (2008), 908-912.

[61] R.A. Horn and C.R. Johnson, *Matrix Analysis*, Cambridge University Press, 1990.

[62] G.E. Hutchinson, circular causal systems in ecology, Annals of the New York Academy of Science **50**(1948), 221-246.

[63] H. Iland, M. Hertzburg and P. Marlton, *Myeloid Leukemia: Methods and Protocols*, Humana Press Inc., Totowa, Newjersy, 2006.

[64] K.J. in 't Hout, Convergence of Runge-Kutta methods for delay differential equations, **Technical report number TW-98-11**, University of Leiden, 1999.

[65] F. Ismail and M. Suleiman, Solving delay differential equations using intervalwise partitioning by Runge-Kutta method, *Applied Mathematics and Computation*, **121** (2001), 37-53.

[66] K. Ito, H.T. Tran and A. Manitius, A fully-discrete spectral method for delay differential equations, *SIAM Journal on Numerical Analysis* **28(4)** (1991), 1121-1140.

[67] Z. Jackiewicz and B. Zubik-Kowal, Spectral collocation and waveform relaxation methods for nonlinear delay partial differential equations, *Applied Numerical Mathematics* **56(3-4)** (2006), 433-443.

[68] Z. Jackiewicz and E. Lo, Numerical solution of neutral functional differential equations by Adams methods in divided difference form, *Journal of Computational and Applied Mathematics* **18** (2006), 592-605.

[69] E. Jarlebring and T. Damm, The Lambert W function and the spectrum of some multidimensional time-delay systems, *Automatica* **43**(2007), 2124-2128.

[70] E. Jarlebring, *The spectrum of delay-differential equations: numerical methods, stability and perturbation*, PhD thesis, Technical University of Braunschweig, 2008.

[71] X. Jiang, X. Zhou, X. Shi and X. Song, Analysis of stability and Hopf bifurcation for a delay-differential equation model of HIV infection of CD4$^+$ T-cells, *Chaos, Solitons and Fractals* **38** (2008), 447-460.

[72] L. Jingwen, Global attractivity in Nicholsons blowflies, *Applied Mathematics - A Journal of Chinese Universities* **11(4)** (1996), 425-434.

[73] M.K. Kadalbajooa, K.C. Patidar, K.K. Sharma, ε-Uniformly convergent fitted methods for the numerical solution of the problems arising from singularly perturbed general DDEs, *Applied Mathematics and Computation* **182(1)** 2006, 119-139.

[74] T.K. Kar and A. Batabyal, Stability and bifurcation of a prey predator model with time delay, Comptes Rendus Biologies, Ariticle to appear 2009, available online at the sciencedirect website.

[75] A. Karoui and R. Vaillancourt, A numerical method for vanishing-lag delay differential equations, *Applied Numerical Mathematics* **17** (1995), 383-395.

[76] J. Keener and J. Sneyd, *Mathematical Physiology I: Cellular Physiology*, Springer, 2009.

[77] R.B. Kellogg and A.Tsan, Analysis of some difference approximations for a singular perturbation problem without turning points, *Mathematics of Computation* **32** (1978), 1025-1039.

[78] L. Edelstein-Keshet, *Mathematical Models in Biology*, SIAM, Pheladelphia, 2005.

[79] J.F.C. Kingman, *Poisson processes*, Oxford University Press, 1993.

[80] Y.N. Kyrychko and K.B. Blyuss, Global properties of a delayed SIR model with temporary immunity and nonlinear incidence rate, *Nonlinear Analysis: Real World Applications* **6** (2005), 495-507.

[81] C.G. Lange and R.M. Miura, Singular perturbation analysis of boundary value problems for differential-difference equations, *SIAM Journal on Applied Mathematics* **42 (3)** (1982), 502-531.

[82] C.G. Lange and R.M. Miura, Singular perturbation analysis of boundary-value problems for differential-difference equations II. Rapid oscillations and resonances, *SIAM Journal on Applied Mathematics* **45 (5)** (1985), 687-707.

[83] C.G. Lange and R.M. Miura, Singular perturbation analysis of boundary-value problems for differential-difference equations III. Turning point problems, *SIAM Journal on Applied Mathematics* **45 (5)** (1985), 708-734.

[84] C.G. Lange and R.M. Miura, Singular perturbation analysis of boundary-value problems for differential-difference equations. V. small shifts with layer behaviour, *SIAM Journal on Applied Mathematics* **54 (1)** (1994), 249-272.

[85] C.G. Lange and R.M. Miura, Singular perturbation analysis of boundary-value problems for differential-difference equations. VI. Small shifts with rapid oscillations, *SIAM Journal on Applied Mathematics* **54 (1)** (1994), 249-272.

[86] W. Li, X. Yan and C. Zhang, Stability and Hopf bifurcation for a delayed cooperation diffusion system with Dirichlet boundary conditions *Chaos, Solitons and Fractals* **38** (2008), 227-237.

[87] J.M.-S. Lubuma and K.C. Patidar, Contributions to the theory of non-standard finite difference methods and applications to singular perturbation problems, Advances in the Applications of Nonstandard Finite Difference Schemes, R.E. Mickens (editor), World Scientific, Singapore, 2005, 513-560.

[88] J.M.S. Lubuma and K.C. Patidar, Non-standard methods for singularly perturbed problems possessing oscillatory/layer solutions, *Applied Mathematics and Computation* **187**(2007), 1147-1160.

[89] T. Luzyanina and D. Roose, Numerical stability analysis and computation of Hopf bifurcation points for delay differential equations, *Journal of Computational and Applied Mathematics* **72** (1996), 379-392.

[90] T. Luzyanina, D. Rooseaand G. Bocharov, Numerical bifurcation analysis of immunological models with time delays, *Journal of Computational and Applied Mathematics* **184** (2005), 165-176.

[91] M.C. Mackey and L. Glass, Oscillation chaos in physiological control systems, *Science, New Series* **197 (4300)** (1977),287-289.

[92] M.C. Mackey and R. Rudnicki, Global stability in a delayed partial differential equation describing cellular replication, *Journal of Mathematical Biology* **33**(1994), 89-109.

[93] M.C. Mackey, C. Ou, L. Pujo-Menjouet and J. Wu, Periodic oscillations of blood cell populations in chronic myelogenous leukemia, SIAM Journal in Mathematical Analysis **38(1)** (2006), 166-187.

[94] J. Mahaffy, J. Bélair And M. C. Mackey, Hematopoietic model with moving boundary condition and state dependent delay applications in Erythropoiesis, *Journal of Theoretical Biology* **190** (1998), 135-146.

[95] S.M. Mahmoud, A class of three-point spline collocation methods for solving delay differential equations, *International Journal of Computer Mathematics* **84 (10)**(2007), 1495-1508.

[96] M.B. Marcus and J. Rosen, *Markov processes, Gaussian processes and local times*, Cambridge University Press, 2006.

[97] R.M.M. Mattheij, S.W. Rienstra and J.H.M. ten Thije Boonkkamp, *Partial Differential Equations*, SIAM, Philadelphia, 2005.

[98] J. Mead and B. ZubikKowal, Pseudospectral Iterated Method for Differential Equations with Delay Terms, *Computational Science - ICCS 2004 (Book Chapter)*, Springer Berlin / Heidelberg, 451-458

[99] L. Pujo-Menjouet, M.C. Mackey, Contribution to the study of periodic chronic myelogenous leukemia, *Comptes Rendus Biology* **327(3)** 2004, 235-244.

[100] L. Pujo-Menjouet, S. Bernard and M. C. Mackey, Long period oscillations in a G_0 model of hematopoietic stem cells, *SIAM Journal in Applied Dynamical Systems* **4 (2)** (2005), 312-332.

[101] M.J. Wester, *Michael J. Wester*, Wiley, 1999.

[102] R.E. Mickens, *Nonstandard Finite Difference Models of Differential Equations*, World Scientific, Singapore, 1994.

[103] R.E. Mickens, Positivity preserving discrete model for the coupled ODE's modelling glycolysis, *Proceedings of the fourth international conference on dynamical systems and differential equations*, Wilmington, USA, 2002, 623-629.

[104] R.E. Mickens, A nonstandard finite-difference scheme for the Lotka Volterra system, *Applied Numerical Mathematics* **45**(2003), 309-314.

[105] R.E. Mickens, *Advances in the Applications of Nonstandard Finite Difference Schemes*, World Scientific, Singapore, 2005.

[106] J.J.H. Miller, E. O'Riordan and G.I. Shishkin, *Fitted Numerical Methods for Singular Perturbation Problems*, World Scientific, Singapore, 1996.

[107] J.J.H. Miller, E. O'Riordan, G.I. Shishkin and L.P. Shishkina, Fitted mesh methods for problems with parabolic boundary layers, *Mathematical Proceedings of the Irish Academy* **98A(2)** (1998), 173-190.

[108] K.W. Morton and D.F. Mayers, *Numerical Solution of Partial Differential Equations*, Cambridge University Press, 2005.

[109] Z. Mukandavire, W. Garira, C. Chiyaka, Asymptotic properties of an HIV/AIDS model with a time delay, *Journal of Mathematical Analysis and Applications* **330(2)** (2007), 916-933.

[110] J.D. Murray, *Mathematical Biology I: An Introduction*, Springer-Verlag, Berlin, third edition, 2001.

[111] J.D. Murray, *Mathematical Biology II: Spatial Models and Biomedical Applications*, Springer-Verlag, Berlin, second edition, 1993.

[112] O. Orino, M.L. Hbid and E. Ait Dads, *Delay Differential Equations and Applications*, Proceedings of the NATO Advanced Study Institute held in Marrakech, Morroco, 2002.

[113] S. Panunzi, P. Palumbo and A. De Gaetano, A discrete single delay model for the intra-venous Glucose tolerance test, *Theoretical Biology and Medical Modelling* **4**:35 (2007).

[114] K.C. Patidar, On the use of nonstandard finite difference methods, *Journal of difference equations and applications* **11(8)** (2005), 735-758.

[115] K.C. Patidar, High order fitted operator numerical method for self-adjoint singular perturbation problems, *Applied Mathematics and Computation* **171** (2005), 547-566.

[116] K.C. Patidar and K. K. Sharma, Uniformly convergent nonstandard finite difference methods for singularly perturbed differential difference equations with delay and advance, *International Journal for Numerical Methods in Engineering* **66(2)** (2006), 272-296.

[117] K.C. Patidar and K.K. Sharma, ε-Uniformly convergent non-standard finite differece methods for singularly perturbed differential difference equations with small delay, *Applied Mathematics and Computation* **175** (2006), 864-890.

[118] K.C. Patidar, A robust fitted operator finite difference method for a two-parameter singular perturbation problem, *Journal of Difference Equations and Applications* **14 (12)** (2008), 1197-1214.

[119] C.A.H. Paul, A Test Set of Functional Differential Equations, *Numerical Analysis Report No. 243*, 1994.

[120] C.A.H. Paul, A User-Guide to Archi An Explicit Runge-Kutta Code for Solving Delay and Neutral Delay differential Equations and Parameter Estimation Problems, *Numerical Analysis Report No. 283*, University of Manchester, 1997.

[121] C.A.H. Paul, Designing Effcient Software for Solving Delay Differential Equations, *Numerical Analysis Report No. 368*, Oct 2000.

[122] M.H. Protter and H.F. Weinberger, *Maximum Principles in Differential Equations*, Prentice Hall, Englewood Cliffs, NJ, 1967.

[123] A.D. Ray and M.C. Mackey, Transition and kinematic of reaction-convection fronts in a cell population model, Physica D **80**(1995), 120-139.

[124] H.G. Roos, M. Stynes and L. Tobiska, *Numerical Methods for Singularly Perturbed Differential Equations*, Springer-Verlag, Berlin, 1996.

[125] R.D. Richtmyer and K.W. Morton, *Difference Methods for Initial-Value Problems*, Interscience, New York, 1967.

[126] S. Ruana, D. Xiaob and J. C. Beierc, On the delayed Ross-Macdonald model for malaria transmission, *Bulletin of Mathematical Biology* **70** (2008), 1098-1114.

[127] J.L. Schiff, *The Laplace Transform: Theory and Applications*, Springer, 1999.

[128] L.L. Schumaker, *Spline Functions: Basic Theory*, Wiley-Interscience, New York, 1981.

[129] L.F. Shampine and S. Thompson, Solving Delay Differential Equations with dde23, available on line at http://www.runet.edu/ thompson/webddes/ddetutwhite.html.

[130] L.F. Shampine and S. Thompson, Solving DDEs in Matlab, *Applied Numerical Mathematics* **37** (2001), 441-458.

[131] L.F. Shampine, Solving ODEs and DDEs with residual control, *Applied Numerical Mathematics* **52** (2005), 113-127.

[132] G.D. Smith, *Numerical Solution of Partial Differential Equations: Finite Difference Methods*, 3rd ed., Clarendon Press, Oxford, 1985.

[133] J.W.H. So, J. Wu b and Y. Yang, Numerical steady state and Hopf bifurcation analysis on the diffusive Nicholson's blowflies equation, *Applied Mathematics and Computation* **111** (2000), 33-51.

[134] Y. Song, M. Han and Y. Peng, Stability and Hopf bifurcations in a competitive Lotka-Volterra system with two delays, *Chaos, Solitons and Fractals* **22** (2004), 1139-1148.

[135] G. Stepan, *Retarded Dynamical Systems: Stability and Characteristic Functions*, Longman, London (1989).

[136] O. Stormark, *Lie's Structural Approach to PDEs*, Cambridge University Press, Cambridge, UK, 2000.

[137] K. Strehmel, R. Weinerand H. Claus, Stability analysis of linearly implicit One-Step interpolation methods for stiff retarded Differential Equations, *SIAM Journal on Numerical Analysis* **26 (5)** (1989), 1158-1174.

[138] M. Suleiman and F. Ismail, Solving delay differential equations using component-wise partitioning by Runge-Kutta method, *Applied Mathematics and Comutation* **122** (2001), 301-323.

[139] S. Thompson and L.F. Shampine, A friendly fortran DDE solver, *Applied Numerical Mathematics* **56** (2006), 503-516.

[140] H.C. Tukwell, On the first exit time problem for temporally homogeneous Markov processes, Journal of Applied Probability **13** (1976), 39-48.

[141] K. Verheyden, T. Luzyaninab and D. Roosea, Efficient computation of characteristic roots of delay differential equations using LMS methods,*Journal of Computational and Applied Mathematics* **214** (2008), 209-226.

[142] M. Villasana and A. Radunskaya, A delay differential equation model for tumor growth, *Journal of Mathematical Biology* **47** (2003), 270-294.

[143] G. de Vries, T. Hillen, M. Lewis, J. Müler and B. Schönfisch, *A Course in Mathematical Biology, Qnantitative Modelling With Mathematical and Computational Methods*, SIAM, Pheladelphia, 2006.

[144] L. Wen and S. Li, Nonlinear stability of linear multistep methods for stiff delay differential equations in Banach spaces, *Applied Mathematics and Computation* **168** (2005), 1031-1044.

[145] C.W. Wu, On bounds of extremal eigenvalues of irreducible and m-reducible matrices, *Linear algebra and its applications* **402** 2005, 29-45.

[146] R. Yafia, Hopf bifurcation in differential equations with delay for tumor-immune system competition model, *SIAM Journal in Applied Mathematics* **67(6)** (2007), 1693-1703.

[147] P. Yan and S. Liu, SEIR epidemic model with delay, *ANZIAM Journal* **48** (2006), 119-134.

[148] N. Yoshida and T. Hara, Global stability of a delayed SIR epidemic model with desnsity dependant birth and death rates, *Journal of Computational and Applied Mathematics*, **201** (2007), 339-347.

[149] P.H. Young and P.A. Young, *Basic Clinical Neuroscience*, Lippincott Williams & Wilkins, 2007.

[150] J. Zhang, Z. Jin, Q. Liu and Z. Zhang, Analysis of delayed SIR model with nonlinear incidence rate, *Discrete Dynamics in Nature and Society* **2008**(2008), 16 pages.

[151] L. Zhou, Y. Tang and S. Hussein, Stability and Hopf bifurcation for a delay competition diffusion system, *Chaos, Solitons and Fractals* **14** (2002), 1201-1225.